THERMODYNAMICS OF THE INTERSTITIAL PHASES OF NIOBIUM IN IRON AUSTENITE

THERMODYNAMICS OF THE INTERSTITIAL PHASES OF NIOBIUM IN IRON AUSTENITE

By

V. K. LAKSHMANAN, B. Tech.

A Thesis

Submitted to the School of Graduate Studies

in Partial Fulfilment of the Requirements

for the Degree

Master of Engineering

McMaster University

September 1977

MASTER OF ENGINEERING (Metallurgical Engineering)

McMASTER UNIVERSITY (Hamilton, Ontario)

TITLE: Thermodynamics of the Interstitial Phases of Niobium in Iron Austenite

AUTHOR: V.K. Lakshmanan, B. Tech. (Indian Institute of Technology, Madras)

SUPERVISOR: Professor J.S. Kirkaldy

NUMBER OF PAGES: xv, 136

ABSTRACT

The austenite-niobium carbonitride equilibrium has been accurately characterized between 1000°C and 1250°C for commercial steel compositions. A closed capsule technique using hydrogen as carrier gas has been employed to equilibrate Fe-Nb alloys with Fe-C alloys and determine the $\gamma/\gamma+NbC_x$ phase boundary in the temperature range 1000-1250°C. The results have been used to define the solubility of niobium carbide in austenite with improved accuracy. Solubility limits have also been determined by chemical analysis of carbides extracted from a laboratory melted steel. A defect carbide $NbC_{0.9}$ and a carbonitride $NbC_{0.91}N_{0.04}$ have been identified as the equilibrium precipitate compositions at 1000°C in two steels.

To test the data for thermodynamic consistency detailed analysis of the thermochemical data of the defect carbides of niobium has been made. The thermodynamics of the binary Fe-C, Fe-Nb and Nb-C systems have been utilized to determine the $\gamma/\gamma+NbC_x$ equilibrium over relevant composition and temperature ranges and this is in good agreement with the experiments. Solubility product relations are given for the carbide $NbC_{0.87}$ as this carbide composition has been shown to be a justifiable average equilibrium composition over the temperature range in this study. The carbide solubility relations have been used along with the reported carbonitride solubilities, to estimate the solubility relation for a metastable cubic nitride of composition $NbN_{0.87}$.

An accurate method for calculating the composition and solubility of nonstoichiometric carbonitride precipitates in steel has been devised using the above carbide and nitride solubility relations and treating the

carbonitrides as compounds with a fixed nonstoichiometry $NbC_xN_{(0.87-x)}$. The effects of Mn, Si, Cr, Ni and Mo on the solubilities of carbonitrides have also been evaluated and it is shown that the carbonitride solubility in a multi-component austenite can be satisfactorily predicted. It is therefore possible to calculate, for example, precipitate fractions and theoretical maximum temperatures required in slab reheating to completely dissolve precipitates.

ACKNOWLEDGEMENTS

The author is indebted to his supervisor, Dr. J.S. Kirkaldy, for introducing the topic of this research and for his inspiring guidance and assistance throughout the course of this study. The advice and assistance of the technical staff and graduate students in the Department of Metallurgy and Materials Science is deeply appreciated.

The generosity of Dr. J. Lapointe of the University of Sherbrooke, Quebec, and Dr. T.M. Hoogendoorn of the Research and Work Laboratories, Hoogovens Ijmuiden B.V., Holland is acknowledged for providing some of the materials used in this study. Due thanks to Mr. B. James of the Department of Biochemistry, McMaster University for providing the Spectrophotometer facility and Mr. H. Hodds of the Steel Company of Canada Research Laboratories for assisting in the chemical analyses.

And also, thanks to Mrs. Jan Gallo for her excellent typing.

The financial support of the National Research Council of Canada is gratefully acknowledged.

TABLE OF CONTENTS

CHAPTER PAGE

LIST OF TABLES

LIST OF ILLUSTRATIONS

LIST OF SYMBOLS

γ	iron austenite
ΔG°	change in the Gibbs standard free energy
ΔH°	change in the standard enthalpy
ΔS°	change in the standard entropy
T	absolute temperature in degrees Kelvin
f	(subscript) formation of the product from the elements
K	equilibrium constant for the reaction as written
[ ]	represents a component in solution in austenite
[i]	concentration of component i in mole fraction
K'	"solubility product"
a_i	Raoultian activity of component 'i'
$\mathfrak{a}_i$	activity of the ith component based on a standard state of infinite dilution in austenite
γ_i	activity coefficient of component 'i' referred to the infinite dilution standard state
γ_i°	Henry's Law coefficient of the ith component in austenite based on a standard state of pure components
ϵ_j^i	Wagner first order interaction coefficient
$\sum_{i=1}^{n}$	'n' represents the number of additional alloying elements besides niobium
ma	milli amperes
R	gas constant, 1.987 cal/mol-deg.
gef_T	Gibbs energy function, $(G^\circ - H^\circ_{298})/T$

ℓn	logarithm to the base 'e'
log	logarithm to the base '10'
$\mathring{A}$	Angstroms (10^{-8} cm)
μ	micron (10^{-4} cm or 10^{4} $\mathring{A}$)

CHAPTER I

INTRODUCTION

The development of structural steels with yield strengths in the range of 60-80 Ksi and improved ductility for line pipe and other applications has been one of the most important metallurgical endeavours of the past decade. Reducing the carbon and micro-alloying with elements such as niobium, titanium and vanadium have made it possible to attain the above objective. These elements, in view of their strong carbide or nitride forming tendency, react with the carbon and nitrogen in steel to precipitate fine second phase particles which influence the strength. Familiarly known as "interstitial phases", these carbides and nitrides exist over wide ranges of nonstoichiometry (e.g., TiC_x $0.4 < x < 1.0$; NbC_x $0.70 < x \leq 0.98$). When precipitated in steels the degree of nonstoichiometry of these interstitial phases is governed by the steel chemistry and temperature.

In the heat treatment and thermomechanical working of micro-alloyed steels, it is a matter of importance to know the limits of homogeneity of austenite and understand the thermodynamics governing the solution behaviour of the interstitial phases in order to schedule the respective processing routes effectively. A low solubility would mean that the second phase particles are more stable and as a result would be mostly undissolved during reaustenitizing treatment of the steel. The undissolved particles inhibit austenitic grain coarsening making the steel amenable for thermomechanical working. Furthermore, the ferritic grain size developed after allotropic transformation strongly depends on the prior austenitic grain size because of ferritic nucleation on the grain boundaries. Thus a desireable fine ferritic grain size results and contributes to higher strength and ductility. A relatively high solubility of an interstitial phase, on the other hand, leads to precipitation-hardening in the ferrite. Such steels can be normalized after prior solution treatment. The solubility must not be too high, however, because undercooling and precipitation must take place in a temperature range which permits reasonable diffusion. The interstitial phases satisfy the above stringent solubility requirements and contribute to improved combinations of strength and ductility.

Among niobium, titanium and vanadium, the more commonly used additive is niobium in view of its better ability to grain refine and moderately precipitation harden the ferritic matrix. Niobium is also used as an important additive in Type 347 austenitic stainless steels for power plant applications. The beneficial creep rupture properties of these steels are attributed to the precipitation-hardening caused by niobium carbide. Correlation of these properties with steel chemistry and precipitate solubility and stoichiometry has been the object of recent investigations.[2-4]

There have been many experimental determinations of the niobium carbide solubility in austenite.[8-16] Most of the investigators have assumed a stoichiometric carbide, NbC, for interpretation of the data and show considerable disagreement. The published theoretical treatments,[6] in spite of good thermochemical data being available, fail to correctly predict the defect carbide solubility.

Precipitates formed in equilibrium with austenite in commercial steels containing niobium have been shown to contain appreciable proportions of nitrogen as well as carbon. Mandry and Dornelas,[21] for example, obtained precipitates with the formula $NbC_{0.83}N_{0.14}$ while Mori et al.[7,18,22] have obtained carbonitrides that were nonstoichiometric to an even greater extent. The latter author's extensive studies has clearly demonstrated that the equilibrium composition of the precipitate depends markedly on the composition of the steel and temperature.

In the present study a systematic experimental and theoretical investigation of the solubility of niobium carbide in austenite has been made. The results have been used, along with the reported data on carbonitrides, to satisfactorily predict the composition and solubility relation for any carbonitride precipitated in a multicomponent austenite.

CHAPTER II

LITERATURE REVIEW

2.1 INTRODUCTION

The objective of the present study is to make use of direct and indirect experiments, binary and higher order phase diagrams, structural information and solution thermodynamics to obtain the best possible $\gamma/\gamma+NbC_xN_y$ phase equilibria. This chapter comprehensively reviews the work reported in the literature related to the investigation. The review is divided into three main sections: the structure-phase relationships in the Nb-C, Nb-N and the Nb-C-N systems; the direct experimental determinations of the solubility products $K_C' = [\%Nb][\%C]^x$, $K_N' = [\%Nb][\%N]$ and $K_{CN}' = [\%Nb][\%C]^x[\%N]^y$; and, the thermochemical data required for the calculation of the standard free energies of formation, ΔG_f^o; of niobium carbide, NbC_x; of niobium nitride, NbN and the free energy of solution of niobium, carbon and nitrogen in austenite.

2.2 STRUCTURE-COMPOSITION RELATIONSHIPS IN THE Nb-C, Nb-N AND Nb-C-N SYSTEMS

2.2.1 The System Nb-C

The most recent and accurate of the phase diagrams of the Nb-C system given by Storms et al.[54] is presented in Fig. 2.1. The composition range of interest is 35 at %C - 50 at %C which is the range of nonstoichiometry of the carbide phase NbC_x. The structural type of this carbide is cubic B1 as shown in Fig. 2.2. This is the only carbide of niobium

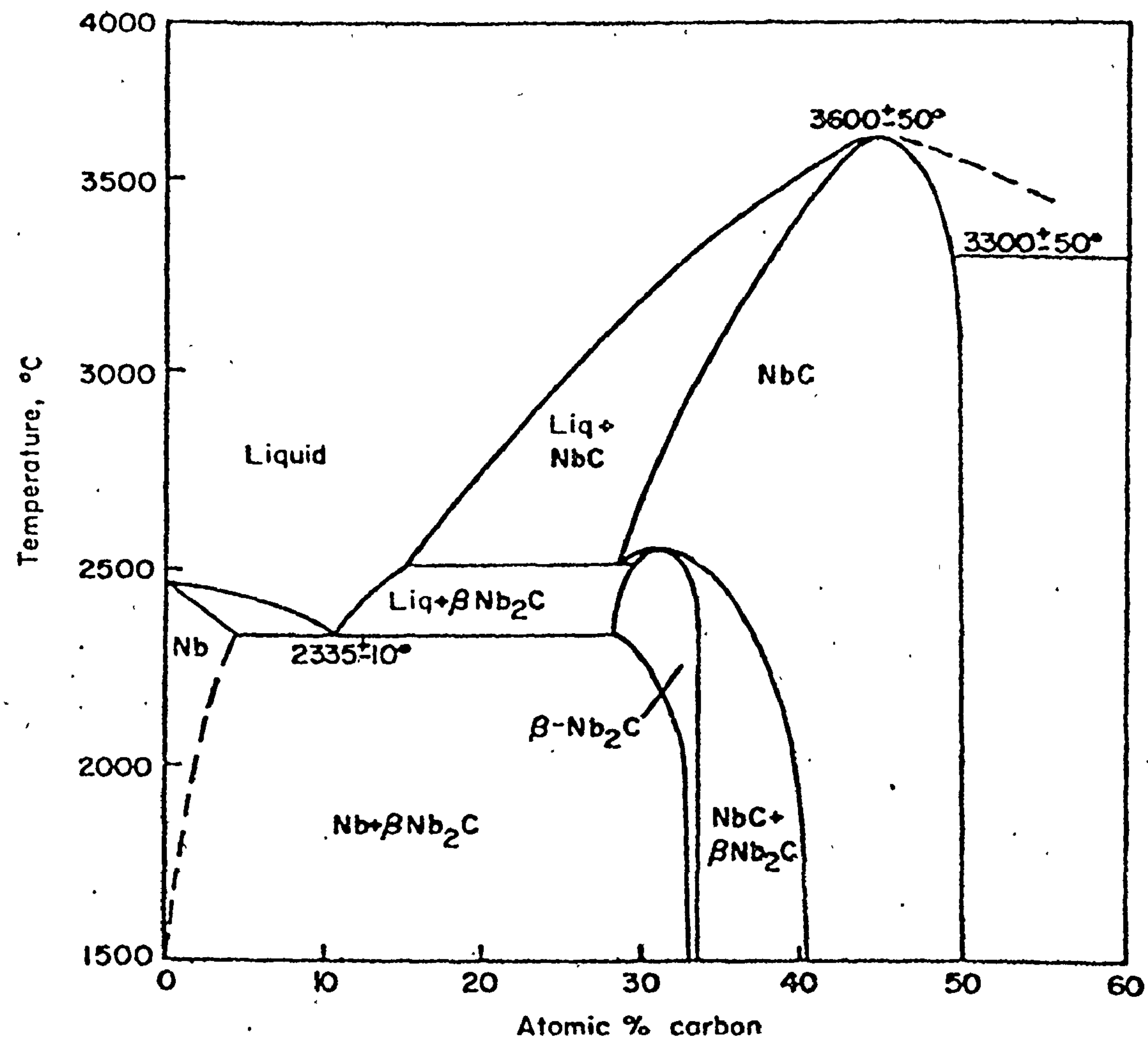

Figure 2.1 The niobium-carbon phase diagram (after Storms et al.[54])

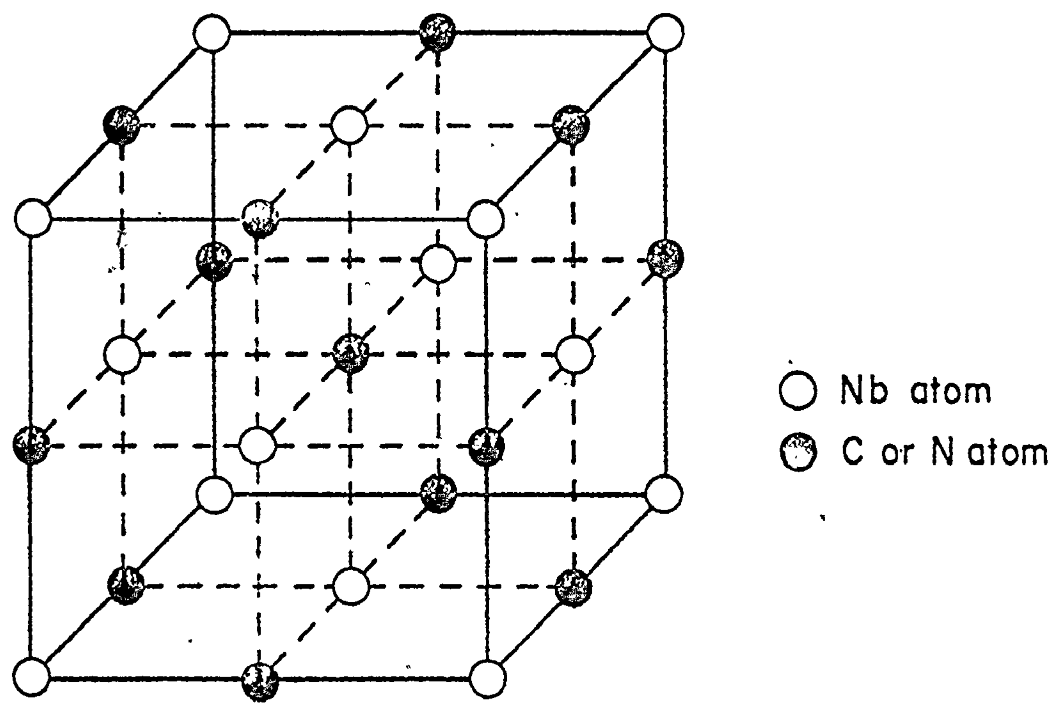

Figure 2.2 . Crystal structure of cubic carbides, nitrides and carbonitrides of niobium

that precipitates in steel. The features of the phase diagram at the lowest temperature indicated (1500°C) are retained to the even lower temperatures, which are of interest to this study and to the general precipitation reactions in steels. At room temperature, the range of homogeneity of the NbC_x phase has been shown[23,24] to be from x = 0.70 to 0.98. The strong covalent nature of this phase assures no change to this composition range for temperatures up to 1700°C.[44] The carbide $NbC_{0.98}$ which is in equilibrium with graphite in the pure Nb-C system suggests that the cubic carbide precipitated in a low carbon steel is bound to be even more defective. Accurate information on the lattice dimensions of the cubic carbide as a function of nonstoichiometry are available through a number of sources.[24-30] The relationship between the lattice parameter and nonstoichiometry that is widely used for identifying these compounds is shown in Figure 2.3. There is considerable uncertainty about the range of homogeneity of the hexagonal carbide at high temperatures. The upper limit has been well established as $NbC_{0.5}$ and there is some experimental information around 1000°C on the composition ranges of this phase.[44,46]

2.4.2 The System Nb-N

The most recently proposed Nb-N constitution diagram of Guard et al.[31] is shown in Fig. 2.4. The crystal structure types and lattice parameters are summarized in Table 2.5. The wide variety of crystal structures exhibited in the composition range 40-50 atomic % nitrogen suggests a possible complexity of the phases when precipitated in steels. However, pure niobium nitrides have been observed only in steels

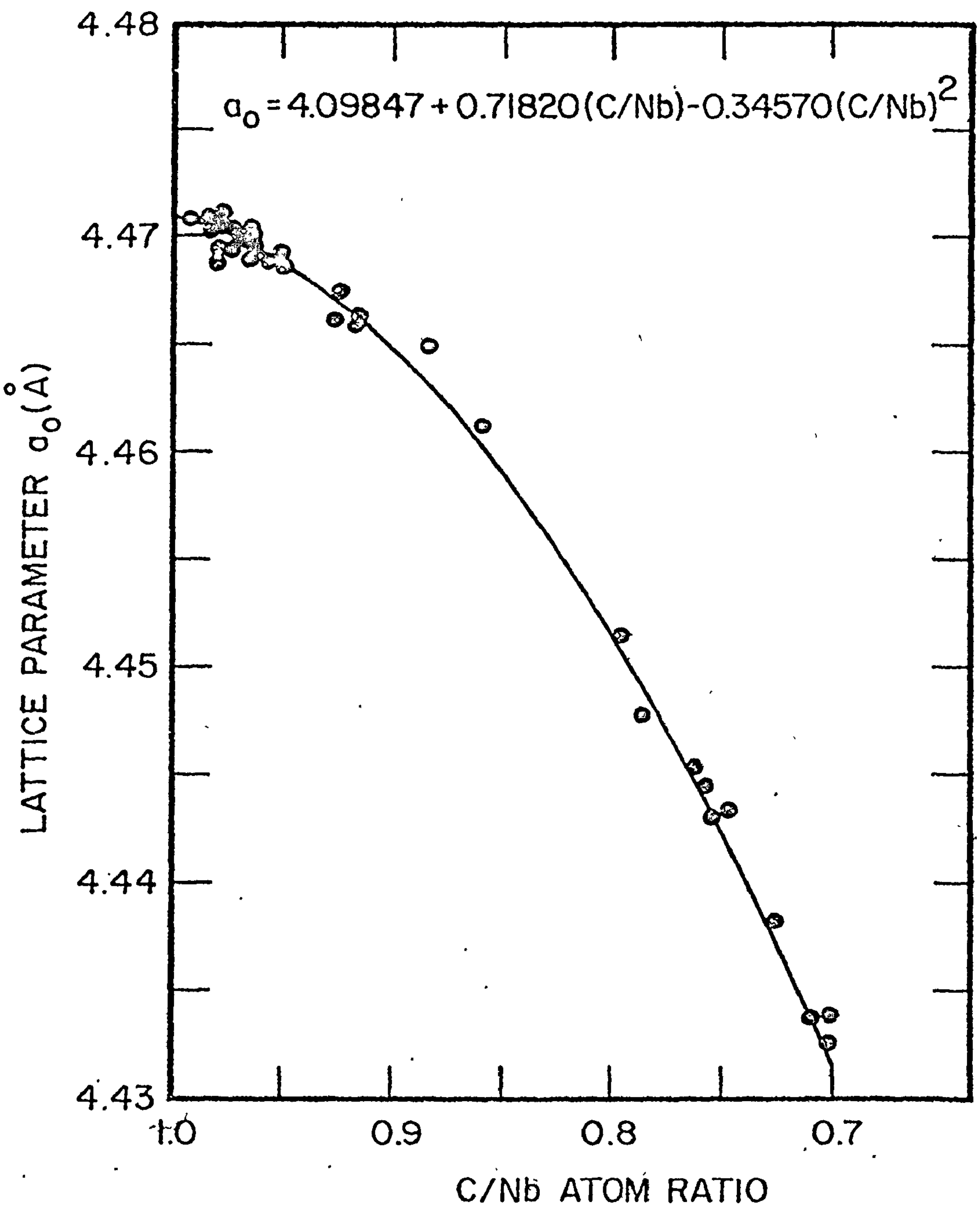

Figure 2.3 Relation between lattice parameter and nonstoichiometry for the cubic niobium carbide

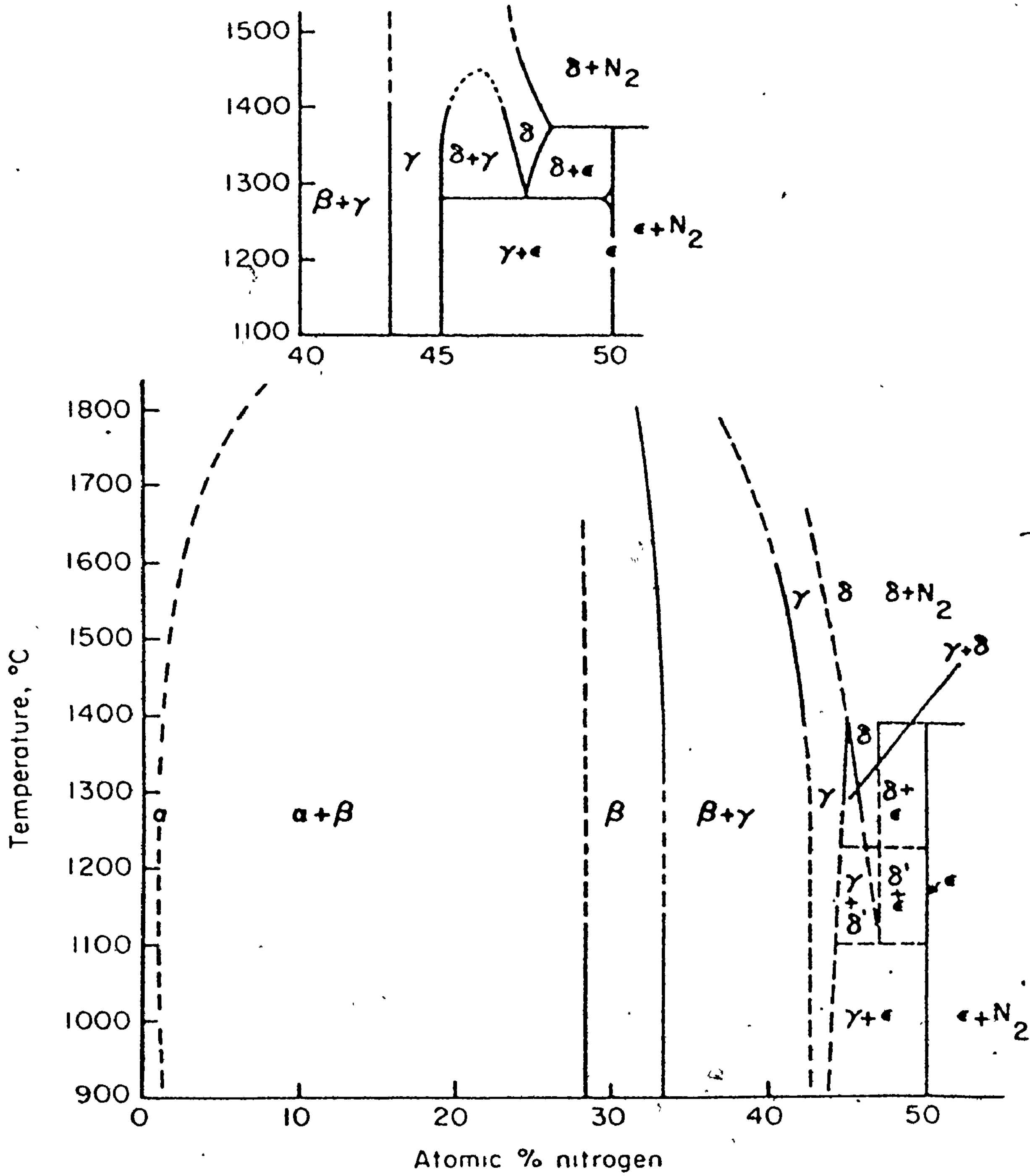

Figure 2.4 The Nb-N phase diagram earlier proposed by Brauer et al.[34] (shown below) and modified by Guard et al.[31] (shown above)

TABLE 2.5

Phases, their Crystal Structures and Lattice Parameters in the Nb-N System in the Temperature Range 1100-1450°C at 1 Atm. N_2 Pressure (after Guard et al.[31])

Phase	Crystal Structure	N/Nb Atom Ratio	Lattice Parameter Å a	c
α-solid solution	Basic niobium (BCC) with nitrogen contained interstitially	0.4		
β-NbN_x	Hexagonal	0.39-0.45	3.058	4.961
γ-NbN_x	Tetragonal	0.75-0.80	4.386	4.332
δ-NbN_x	Cubic B1	0.88-0.91	4.3885	---
ε-NbN_x	Hexagonal	0.92-1.00	2.958	11.272
δ'-NbN_x	Hexagonal (metastable transition phase)	0.96	2.94	5.46

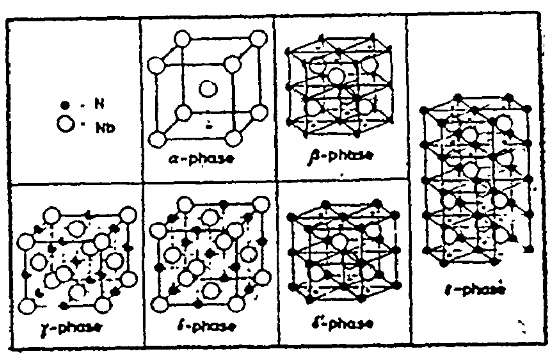

of extreme compositions ($C/N < 1$) and these nitrides have always been of the stoichiometric composition of ε-NbN or very close to stoichiometric ε-$NbN_{0.92-1.0}$. The other nitrides have never been observed in steels.

2.4.3 The System Nb-C-N

The normal carbon and nitrogen levels in steels are always associated with a cubic carbonitride, the structure type of which is shown in Fig. 2.2. Brauer and Lesser[26] have studied the Nb-C-N system most extensively and in particular, have estimated the wide ranges of stability of the cubic carbonitride phase. They have measured accurate lattice parameters for a variety of carbonitride compositions, NbC_xN_y, for x and y ranging from very small to very large values. Their work has been the only source of information available for identification of carbonitrides precipitated in steels. Fig. 2.6 shows a line drawing of a model constructed by plotting their data as the ratios C/Nb, N/Nb and vacancies/Nb on the ternary axes and the lattice parameter on the vertical axis. The lattice parameter curve for pure NbC_x is based on Fig. 2.2. The surface thus created shows that dissolved nitrogen causes a lowering of the lattice parameters of the particular carbide but in a manner dependent on the number of vacancies in the lattice, A small amount of nitrogen will cause a smaller decrease in the lattice parameter of $NbC_{0.9}$ than would be produced if it were dissolved in $NbC_{0.7}$, for example. Fig. 2.7 is another useful representation of the data of Brauer and Lesser.[26]

In addition, these figures make it clear that a study of lattice parameters in any binary system in which the starting materials have a range of nonstoichiometry is not unique unless the amount of vacancies

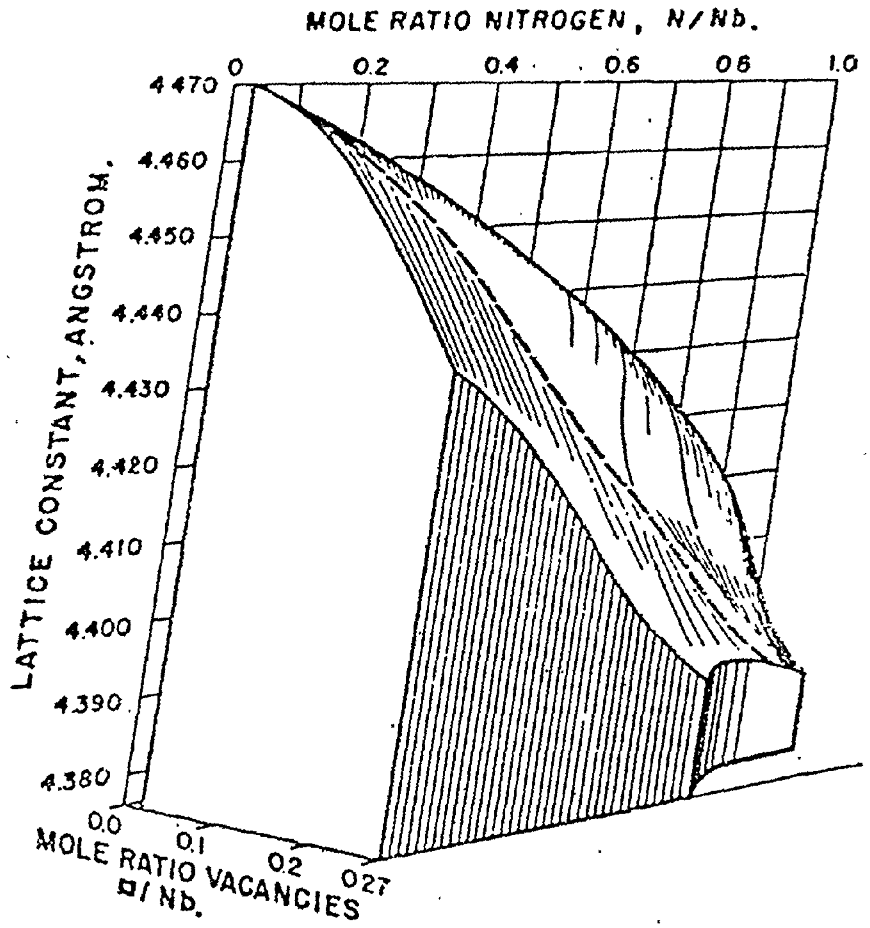

Figure 2.6 Lattice parameter vs composition in the system Nb-NbC-NbN

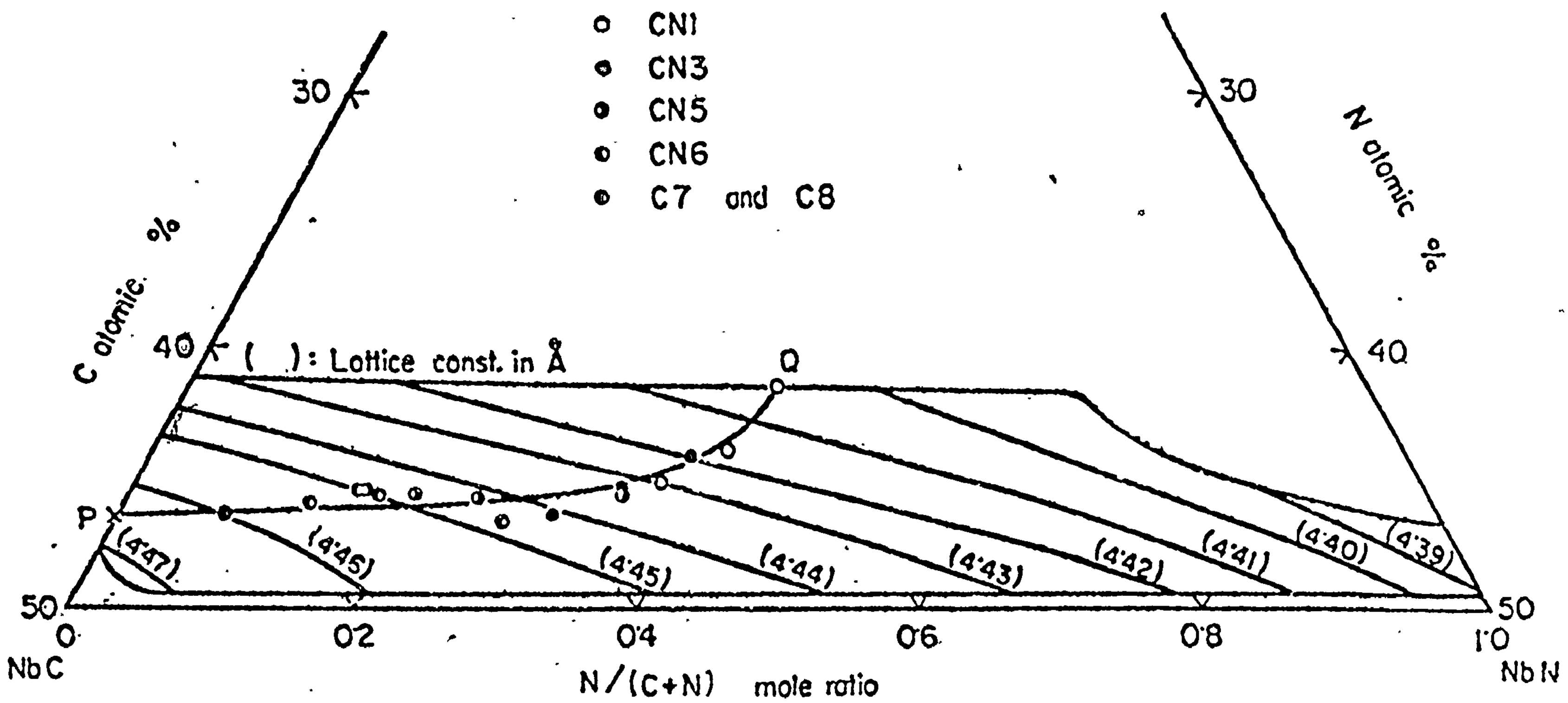

Figure 2.7 Representation of the lattice parameter-composition relationships in the Nb-NbC-NbN system

is specified. For example, Duwez and Odell[20] give the variation in a_o, the lattice parameter for the system NbC-NbN as well as other systems. Based on the lattice parameter given, their NbC was nearly stoichiometric (4.470 Å = $NbC_{0.99}$), but the NbN apparently contained a large number of vacancies (4.379 Å ≈ $NbN_{0.81}$). As a result their data shows a slight positive deviation from linearity and cuts across the surface as indicated by the solid line in Fig. 2.15. Had $NbC_{0.86}$ and $NbN_{0.86}$ been the starting compounds, a linear change in the lattice parameter would have been obtained. Furthermore, by choosing the appropriate starting materials any number of odd shaped curves can be produced. In a steel when a carbonitride precipitates, it is difficult to say what carbide and nitride would have mixed to yield that particular carbonitride. In a sense therefore, carbonitride compositions reported in the literature are not very accurate since the master interpolation curve used corresponds to the mixing of a particular carbide and nitride and the initial compounds that mixed to yield the carbonitride in the steel might not necessarily have been the same. Excepting for Mori et al.[7] this important fact was overlooked by workers reporting carbonitride composition in steels. Also prior knowledge of any impurities such as oxygen or sulphur is necessary while dealing with compounds of niobium. Appreciable quantities of these impurities will change the lattice parameter or make the compound appear richer in the metal.

2.3 DIRECT DETERMINATIONS OF THE "SOLUBILITY PRODUCT"

There have been many determinations of the solubility products $K_C' = [\%Nb][\%C]$, $K_N' = [\%Nb][\%N]$ and $K_{CN}' = [\%Nb][\%C]^x[\%N]^y$. The experimental procedures have been one of the following:

(i) Extraction of the carbides, nitrides or carbonitrides from steel specimens held at the desired temperature for long durations after prior solution treatment and chemical analysis of the extracts.

(ii) Equilibration of Fe-Nb alloys in CH_4/H_2 gas mixtures at fixed carbon potentials and examination of the phase fields metallographically to delineate the single and two phase regions.

(iii) Hardness measurements on quenched and tempered steels and analysis of the data using precipitation hardening models to estimate solubility limits.

2.3.1 Solubility of Niobium Carbide in Austenite

There have been a number of experiments in the Fe-Nb-C system to determine the solubility of niobium carbide. All experimentors to date have analysed their data on the basis of a solubility product

$$\log[\%Nb][\%C] = A - \frac{B}{T} \qquad 2.1$$

where A and B have been determined from the experimental results. The limited experimental accuracies did not permit inclusion of further terms.

The carbide equilibrium in austenite is strictly represented by

$$[Nb] + x[C] \rightleftharpoons NbC_x(s) \qquad 2.2$$

where [ ] signifies that the component is in solution in austenite, the concentration of the component is in atom fraction and the standard state referred to is at infinite dilution in austenite. Unfortunately, the value of x is not fixed in this system so a fixed stoichiometry for the carbide composition is an approximation at best. Such an approximation only helps to interpret measured solubility data and does not help to determine the actual tie lines.

The equilibrium constant for the carbide dissolution is given by

$$K_C = a_{Nb} \cdot a_C^x / a_{NbC_x} = \gamma_{Nb} \cdot \gamma_C^x [Nb][C]^x \qquad 2.3$$

where a_{NbC_x}, the Raoultian activity of the phase NbC_x, is assumed to be equal to unity; and γ_{Nb} and γ_C are the activity coefficients referred to the infinite dilution standard state.

There is considerable conflict as to the exact value of x to choose as an average representation of the carbide composition over a temperature range of investigation. Earlier experimentors assumed x = 1, i.e., perfect stoichiometry for the carbide and also assumed the activity coefficients γ_{Nb} and γ_C to be unity. With these assumptions, they interpreted their experimental data in the form of a solubility product given by Eq. 2.1. The details of the previous experiments and their results are summarized in Tables 2.8 and 2.9.

Nordberg and Aronsson,[6] who reviewed most of the above data, found that the experimental solubility products lacked good agreement for the precipitate composition NbC and that the agreement was better if the carbide was assumed to be $NbC_{0.87}$. Reinterpreting all the earlier direct experimental results, they gave the solubility product relations for the carbide $NbC_{0.87}$ as

$$\log[\%Nb][\%C]^{0.87} = 3.11 - \frac{7520}{T} \pm 0.1 \qquad 2.4$$

TABLE 2.8

Details of Previous Experiments

Type of steel	Composition (wt.-%)				Method	Type of Precipitate Assumed	Reference
	C	N	Nb	Mn			
Commercial	0.11	---	0.036	1.0	A	NbC	8
Laboratory	0.08	---	0.031	1.1-1.8	A	NbC	6
Laboratory	0.3	---	0.5	0.2-3.9	B	NbC	10
Commercial	0.17	0.010	0.023	1.4	B	NbC	11
	0.04	0.009	0.019	2.2	B	NbC	11
Laboratory		---	0-0.8	0.0	C	NbC	12
Laboratory		0.001	0.190	0.0	C	NbC	13
Laboratory	0.21	0.0036	0-0.11	1.2	B	NbC	9
Laboratory	0.03-0.10	0.002-0.02	0.2-0.9	0.0	B	$NbC_{0.87}$	7
Laboratory			0-0.5	0.0	C	NbC	16
Laboratory				0.0	C	NbC	15

The methods used are as follows:
A Hardness measurement after quenching and tempering;
B Isolation of precipitate and chemical analysis; and,
C Equilibration using H_2/CH_4 gas mixtures.

TABLE 2.9

Previous Results for the Solubility of Niobium Carbide in Austenite

Author	Reference	Austenitization temperature, °C	Solubility product Log K_C'	K_C'
de Kazinczy et al.	8	900-1200	-0.63-2500/T	%Nb %C
			2.90-7500/T*	%Nb %C
Nilsson	6	1115-1085	-2.61,-2.84	%Nb %C
Wilson and Gieselman	10	1204	-1.97,-2.14,-2.37	%Nb %C
Reistad and Sehlstedt	11	880,900,1000	-3.38,-3.38,-2.93	%Nb %C
Smith	12	1000-1300	3.7-9100/T	%Nb %C
Johansen et al.	13	950-1050	4.37-9290/T	%Nb %C
Mori et al.	7	1000-1300	3.18-7700/T	%Nb $\%C^{0.87}$
Meyer	9	900-1300	3.04-7290/T	%Nb %C
Koyama et al.	16	1050-1150	3.31-7970/T	%Nb %C
Narita and Koyama	15	1050-1300	3.42-7900/T	%Nb %C

* Recalculated under the assumption that the hardness is proportional to the average distance between the coherent NbC particles.

A theoretical calculation using thermochemical data was also made by the authors and the calculated solubility product was

$$\log[\%Nb][\%C]^{0.87} = 3.4 \pm 0.4 - \frac{7200 \pm 350}{T} \qquad 2.5$$

Thus the existing assumed values for average carbide composition range from 0.87 to 1.0. The important limitation of assuming a fixed stoichiometry (or nonstoichiometry) is that the measured solubilities cannot include tie line determinations.

To characterize the $\gamma/\gamma+NbC_x$ equilibrium better and improve upon the earlier solubility data, a rigorous thermodynamic analysis and detailed direct experiments (to be discussed in a later chapter) have been made in the present study.

2.3.2 Solubility of ε-NbN in Austenite

Extensive studies have been made by Mori et al.[18,7] to identify compounds precipitated in the Fe-Nb-N system. Their results, summarized in Table 2.10, clearly demonstrate two facts. The compound precipitated in the pure Fe-Nb-N system is always of the hexagonal type ε or δ'. While the ε phase is a pure stoichiometric niobium nitride, the δ' phase was identified by these authors as a carbonitride with substantial amounts of nitrogen. Smith[17] and Narita and Koyama[15] who have also identified niobium nitrides precipitated in steels, found them to be ε-NbN. On the other hand, this nitride was found to be present only in steels with an extremely low carbon and high nitrogen (C/N < 1) and these compositions are nowhere near the commercial steel compositions normally encountered.

From the point of view of the present investigation, interest in a study of the literature data on the hexagonal niobium nitride is mainly

TABLE 2.10

Chemical Composition of Samples

Sample No.	Concentration (%)					Reference	C/N
	Nb	C	N	S	O		
C13	0.317	0.108	0.001	0.010	0.0010	Mori[18]	126
CN34	0.329	0.074	0.036	0.010	0.0006	Mori[18]	2.4
CN23	0.262	0.010	0.027	0.010	0.0019	Mori[18]	0.5
N7	0.159	0.008	0.022	0.011	0.0015	Mori[18]	0.4
N8	0.202	0.008	0.020	0.010	0.0020	Mori[7,18]	0.5
NA	0.094	0.004	0.017	0.007	0.0047	Mori[7]	0.3

TABLE 2.11

Phases Identified and Their Lattice Constants

Sample No.	Heat treatment	Phase	Lattice Constant a(Å)	Lattice Constant c(Å)
C13	As cast	δ NbC$_x$	4.460	---
	800°C		4.460	---
	1200°C		4.453	---
CN34	As cast	δ NbCN	4.420	---
	800°C		4.415	---
	1200°C		4.428	---
CN23	As cast	δ	4.390	---
		δ'	2.98	5.53
	800°C	δ'	2.98	5.58
	1200°C		2.97	5.57
N7	1000°C	ε	2.96	11.30
		(δ')	2.96	5.61
	1250°C	ε	2.99	11.25
N8	1000°C	δ'	2.97	5.53
		(ε)	2.95	11.50
	1250°C	ε	2.78	11.28
		(δ')	2.96	5.58
NA	1000°C - 1300°C	ε	2.78	11.28

of an academic nature. The data surveyed here, however, help to strengthen the assumptions to be made later on while treating carbonitrides precipitated in steels and to revise certain assumptions of earlier workers.

A summary of the existing direct determinations of ε-NbN solubility is presented in Tables 2.12 and 2.13.

2.3.3 Direct Determinations of Carbonitride Solubilities in the Fe-Nb-C-N System

Irvine, Pickering and Gladman[19] determined the solubility relationships for a number of laboratory melted steels using chemical analysis techniques for soluble and insoluble niobium, carbon and nitrogen. They found that there was no marked tendency for niobium to form a separate nitride phase. Since empirically the ratio of nitrogen to carbon is similar for both austenite and niobium carbonitride; and it is known that niobium carbide and niobium nitride are mutually soluble;[20] these authors considered the nitrogen content in terms of an equivalent carbon content; i.e.: carbon equivalent = C + (12/14)N and the solubility product of Nb(C,N) determined over the temperature range of 900°C to 1200°C was given as

$$\log[\%Nb][\%C + 12/14\ \%N] = 2.26 - \frac{6770}{T} \qquad 2.6$$

Their results are shown in Fig. 2.14.

Mandry and Dornelas[21] identified electrolytically extracted carbonitride residues from a single laboratory melted steel heat treated at different temperatures over the range 950°C to 1250°C. The precipitated carbonitride, $NbC_{0.83}N_{0.14}$ remained constant in composition over the range

TABLE 2.12

Details of Previous Experiments

Type of Steel	Composition C	N	Nb	Mn	Method	Precipitate Observed	Reference
Laboratory	---	---	0-0.8	0.0	C	ε-$NbN_{0.9-1.0}$ ε-$NbN_{0.9-1.0}$	17
Laboratory	0.004-0.008	0.017-0.022	0.04-0.2	0.0	B	ε-$NbN_{0.9-1.0}$	15
Laboratory	---	---	---	---	C	ε-$NbN_{0.9-1.0}$	7

TABLE 2.13

Previous Results for the Solubility of ε-NbN in Austenite

Author	Reference	Austenitization Temperature, °C	Solubility Product Log K'_N	K'_N
Smith	17	1191-1336	4.04-10230/T	%Nb %N
Narita and Koyama	15	1100-1300	2.89-8500/T	%Nb %N
Mori et al.	7	1000-1300	3.79-10150/T	%Nb %N

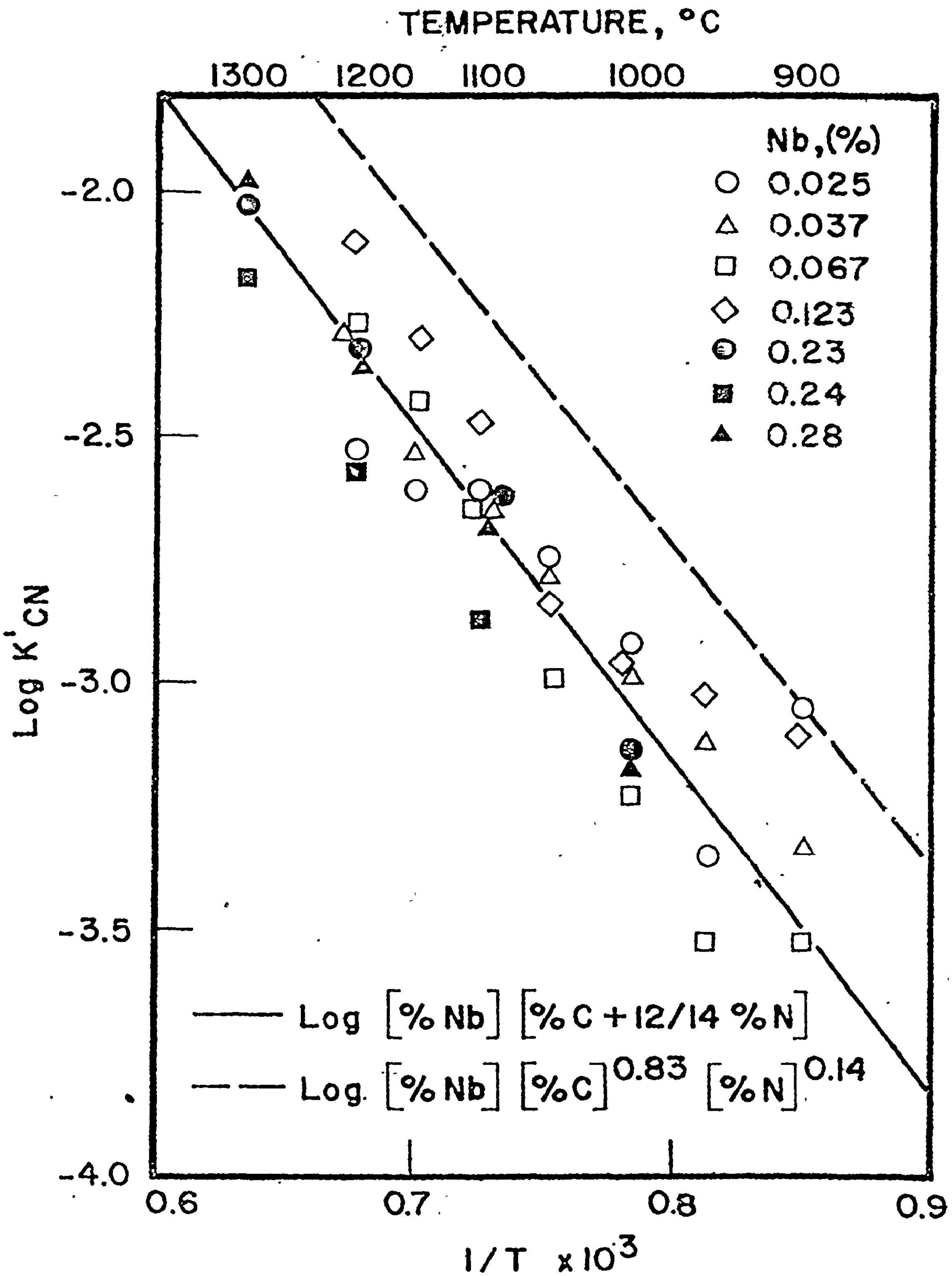

Figure 2.14 Carbonitride solubility product relationships given by Irvine et al.[19] (solid line) and Mandry and Dornelas[21] (dotted line)

of temperatures studied. Their experimental solubility product was

$$\log[\%Nb][\%C]^{0.83}[\%N]^{0.14} = 4.46 - \frac{9800}{T} \qquad 2.7$$

and is shown in Fig. 2.14. Their experimental results along with other reported determinations are shown in Table 2.15.

Mori et al.[18,22,7] carried out the most detailed solubility determinations and precipitate identifications by extracting carbonitrides from very pure laboratory melted steels using chemical dissolution methods. Their steel compositions are shown in Table 2.16 and results are shown in Table 2.17. It can be seen that the carbonitrides are nonstoichiometric and the degree of nonstoichiometry is greater at higher temperatures. The proportion of nitrogen in the precipitate is more at higher temperatures. It can also be seen that at very low N/C mole ratios in the steels, a carbonitride of fixed composition was observed.

2.4 THERMOCHEMICAL DATA

In principle, if complete thermochemical data were available it would be possible to calculate via solution thermodynamics the complete austenite-niobium carbide equilibrium including solubilities and tie lines. As it turns out, the data available is quite comprehensive and is able to reproduce the solubility products to good accuracy and furthermore, yield good estimates of carbide compositions (i.e., the tie lines or varying degrees of nonstoichiometry). In view of the experimental difficulty of establishing the tie lines (i.e., the changes in stoichiometry) the finally recommended phase diagrams must be based on a self-consistent calculation involving direct solubility measurements and indirect prediction of tie lines.

TABLE 2.15

Experimental Results Reported in the Literature for the Solubility of Niobium Carbonitride in Austenite

Author	Ref.	Temp. °C	Steel Composition, Wt%									x*	y*	w^*_{Nb}
			Nb	C	N	S	O	Mn	Si	Al	P			
Meyer	9	900	0.035	0.220	0.0050	---	---	---	---	---	---	0.90	0.10	0.030
		900	0.110	0.200	0.0039	0.020	0.0020	1.21	0.08	< 0.007	< 0.009	---	---	0.010
		900	0.038	0.036	0.0073	0.014	0.0050	0.31	0.03	< 0.001	< 0.007	---	---	0.030
		900	0.105	0.025	0.0065	0.013	0.0050	0.31	0.03	< 0.001	< 0.007	0.65	0.35	0.090
		1000	0.105	0.025	0.0065	0.013	0.0050	0.31	0.03	< 0.001	< 0.007	0.61	0.39	---
Mandry & Dornelas	21	950												0.061
		1050												0.054
			0.065	0.180	0.0036	0.010	0.0180	0.65	0.01	---	< 0.025	0.83	0.14	
		1100												0.045
		1150												0.031
Mori	18	1200	0.329	0.074	0.0360	0.010	0.006	---	---	---	---	0.2-0.3	0.7-0.8	0.220
Mori	22	1000	0.094	0.004	0.017	0.007	0.0047	---	0.05	< 0.001	< 0.010	0.08	0.88	0.075

* x,y atomic proportion of interstitial in the carbonitride NbC_xN_y

w_{Nb} Niobium present as carbonitride, Wt%.

TABLE 2.16

Compositions of steels used in the work of Mori *et al.*[7] for the determination of the solubility and compositions of niobium carbonitrides in austenite

Steel	Composition, wt.-%				
No.	Nb	C	N	S	O
C7	0.531	0.081	0.002	0.009	0.0010
C8	0.817	0.090	0.002	0.010	0.0013
CN1	0.197	0.029	0.012	∿ 0.01	0.0033
CN3	0.207	0.101	0.016	∿ 0.01	0.0021
CN5	0.641	0.081	0.017	∿ 0.01	0.0018
CN6	0.957	0.102	0.018	∿ 0.01	0.0024

Other impurities Si ∿ 0.05; P < 0.01

Ni ∿ 0.02; Cr < 0.004; total Ti ∿ 0.005

V ∿ 0.002 and total Al ∿ 0.001, all wt-%

TABLE 2.17

The Experimental Results of Mori et al.[7]

Steel No.	Holding Temperature °C	Composition of the Carbonitride	Niobium, wt.% present as Carbonitride
C7	1000	$NbC_{0.8}N_{0.7}$	0.512
	1100		0.444
	1200		0.381
	1300		0.230
C8	1000	$NbC_{0.8}N_{0.07}$	0.777
	1100		0.729
	1200		0.619
	1300		0.438
CN1	1000	$NbC_{0.49}N_{0.34}$	0.177
	1100	$NbC_{0.42}N_{0.36}$	0.151
	1200	$NbC_{0.34}N_{0.36}$	0.102
CN3	1000	$NbC_{0.57}N_{0.28}$	0.203
	1100	$NbC_{0.51}N_{0.32}$	0.183
	1200	$NbC_{0.45}N_{0.34}$	0.117
CN5	1000	$NbC_{0.69}N_{0.15}$	0.625
	1100	$NbC_{0.65}N_{0.18}$	0.546
	1200	$NbC_{0.60}N_{0.23}$	0.442
	1300	$NbC_{0.52}N_{0.32}$	0.320
CN6	1000	$NbC_{0.73}N_{0.12}$	0.925
	1100	$NbC_{0.70}N_{0.14}$	0.851
	1200	$NbC_{0.68}N_{0.16}$	0.757
	1300	$NbC_{0.61}N_{0.25}$	0.544

Referring then to the schematic Fe-Nb-C free energy-composition diagram (Fig. 2.18) for the austenite-carbide (NbC_x) equilibrium, the problem of prediction reduces to the evaluation of the two integral free energy of mixing surfaces. These can be obtained directly from activity measurements or from the reference standard heat of formation, ΔH°_{298}, of the carbide NbC_x as a function of nonstoichiometry via a Third Law analysis. Unfortunately, the available activity measurements were obtained at temperatures well above those of interest here. Consequently, the use of a Third Law analysis is unavoidable.

This section accordingly reviews the two sets of thermochemical data required for calculating the $\gamma/\gamma+NbC_x$ equilibrium, viz., the standard free energy of formation (or mixing) of the carbide NbC_x as a function of nonstoichiometry and the free energy of mixing of niobium and carbon in iron.

The standard free energy change for any reaction or transformation, ΔG°_T, at any temperature T can be obtained from the equation

$$\Delta G^\circ_T = \Delta H^\circ_T - T\Delta S^\circ_T \qquad 2.8$$

where ΔH°_T and ΔS°_T are the standard enthalpy and entropy changes for the reaction at the same temperature. The standard heat of formation, ΔH°_T, at the temperature T can be calculated from

$$\Delta H^\circ_T = \Delta H^\circ_{ref,f} + \int_{ref}^{T} \Delta C_p dT \qquad 2.9$$

where $\Delta H^\circ_{ref,f}$ is the standard heat of formation at any reference temperature, usually 298°K, and ΔC_p is the difference between the heat capacities of the products and the reactants. Thus if $\Delta H^\circ_{ref,f}$ and the heat capacities

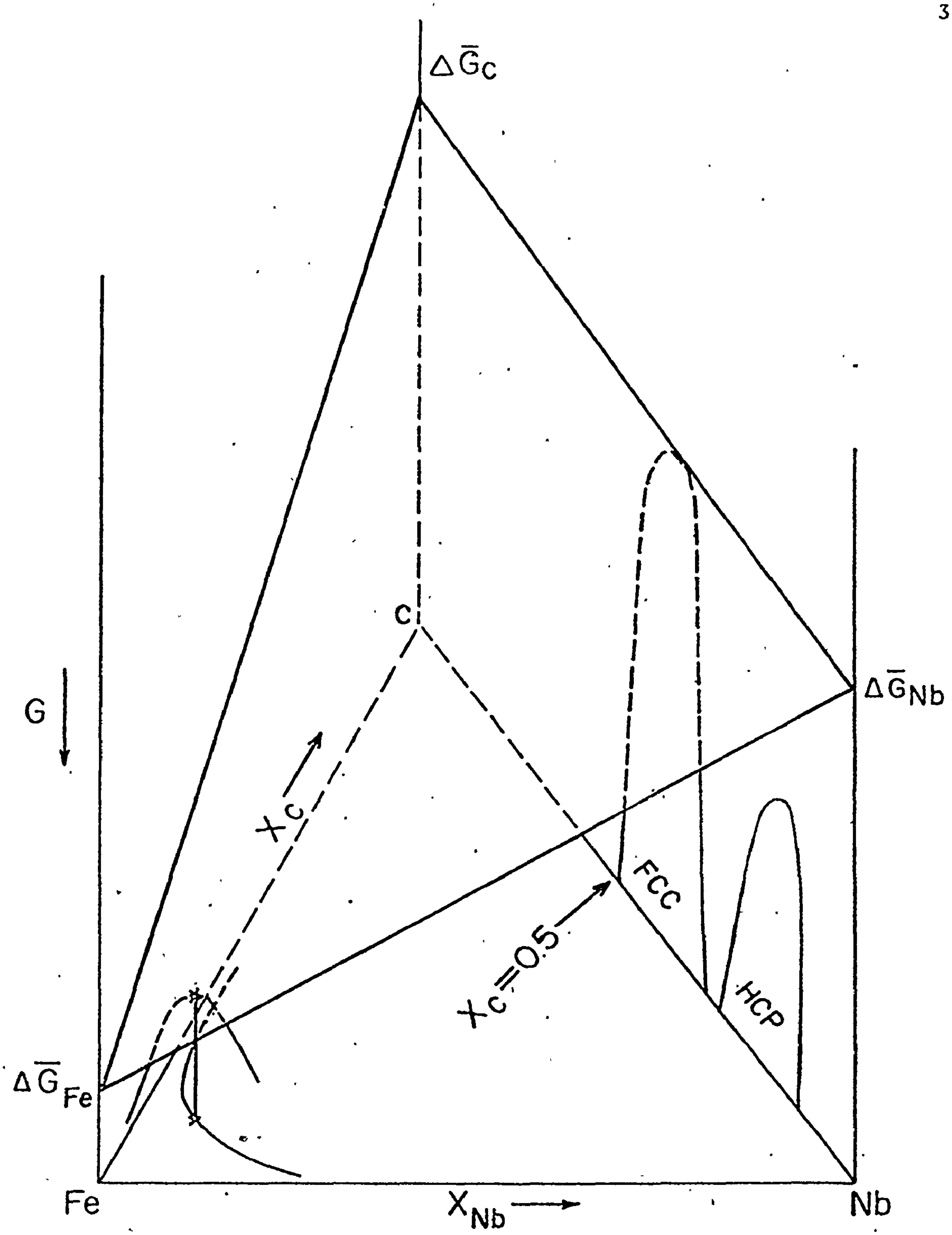

Figure 2.18 Free energy-composition relationships (schematic) in the Fe-Nb-C system

of reactants and products are known over the whole temperature range, ΔH_T° can be calculated at any temperature T in that range. If a phase change of any component occurs in the temperature range, the heat of transformation must be included in equation (2.9) and any change in C_p value must be incorporated in ΔC_p.

The entropy change for a reaction, ΔS_T°, can be calculated from the entropies of the components at the reaction temperature. Standard entropy of any substance, S_o^T, can be calculated from the equation

$$S_T^\circ = \int_o^T \frac{C_p}{T}\, dT \qquad 2.10$$

Thus, calculations of $\Delta G_{T,f}^\circ$ require the experimental determination of the following thermochemical quantities:

(1) the standard heat of formation, $\Delta H_{ref,f}^\circ$, at any reference temperature, usually 298°K;

(2) the heat of transformation of the components in the relevant temperature range; and,

(3) the heat capacity of the components from °K to the required temperature.

If we consider the reaction

$$Nb + x \cdot B = NbB_x$$

where B is carbon or nitrogen, the standard free energy change, $\Delta G_{T,f}^\circ$ for the above reaction will be given for each x by

$$\Delta G_{T,f}^\circ = \Delta H_{298}^\circ + T\Delta gef_T \qquad 2.11$$

where

ΔH°_{298} = standard reference heat of formation of the compound NbB_x

$$\Delta gef_T = gef_T(NbB_x) - gef_T(Nb) - x \cdot gef_T(B) \qquad 2.12$$

and gef_T is the Gibbs energy function, given by

$$gef_T = -S^\circ_T + \frac{H^\circ_T - H^\circ_{298}}{T} \qquad 2.13$$

or

$$gef_T = (G^\circ_T - H^\circ_{298})/T \qquad 2.14$$

Normally, thermodynamic data compilations, list S°_T, $\frac{H^\circ_T - H^\circ_{298}}{T}$ and gef_T for all the elements and compounds. The gef_T value derived from the first two functions is a more convenient form of the data from the viewpoint of the user. Fortunately, for present purposes, NbC_x is one of the few compounds for which data are available for a range of values of x.[55-62,44]

2.4.1 The Standard Heats of Formation, ΔH°_{298}, of Niobium Carbide as a Function of Nonstoichiometry

The various heat of formation measurements[48-53] are compared in Fig. 2.19. A critical review of these measurements has been made by Storms.[44] The combustion calorimetric data of Huber et al.[48] has been assessed as the best of the reported calorimetric measurements. These workers have given proper weights to each one of their measurements across the composition range and fit their data by the equation

$$\Delta H^\circ_f(298) = 6.60 - 70.95(C/Nb) + 30.75(C/Nb)^2 \qquad 2.15$$

which is shown as the solid curve in the figure. The additional data shown agree reasonably well with the curve.

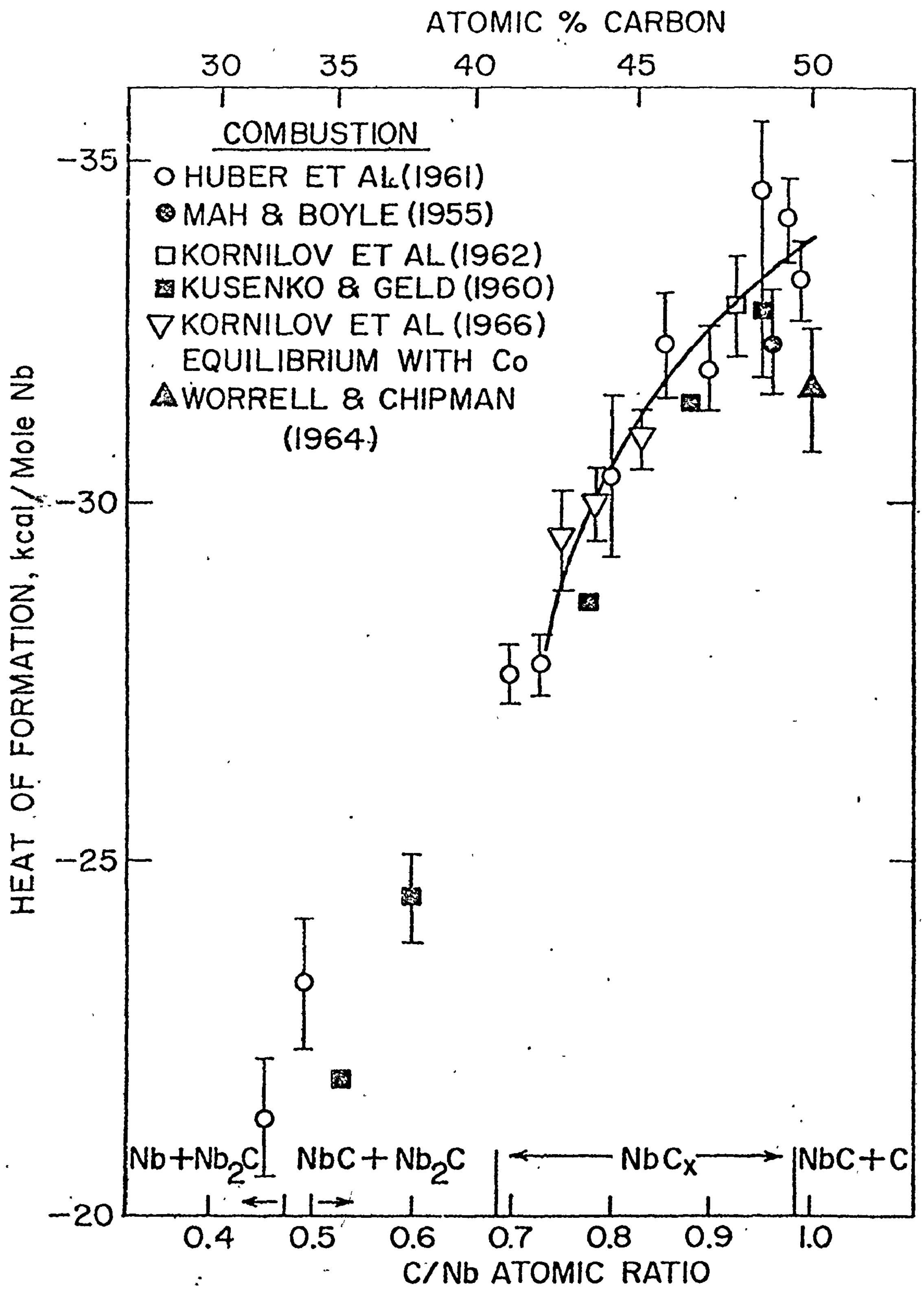

Figure 2.19 Reference heat of formation, ΔH°(298), of niobium carbide.

Storms et al.[54] have recently measured the vapour pressure of Nb in the cubic monocarbide as a function of composition and temperature using Knudson effusion in a mass spectrometer. Their measured Nb activities at the upper and lower limit of their experimental temperature range, i.e., 2300°K and 2500°K are shown in Fig. 2.20. The C activities were derived from the Nb activities by Gibbs-Duhem integration. These data are inadequate for direct evaluation of the free energy of mixing of the carbide NbC_x as a function of x, in the temperature ranges of interest in this study. However, the high temperature data serve through a Third Law analysis as a check on the combustion calorimetric data of Huber et al.[48] The details of the Third Law analysis are given in the next chapter.

2.4.2 Heat Capacities of Niobium Carbides, Niobium and Carbon

Niobium Carbides:

Among the refractory compounds, reliable high temperature heat capacity data as a function of composition exist only for the defect carbides of niobium. These data have been adequately reviewed by a number of workers.[44,45,62,63] Extensive high temperature heat capacity measurements have been reported for four carbides, $NbC_{0.5}$, $NbC_{0.75}$, $NbC_{0.87}$ and $NbC_{0.98}$. Sandenaw and Storms[60,61] have measured the low temperature heat capacities of the defect carbides between 7.5° and 320°K. The best compilations of the specific heat, heat capacity and entropy values over a wide temperature range of 0°K to 3000°K, have been made by Storms et al.[44,45] The following relative enthalpy values reported in their work have been used in the present study.

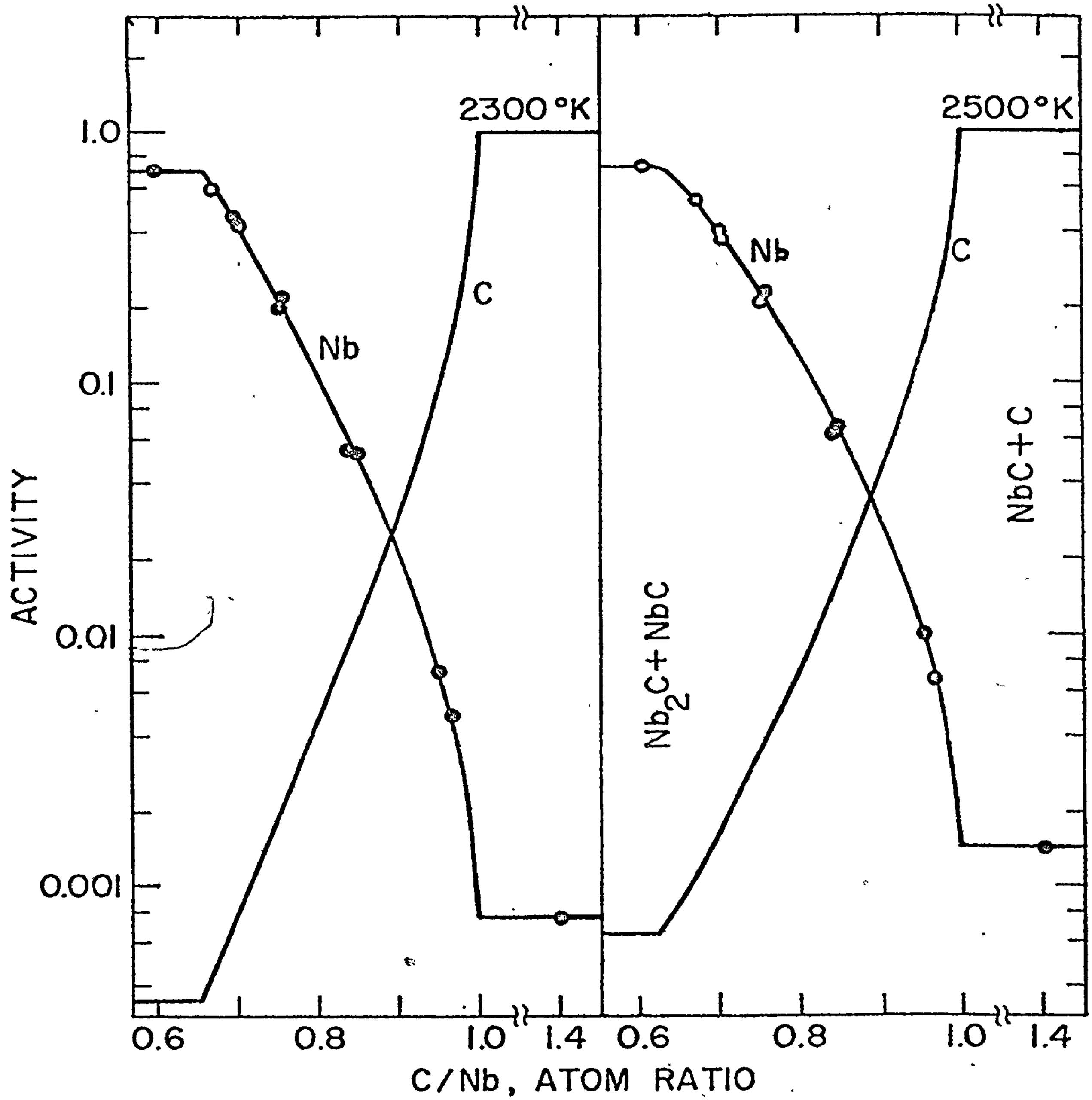

Figure 2.20 High temperature activity data of Storms *et al.*[54] for niobium carbide

$NbC_{0.5}$

$$H^\circ_T - H^\circ_{298} = -2.1417 \times 10^3 + 6.7057\ T + 1.5942 \times 10^{-3}\ T^2 - 1.8076 \times 10^{-7}\ T^3 + 1.6148 \times 10^3/T \text{ (cal/mole, 298-1800°K, } \pm 0.4\%)$$

$NbC_{0.75}$

$$H^\circ_T - H^\circ_{298} = -3.2096 \times 10^3 + 8.8844\ T + 1.2409 \times 10^{-3}\ T^{-2} - 3.8370 \times 10^{-8}\ T^3 + 1.3460 \times 10^5/T \text{ (cal/mole, 298-1800°K, } \pm 0.2\%)$$

$NbC_{0.87}$

$$H^\circ_T - H^\circ_{298} = -3.5738 \times 10^3 + 9.8318\ T + 9.2474 \times 10^{-4}\ T^2 + 1.6788 \times 10^{-8}\ T^3 + 1.6691 \times 10^5/T \text{ (cal/mole, 298-1800°K, } \pm 0.2\%)$$

and $NbC_{0.98}$

$$H^\circ_T - H^\circ_{298} = -4.0918 \times 10^3 + 10.8561\ T + 9.1724 \times 10^{-4}\ T^2 - 5.2003 \times 10^{-8}\ T^3 + 2.3105 \times 10^5/T \text{ (cal/mole, 298-3000°K, } \pm 0.3\%)$$

The Gibbs energy function at each temperature is related to the heat capacities as follows:

$$gef_T = -S^\circ_T + \frac{H^\circ_T - H^\circ_{298}}{T}$$

As discussed earlier, specific heats have been measured only for three carbide compositions $NbC_{0.75}$, $NbC_{0.87}$ and $NbC_{0.98}$. The Gibbs energy function, the enthalpy and vibrational entropy data have therefore been tabulated only for these three carbides. In Figs. 2.21 and 2.22, these thermal functions have been plotted against the C/Nb atom ratio, of each of the defect carbides NbC_x. The temperatures in these figures correspond to the limits of the range of temperatures of interest to this study. All three thermal functions, the enthalpy, the vibra-

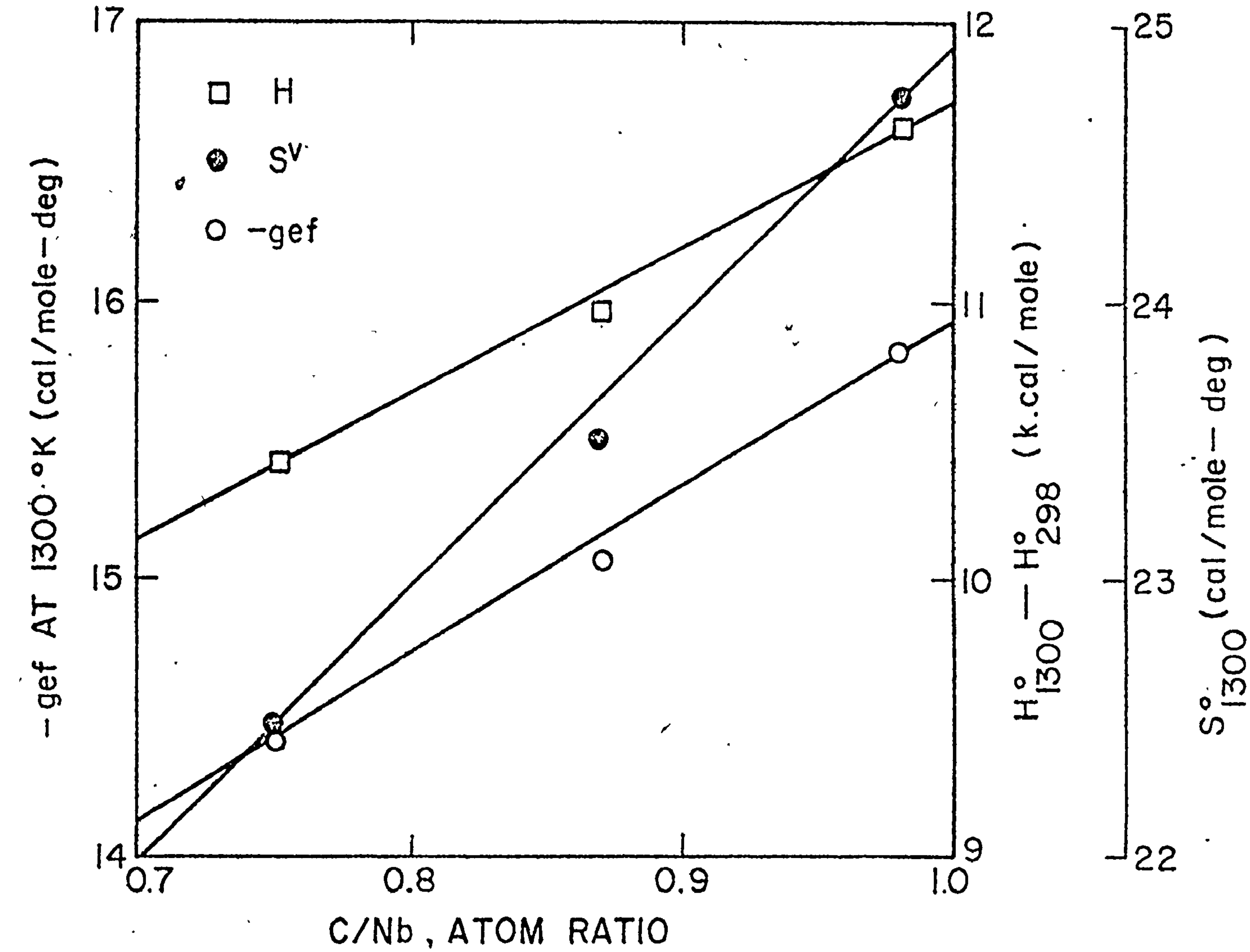

Figure 2.21 Thermal functions of NbC_x as a function of x at 1300°K

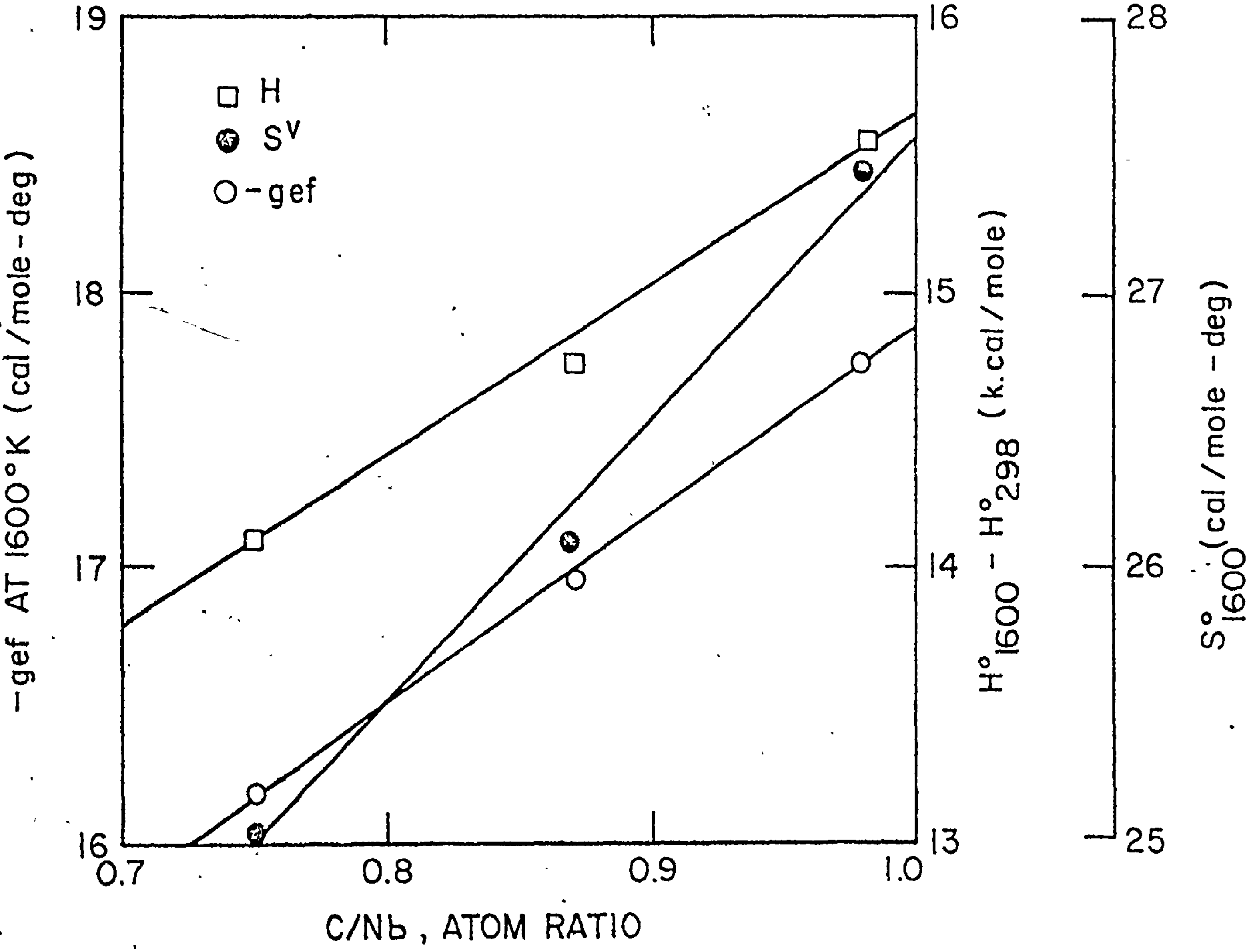

Figure 2.22 Thermal functions of NbC_x as a function of x at 1600°K

tional entropy and the Gibbs energy function exhibit good linear relationships across the composition range of interest, ($x = 0.70$ to $x = 0.98$) at both these temperatures and at the intermediate temperatures (not shown). The thermal functions of all the carbide compositions over the indicated range of composition and temperature can therefore be safely extrapolated from the fortuitous straight line relationships.

Besides the standard reference heat of formation and the aforementioned thermal functions, both of which are now known as a function of composition, there is a configurational entropy contribution to the free energy of formation of each carbide to be taken into account. This arises as a result of the mixing of the carbon atoms and the vacancies in the carbon sublattice. This is also referred to as the randomization entropy and it varies across the composition range. For each nonstoichiometric carbide NbC_x, the configurational entropy S^c, is given by[112]

$$S^c = -R(x \ln x + (1-x)\ln(1-x))$$

The calculated S^c values for the composition range of interest ($x = 0.70$ to 0.98) are shown in Fig. 2.23. At any temperature T, the additional free energy change for each carbide composition NbC_x would then be $-S^c \cdot T$. While using the above relationship, it is assumed that there is random mixing of the carbon atoms and the vacancies; thus no ordering.

<u>Niobium</u>:

A large number of heat capacity measurements[64-70,55] have been reported in the literature. Storms et al.[44,45] have critically reviewed all the above data, re-examined them and found that the specific heat measurements compared very well. They have tabulated more accurate thermal

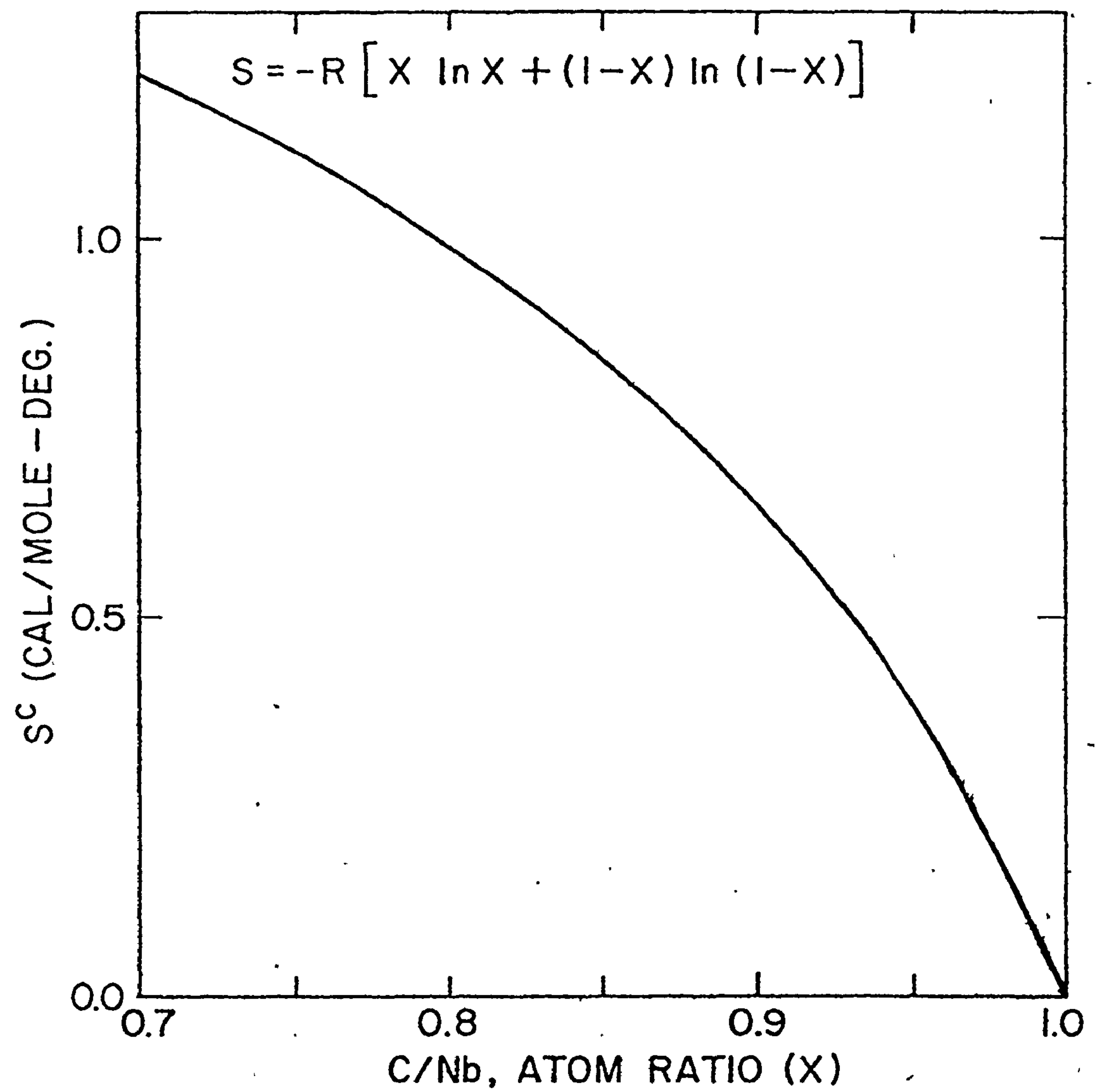

Figure 2.23 Configurational entropy for niobium carbide

functions of Nb and their data has been used in the present study. The relative enthalpy value which they report for niobium is:

$$H_T^\circ - H_{298}^\circ = -2.1963 \times 10^3 + 6.7326\ T - 3.7989 \times 10^{-4}\ T^2 + 2.5601 \times 10^{-7}\ T^3 + 4.6391 \times 10^4/T \quad (298°\text{-}2740°K,\ \text{cal/mole},\ \pm\ 1.0\%)$$

The Gibbs energy function, gef_T, $-(G_T^\circ - H_{298}^\circ)/T$ is also tabulated by these authors at each temperature.

Carbon:

Very good compilations of the thermal functions of carbon[71,72,73] are available in the literature and the values show excellent agreement. Gibbs free energy function gef_T has been tabulated in all the above sources and the data of Barrin and Knacke[72] has been used in the present study.

2.4.3 Thermal Properties of ε-NbN

It is well known that stable hexagonal nitride of niobium never forms in commercial steels, the nitrogen appearing dissolved in the cubic carbonitrides. The free energy of formation of this compound, ε-NbN, is usefully compared with the free energy of formation of a metastable cubic niobium nitride, $NbN_{0.87}$, as discussed later. The existing thermochemical data on ε-NbN are limited in accuracy and the free energy of formation calculated via a Third Law analysis and solution thermodynamics is not as accurate as the direct solubility product determinations discussed earlier. However, for the sake of completeness the limited thermochemical data on the ε-NbN is briefly described below.

The standard heat of formation $\Delta H_f^\circ(298)$ of ε-NbN has been measured through combustion calorimetry by Mah and Gellert[77] and recalculated by Barrin and Knacke[72] as $\Delta H^{\circ}_{f,298.15}$ = -56.5 ± 0.4 kcal/mole. Only estimated low temperature heat capacities are available.[75,78] Kelley's[74] tabulations of high temperature heat capacity equations for ε-NbN based on the work of Sato and Sogube[76] is the only source of this thermochemical quantity. Estimations of the high temperature heat capacities by Schick et al.[63] are in excellent agreement with Kelley's[74] tabulations. The free energies of transition to other crystal structures are unknown and there is very little information even to aid an estimate. With the present data available in the literature, free energies of formation of ε-NbN alone can be estimated, and this with limited accuracy. Thermal functions of N_2, tabulated by many authors,[71,72,73] and those of niobium discussed earlier are also necessary for such an estimation.

2.4.4 Free Energies of Solution of Niobium, Carbon and Nitrogen in Austenite

The thermochemical data discussed thus far aid in calculating free energies of formation of niobium carbide, NbC_x, as a function of x and ε-NbN the products and the reactants all being in the standard states of pure substances. Besides this, a knowledge of the solution behaviour of niobium, carbon and nitrogen in austenite is necessary for calculation of the ternary or quaternary phase diagrams.

Niobium:

Considerable uncertainty exists over the values of Henry's law constant γ°_{Nb} for Nb in γ-iron reported by Hawkins,[79] whose solid electrolyte measurements are the only ones that yield experimental information on the solution behaviour of Nb. The reported value of γ°_{Nb} is 2.1 at 1000°C and 1100°C. Argent,[80] who has reviewed experimental information on all the substitutional alloying elements in iron, has pointed out that Hawkins' results are unsatisfactory. Recently, Robinson and Argent[81] have studied the solution behaviour of Vanadium among other elements, using Knudsen cell mass spectrometry in the temperature range 1200-1650°K. They have given a value of 0.5 over the temperature range for the Henrian activity coefficient of vanadium, γ_V°, in austenite. Hawkins[79] has reported more reliable γ° values for Tantalum as 1.1 and 0.96 at 1100°C and 1000°C. V, Nb and Ta form the elements of group Va of the periodic table and the value of 2.1 for γ_{Nb}° is probably too high. Equilibration experiments carried out in this study and other reliable ones reported in the literature on the austenite/austenite+NbC_x equilibrium, yield solubility limits of Nb in austenite when combined with the thermochemical data on the defect carbides, yield γ_{Nb}° values ranging between 1.0 and 1.5 over the temperature range 1000-1300°C. These values are in better agreement with the conclusions of Bodsworth et al.[102] who have suggested a solution behaviour of Nb in austenite close to ideal. For present calculations, the solution behaviour of niobium has been assumed as ideal over the temperature range 1000-1250°C.

Carbon and Nitrogen:

The solution behaviour of carbon in γ-iron has been extensively studied experimentally and the results of Ban-ya et al.[82,83] have been accepted as the most accurate among the published data over the temperature range of 900°C to 1400°C. Harvig[84] has analysed the Fe-C system rigorously on the basis of the regular solution models of Hillert and Staffonson[85] and their expressions for the free energy of solution of carbon in austenite describe the information with almost the same precision as that of Ban-ya et al.[82,83]

There are a very large number of reports on the solution behaviour of nitrogen in iron austenite. Hillert and Jarl[86] have made an excellent review of all the available information in the literature and have rationalized and brought them all into mutual agreement after a rigorous thermodynamic analysis. They have reported among other data, the free energy function for the dissolution of nitrogen in austenite.

The changes in free energies accompanying the transfer of carbon and nitrogen from their standard states of graphite and nitrogen gas at one atmosphere respectively, to a standard state based on infinitely dilute solution in austenite are given by Ban-ya et al.[82] and Hillert and Jarl[86] as follows:

$$°G_C^{\gamma} - °G_C^{gr} = -17250 - 12.44\ T \log T + 48.15\ T\ \text{(cal/mole)}$$

$$°G_N^{\gamma} - °G_{N_2} = -13270 - 16.70\ T \log T + 75.87\ T\ \text{(cal/mole)}$$

CHAPTER III

THEORETICAL CALCULATIONS

3.1 SCOPE AND CONTENT

Third Law analysis of the high temperature activity data in the Nb-C system has been carried out to derive the reference heats of formation, $\Delta H_f^\circ(298)$, of niobium carbides, NbC_x, as a function of nonstoichiometry, x. These are compared with the $\Delta H_f^\circ(298)$ values reported through combustion calorimetry and the consistency of this important thermochemical quantity is verified. The chosen heats of formation are used together with the thermochemical data discussed in the earlier chapter to calculate the integral free energies of formation of the defect carbides over the range of nonstoichiometry. Empirical equations have been used to represent the integral free energies of formation. These, together with the activity-composition relationships in the Fe-C and Fe-Nb systems have been used to determine the austenite-niobium carbide equilibrium.

Using the available solubility data on the carbonitrides of niobium, the solubility of a metasatble cubic niobium nitride, $NbN_{0.87}$, is estimated. The experimentally measured carbide solubility and the estimated nitride solubilities are used for predicting carbonitride solubilities. It is shown that the carbonitrides formed in steels can be adequately treated as a compound with a fixed nonstoichiometry and of the composition $NbC_xN_{0.87-x}$. The carbonitride is treated as an ideal mixture of the carbide $NbC_{0.87}$ and the nitride $NbN_{0.87}$ and the austenite-carbonitride equilibrium is determined on this basis.

Finally, the Wagner's interaction coefficients of Mn, Si, Cr, Ni and Mo with niobium are evaluated. The interactions of the above elements with carbon and nitrogen are taken into account in defining the solubilities of niobium carbides, nitrides and carbonitrides in a multicomponent austenite.

3.2 THIRD LAW ANALYSIS OF THE ACTIVITY DATA IN THE Nb-C SYSTEM

Storms et al.[54] have measured the vapour pressure of niobium in the cubic monocarbide as a function of carbide composition. Their results are shown in Fig. 2.17 and discussed in section 2.4.1.

At constant temperature and pressure, the formation of any non-stoichiometric niobium carbide, NbC_x, can be represented by the reaction

$$Nb_{(s)} + xC_{(s)} \overset{K}{\rightleftharpoons} NbC_x \qquad 3.1$$

The thermodynamic equilibrium constant for the above reaction is given by

$$K = \frac{a_{NbC_x}}{a_{Nb} \cdot a_C^x} \qquad 3.2$$

When the product and all the reactants are in their standard state of pure substances, the free energy change for reaction 3.1, $\Delta G^\circ_{f,T}$ may be written as

$$\Delta G^\circ_{f,T} = -RT \ln K \qquad 3.3$$

or

$$\Delta G^\circ_{f,T} = RT \ln a_{Nb} + x\, RT \ln a_C \qquad 3.4$$

in view of the identity (3.2); where a_{Nb} and a_C are the respective activities at equilibrium and R is the gas constant. The activities of niobium and carbon shown in Fig. 2.17 have been used to calculate the free energy changes at 2300°K and 2500°K.

The Gibbs energy function, gef_T, given by

$$gef_T = (G^\circ_T - H^\circ_{298})/T \qquad 3.5$$

is determined for NbC_x, Nb and C using the relationship

$$gef_T = -S^\circ_T + \frac{H^\circ_T - H^\circ_{298}}{T} \qquad 3.6$$

and the thermal functions for these substances chosen in Section 2.4. ΔH°_{298} is then calculated from the free energy data via the equation

$$\Delta H^\circ_{298} = \Delta G^\circ_{f,T} - T\Delta gef_T \qquad 3.7$$

where Δgef_T is given by

$$\Delta gef_T = gef_T(NbC_x) - gef_T(Nb) - x\cdot gef_T(C) \qquad 3.8$$

The configurational entropy is taken into account for each carbide. The results of the calculations for the change in the Gibbs energy function (Δgef_T) and ΔH°_{298} are given in Table 3.1. The latter quantity is evaluated both for the 2300°K and 2500°K free energy data and the mean of these two values is taken to represent the best ΔH°_{298} value for each defect carbide through Third Law analysis. These mean values are compared with the combustion calorimetric values of Huber et al.[48] in Table 3.1 and diagrammatically represented in Fig. 3.2. There is a good agreement and the small systematic deviation could be because of some systematic errors in the high temperature measurements of Storms et al.[54] or due to ordering.

TABLE 3.1

Third Law Heat of Formation of NbC_x

Pressure

Extrapolated from, °K	$T\Delta gef^\circ_T$, kcal/mole	$-\Delta G^\circ_T$, kcal/mole	$-\Delta H^\circ(298)$ kcal/mole	Combustion $-\Delta H^\circ(298)$ kcal/mole	Difference kcal/mole
$NbC_{0.70}$					
2300	0.50	26.92	27.42		
2500	0.42	26.77	27.19		
		ave.	27.31	28.00	-0.69
$NbC_{0.80}$					
2300	0.54	29.80	30.34		
2500	0.48	29.56	30.06		
		ave.	30.20	30.48	-0.28
$NbC_{0.90}$					
2300	0.88	31.76	32.64		
2500	0.87	3.147	32.34		
		ave.	32.49	32.35	+0.14
$NbC_{0.98}$					
2300	1.55	32.67	34.22		
2500	1.61	32.33	33.94		
		ave.	34.08	33.40	+0.68

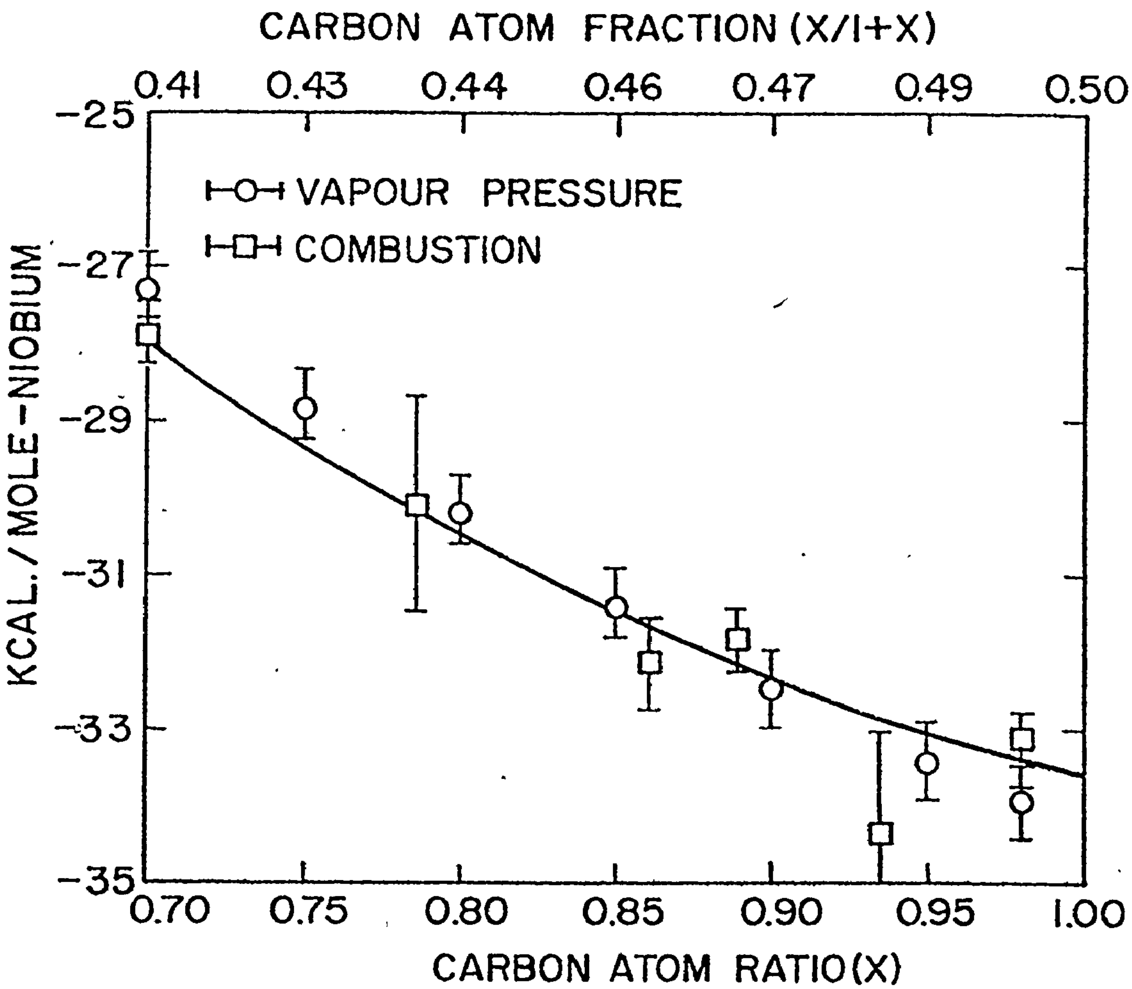

Figure 3.2 Comparison of $\Delta H_f^{\circ}(298)$ values obtained from combustion and activity data

in the defect carbides at lower C/Nb atom ratios. There is no experimental evidence for the latter reported in the literature. Therefore, for the present study, the combustion data of Huber et al.[48] have been chosen and an error of ± 700 cal/mole-Nb at the 2σ level over the entire composition range has been adopted for their heats of formation values.

3.3 REPRESENTATION OF THE INTEGRAL FREE ENERGY OF FORMATION THROUGH EMPIRICAL EQUATIONS

It has been shown by Depoorter[99] that the integral free energy of formation of the carbide NbC_x across the composition range can be adequately represented by an empirical equation of the form,

$$\Delta G^{\circ}_{f,T(NbC_x)} = \{X_C \cdot A(B - \ell n \frac{X_C}{1-2X_C}) + X_{Nb} \cdot A(C + \ell n \frac{X_{Nb}}{1-2X_C})\}RT \qquad 3.9$$

where $\Delta G^{\circ}_{f,T(NbC_x)}$ is the integral free energy of formation (mixing) of a carbide NbC_x of a specific nonstoichiometry x at temperature T; X_C, X_{Nb} are atom fractions of carbon and given by x/1+x and 1/1+x, respectively; and, A, B and C are empirical constants to be determined.

For each carbide composition, using Eq. 3.7 and the chosen standard heat of formation, ΔH°_f, for that carbide, the integral free energy of formation is calculated using the appropriate thermal functions discussed earlier. The calculated integral free energies were fitted consistent with the composition range x = 0.70 to x = 0.98 to obtain the empirical constants A, B and C in Eq. 3.9. The calculated constants are listed in Table 3.3. The agreement between the curve fitted expression and the calculated values at 1000°C is shown in Table 3.4.

Referring to the Nb-C phase diagram (Fig. 2.1) it can be seen

TABLE 3.3

Empirical Constants for NbC_x

$T\ {}^{\circ}C$	-A	B	C
1000	-3.05	0.258	3.89
1050	-2.86	0.330	
1100	-2.70	0.399	
1150	-2.57	0.470	
1200	-2.46	0.532	
1250	-2.31	0.595	

TABLE 3.4

Free energies of formation values calculated at 1000°C from thermochemical data and the curve fitted expression (Eq. 3.9 and Table 3.3)

C/Nb ratio in carbide	Calculated K.cal/mole-carbide	Curve fitted K.cal/mole-carbide
0.70	-16.15	-16.30
0.75	-16.40	-16.48
0.80	-16.57	-16.59
0.85	-16.63	-16.63
0.90	-16.58	-16.58
0.95	-16.45	-16.43
0.98	-16.27	-16.26

that the terminal solid solubilities are negligible. The free energies of formation of the Nb-C (i.e., pure Nb) and C-Nb (i.e., graphite) solid solutions are therefore negligible as compared to those of the intermediate phases, NbC_x (F.C.C.) and NbC_x (h.c.p.). The upper limit of the cubic composition range has been found to be 0.98 up to 1700°C.[26] At higher temperatures, Storms et al.[23] have found this limit to decrease with temperature. The lower limit of nonstoichiometry of the cubic carbide is well known to be 0.70. Uncertainties prevail with regard to the composition range of the hexagonal phase. The upper limit of this phase is well established to be $NbC_{0.5}$ and thermochemical properties of only this carbide composition have been measured in this phase. Storms[44] has summarized the existing, conflicting information on the phase stability of this hexagonal carbide. Fig. 3.5 shows a free energy composition diagram for the Nb-C system at 1000°C. The indicated points ( ) represent the integral free energies of formation, $\Delta G^{\circ}_{f,T}$, computed from the experimental thermochemical data for the NbC_x phase (cubic) and a single value for the h.c.p. composition $NbC_{0.5}$. The solid free energy curve for the cubic phase represents the empirical equation 3.9. The corresponding curve for the hexagonal phase is only estimated, and has been drawn to agree with the maximum known composition range of this phase.[100]

In view of the phase relations in the Nb-C system, the following conditions must be fulfilled.

a) The tangent from the point representing pure Nb must meet the free energy composition curve of the Nb_2C (h.c.p.) phase at the lower limit of its homogeneity.

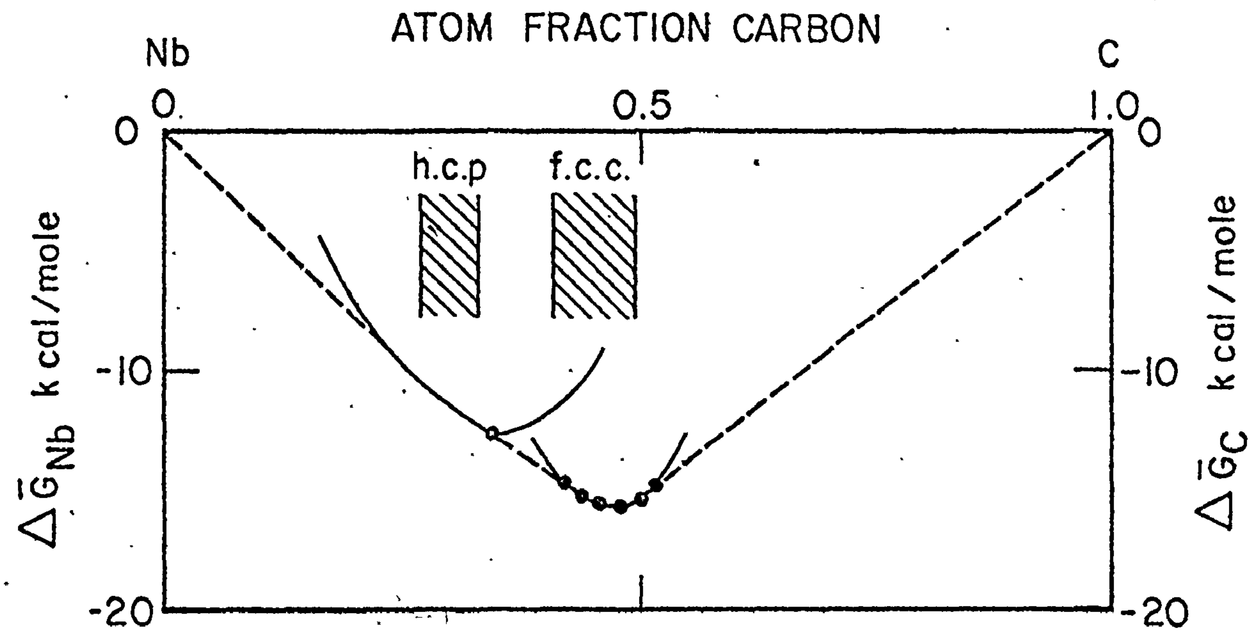

<u>Figure 3.5</u> . Free energy-composition diagram for the Nb-C system at 1000°C

b) The tangent from the point representing pure C must meet the free energy composition curve of the NbC_x (cubic) phase at the upper limit of its homogeneity (at x = 0.98).

c) The tangent joining 'Nb_2C' with 'NbC_x' must meet the curves at the upper composition limit of 'Nb_2C' (at x = 0.5) and the lower limit of 'NbC_x' (at x = 0.7).

d) The free energy composition curves must be concave upwards.

The free energy composition curve of the F.C.C. phase adequately satisfies the conditions (b), (c) and (d) as shown in the figure.

The empirical equation 3.9 is therefore able to describe the integral free energy of formation (or mixing) of any nonstoichiometric carbide in the cubic phase, in a manner which is thermodynamically consistent with the phase relations in the Nb-C system and truly representative of the thermochemical data.

3.4 PREDICTION OF THE $\gamma/\gamma+NbC_x$ PHASE EQUILIBRIUM

Mori et al.[7] have analysed a wide range of cubic defect carbides and carbonitrides precipitated in steels and have proved that their is little iron or other substitutional solutes present in the precipitates. Since the solubility of iron in NbC_x is negligible, the two component free energy diagram shown in Fig. 3.5 can be used to study the precipitation of this phase in steels. The free energy surfaces of the carbides in the ternary schematic free energy diagram (Figure 2.18) can be conceived of as infinitesimally thin.

The integral free energy of formation of each carbide NbC_x can be expressed in terms of the partial molar free energies and the standard free energies of its components as

$$\Delta G^{\circ}_{f,T} = X_{Nb}^{NbC_x}(\overline{G}_{Nb}^{NbC_x} - {}^{\circ}G_{Nb}) + X_{C}^{NbC_x}(\overline{G}_{C}^{NbC_x} - {}^{\circ}G_{C}) \qquad 3.10$$

or

$$\Delta G^{\circ}_{f,T} = X_{Nb}^{NbC_x} \cdot \Delta\overline{G}_{Nb}^{NbC_x} + X_{C}^{NbC_x}\Delta\overline{G}_{C}^{NbC_x} \qquad 3.11$$

Referring then to Fig. 3.5, any tangent to the integral free energy curve at some composition x/1+x, will cut the ordinates at points representing $\Delta\overline{G}^{\gamma}_{Nb}$ and $\Delta\overline{G}^{\gamma}_{C}$, respectively. For the equilibrium between the carbide NbC_x, and the corresponding ternary austenite of composition X^{γ}_{Nb} and X^{γ}_{C} the conditions are

$$\Delta\overline{G}_{Nb}^{NbC_x} = \Delta\overline{G}^{\gamma}_{Nb} \qquad 3.12$$

and

$$\Delta\overline{G}_{C}^{NbC_x} = \Delta\overline{G}^{\gamma}_{C} \qquad 3.13$$

where $\Delta\overline{G}_{Nb}^{NbC_x}$ and $\Delta\overline{G}_{C}^{NbC_x}$ can be evaluated by a tangent construction to the integral free energy curve at $X_{C}^{NbC_x} = x/1+x$ and $\Delta\overline{G}^{\gamma}_{Nb}$ and $\Delta\overline{G}^{\gamma}_{C}$ are related to the activities of niobium and carbon in solution in austenite by

$$\Delta\overline{G}_{Nb}^{\gamma} = RT\ \ell n\ a^{\gamma}_{Nb} \qquad 3.14$$

$$\Delta\overline{G}_{C}^{\gamma} = RT\ \ell n\ a^{\gamma}_{C} \qquad 3.15$$

Since the empirical equation discussed in the last section has been derived for standard states of pure substances, a^{γ}_{Nb} and a^{γ}_{C} also refer to the same standard state. With this choice of standard states, the activities of niobium and carbon in the ternary austenite are related through the Wagner formalism[1] to their concentrations by

$$\ell n\ a^{\gamma}_{Nb} = \ell n\ X^{\gamma}_{Nb} + \ell n\ \gamma^{\circ}_{Nb} + \varepsilon^{Nb}_{Nb}\ X^{\gamma}_{Nb} + \varepsilon^{C}_{Nb}\ X^{\gamma}_{C} \qquad 3.16$$

and

$$\ell n\ a^{\gamma}_{C} = \ell n\ X^{\gamma}_{C} + \ell n\ \gamma^{\circ}_{C} + \varepsilon^{C}_{C}\ X^{\gamma}_{C} + \varepsilon^{Nb}_{C}\ X^{\gamma}_{Nb} \qquad 3.17$$

where γ°_{i} is the Henry's law coefficient for the ith component in austenite based on a standard state of pure components, $\varepsilon^{i}_{i} \cdot X^{\gamma}_{i}$ describes the deviation from the Henrian behaviour in the binary Fe-i system and $\varepsilon^{j}_{i} \cdot X^{\gamma}_{j}$ is the effect of the ternary addition j on the activity of i in the ternary Fe-i-j system.

The higher order terms have been neglected. For the normal compositions encountered in niobium bearing steels X^{γ}_{C} is more than an order of magnitude greater than X^{γ}_{Nb}. It is therefore justifiable to neglect the X^{γ}_{Nb} terms in Eqs. 3.15 and 3.16. As it turns out, the X^{γ} terms are also negligible but since their values are known,[83,5] they are retained for completeness.

As reported in Section 2.4.4, a number of workers have established the activity composition relationships for carbon in iron austenite. The latest results of Ban-ya et al.[83] have been used in the present study. The following relation is given by these authors for the activity of carbon in iron austenite with graphite as the standard state.

$$\log a^{\gamma}_{C} = \frac{3770}{T} + 2.72 \log T - 10.525 + 3860 \cdot \frac{Y^{\gamma}_{C}}{T} + \log Z^{\gamma}_{C} \qquad 3.18$$

where $Y^{\gamma}_{C} = \frac{X^{\gamma}_{C}}{X^{\gamma}_{Fe}}$ (X_C and X_{Fe} being the respective atom fractions) and

$$Z_C^\gamma = \frac{Y_C^\gamma}{1-Y_C^\gamma}\ ,$$

Activities of niobium have been calculated assuming an ideal solution.[81,101,102]

Over the useful range of ternary austenite composition the amounts of niobium and carbon in solution and in equilibrium with the corresponding carbide NbC_x have been calculated using Eqs. 3.9-3.18. This is equivalent to tie line determinations by tangent constructions. In Fig. 2.18, a $\gamma/\gamma+NbC_x$ phase boundary is represented schematically as the trace of the γ contact line. The calculations have been carried out over the range of 1000°C-1250°C and the calculated phase boundaries are shown in Figs. 5.8-5.13 in relation to the experiments. A constant uncertainty of ± 800 calories in the free energy values has been assumed over the entire range and the error band thus calculated. This is found to adequately envelop the present and published experimental information to be discussed later. The equations that approximately describe the calculated phase boundaries are given in Table 3.6.

3.5 TIE-LINE RELATIONS

A direct consequence of the phase boundary calculations discussed in the last section (3.4) is that a knowledge of the range of nonstoichiometry of the precipitated carbides over a given range of the ternary austenite composition in equilibrium, is obtainable. This is particularly useful in interpreting experimentally measured solubility data when it is not possible to identify the precipitated phases. Most of the reported experimental information on the solubility of niobium carbide in austenite

TABLE 3.6

Empirical equations describing the $\gamma/\gamma+NbC_x$ phase boundary

($\log \%C = A1 \cdot \log \%Nb + B1 \pm C1$)

Temperature °C	A1	B1	C1
1000	-1.095	-3.10	0.15
1050	-1.090	-2.80	0.15
1100	-1.085	-2.64	0.15
1150	-1.077	-2.42	0.15
1200	-1.074	-2.24	0.15
1250	-1.068	-1.99	0.15

needs reinterpretation, and in this regard the present relations are useful.

Typical theoretical tie line relations for the temperature range 1000°C-1300°C are shown in Fig. 3.7. The experimental points shown at 1000°C will be discussed later in relation to the experiments. Given a steel composition in the two phase $\gamma/\gamma+NbC_x$ region the austenite composition, the carbide composition and the amounts of the two phases in equilibrium can be obtained through application of the appropriate equations in Table 3.6 and the tie line relations given in Fig. 3.7. The method of calculation can be understood by referring to Fig. 3.8 wherein a schematic representation of the austenite-niobium carbide equilibrium has been made.

Referring to the tie line $T_1T_3T_2$ in Fig. 3.8, let $T_3(Nb_T,C_T)$ be the given composition (in mole fractions) in the two phase $\gamma+NbC_x$ region. One end of the tie line that passes through T_3, i.e., $T_1([Nb],[C])$, determines the austenite composition and the other extremity defines the carbide composition T_3 (1/1+x,x/1+x) as shown. Three relations are needed to determine the three unknowns, [Nb],[C] and x. Application of the Lever rule yields

$$\frac{C_T - [C]}{Nb_T - [Nb]} = \frac{x/1+x - C_T}{1/1+x - Nb_T}$$

Simultaneous solution of this with matched relations from Table 3.6 and Fig. 3.7 in consistent units yield the solution for the desired temperature.

3.6 PREDICTION OF THE AUSTENITE-CARBONITRIDE EQUILIBRIUM

To predict the austenite-niobium carbonitride equilibrium accurately, prior knowledge of the extent of the carbide and nitride phases in the respective binary systems, i.e., Nb-C and Nb-N and that of the cubic carbo-

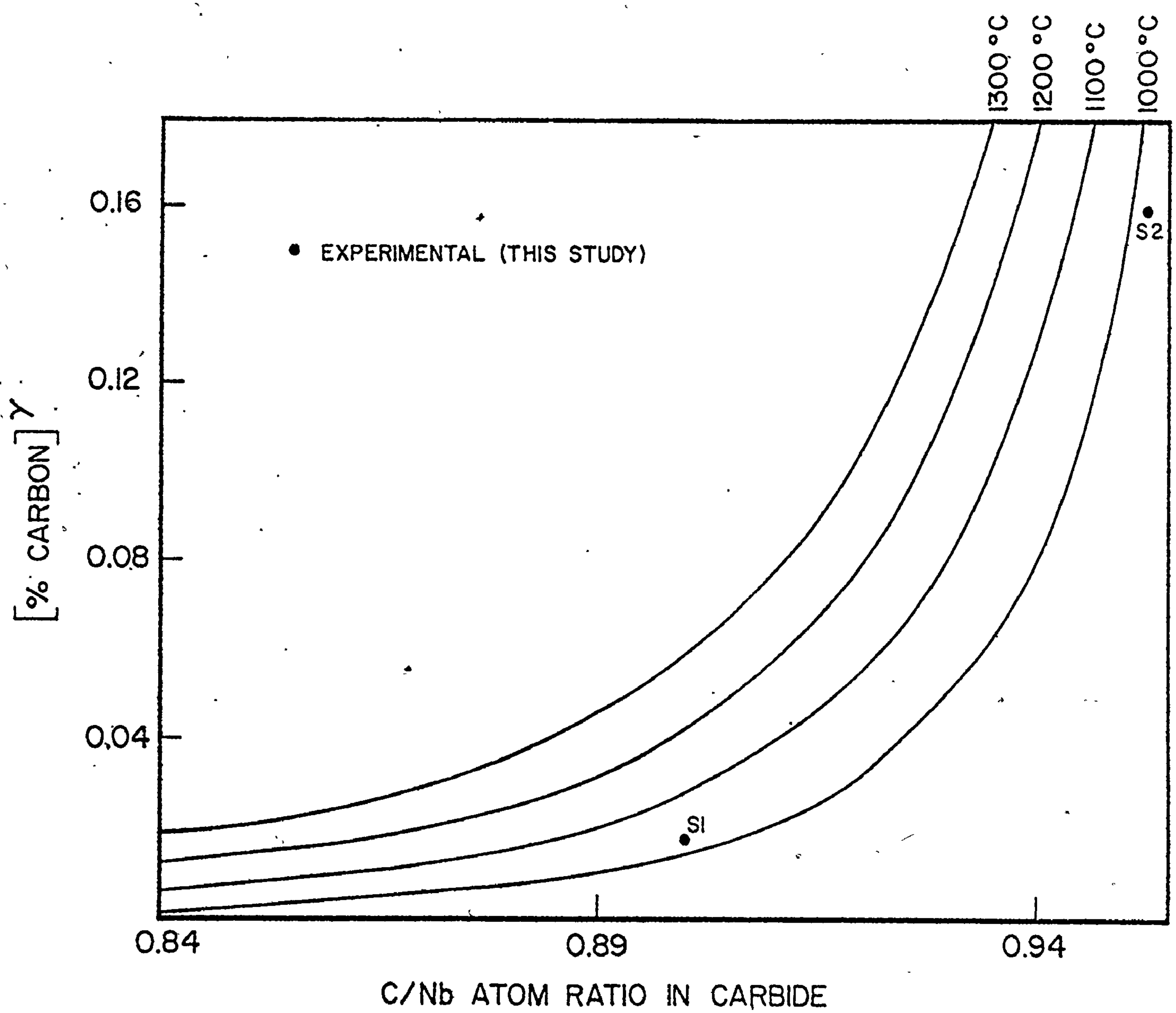

Figure 3.7 Tie-Line Relations

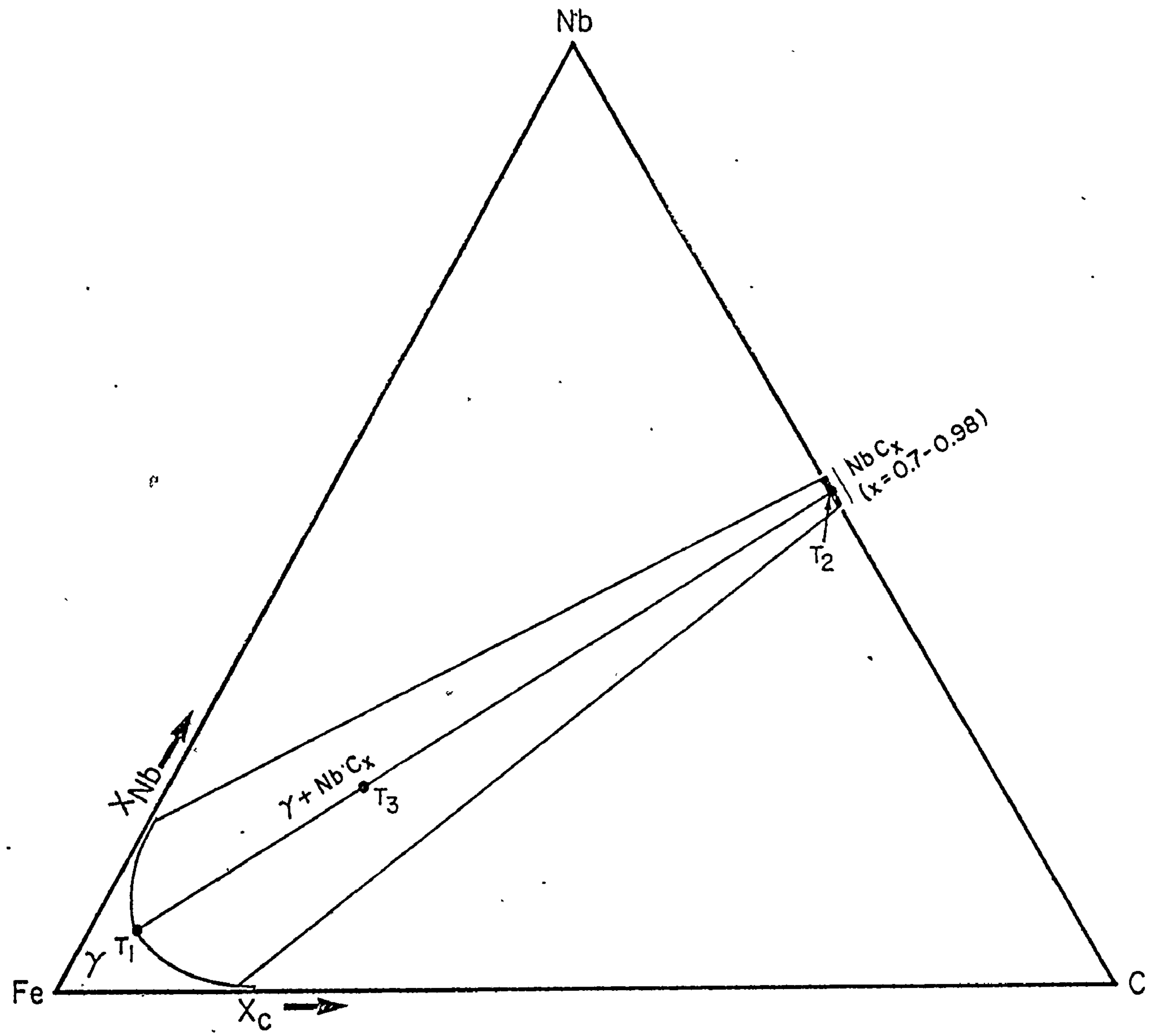

Figure 3.8 Schematic representation of the austenite-carbide equilibrium in the Fe-Nb-C system

nitride phase in the ternary Nb-C-N system is necessary. Thermochemical data should also be available for the phases in the binary and ternary systems seen above. As it turns out, excepting for the Nb-C system, information on the other systems is too meagre and limited in accuracy to permit detailed phase boundary calculations. The few direct carbonitride solubility determinations have been discussed earlier.

A schematic representation of the carbonitride-austenite equilibrium in the quaternary Fe-Nb-C-N system is given in Fig. 3.9. It is known that the composition of the cubic carbonitride is of the form NbC_xN_y $(x+y < 1)$ and this is represented by a hypothetical field on the Nb-C-N triangle. For a given composition, Nb_T, C_T and N_T in the two phase region $\gamma+NbC_xN_y$, prediction of the equilibrium composition of the carbonitride NbC_xN_y and the quaternary austenite composition [Nb], [C] and [N] requires the specification of five relations corresponding to the five unknowns x, y, [Nb], [C] and [N].

The application of the Lever rule yields the following two tie line relations

$$\frac{C_T - [C]}{Nb_T - \frac{x}{x+y}[Nb]} = \frac{\frac{x}{1+x+y} - C_T}{\frac{x/x+y}{1+x+y} - Nb_T} \qquad 3.19$$

$$\frac{N_T - [N]}{Nb_T - \frac{y}{x+y}[Nb]} = \frac{\frac{y}{1+x+y} - N_T}{\frac{y/x+y}{1+x+y} - Nb_T} \qquad 3.20$$

In principle, the conditions for the equality of chemical potentials of the three components in the two phases yield the further three required

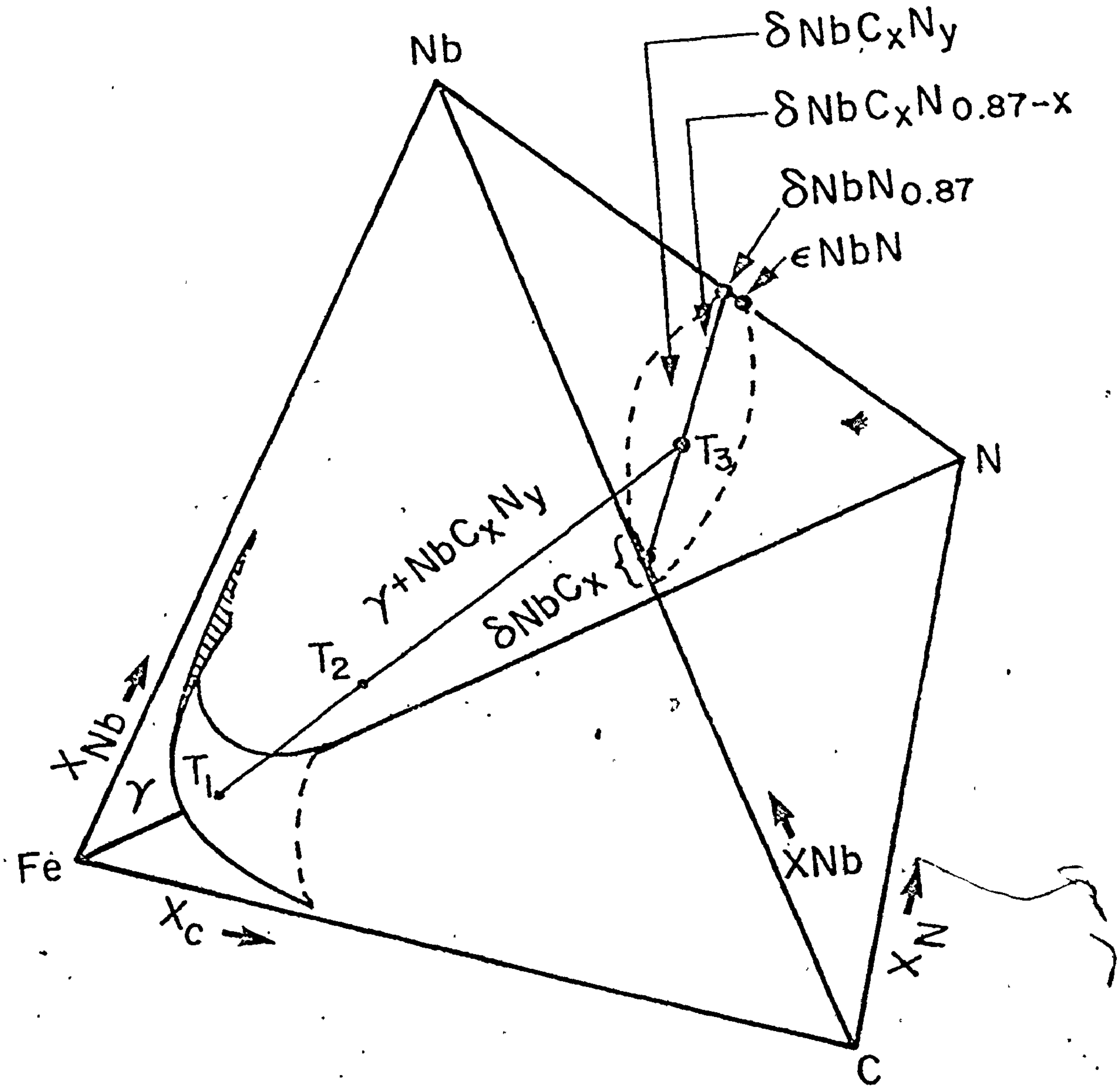

Figure 3.9 Schematic representation of the carbonitride-austenite equilibrium in the Fe-Nb-C-N system

T_1 = [Nb], [C], [N]

$T_2 = Nb_T,\ C_T,\ N_T$

$T_3 = \frac{1}{1+x+y},\ \frac{x}{1+x+y},\ \frac{y}{1+x+y}$

relations. However, to take advantage of these three conditions, thermochemical data for the carbonitride as a function of x and y at any temperature is necessary. Since the latter information is not available, a rigorous and accurate calculation of the austenite-carbonitride equilibrium is not possible. Fortunately, a satisfactory approximate method can be devised to predict the precipitated carbonitride composition and its solubility for any steel composition in the two phase region via certain justifiable assumptions with regard to the composition of the carbonitride, and using the known direct carbonitride solubility determinations available from the literature.

Existing Calculations of the Solubility and Composition of Niobium Carbonitride Precipitated in Steel

Nordberg and Aronsson[6] and Hudd et al.[87] have attempted calculations of carbonitride solubilities. The latter pointed out dimensional inaccuracies in the calculations of Nordberg and Aronsson[6] and presented results of their more comprehensive calculations. Both the earlier treatments involved the following simplifying assumptions:

(i) The precipitated carbonitride is stoichiometric and is of the composition NbC_xN_{1-x};

(ii) The carbonitride is a thermodynamic solution of the carbide NbC and the nitride ε-NbN and is made up of x moles of NbC and 1-x moles of NbN;

(iii) The above solution is ideal and the effective activities of the carbide and the nitride in the carbonitride are equal to their respective concentrations; and,

(iv) In addition to the free energies of formation of the carbide and the nitride given by their respective solubility products, only the entropy of mixing of the two compounds needs to be taken into account.

Eq. 2.10 and the data of Smith[17] were used for the carbide and nitride solubilities in austenite. The reader is referred to the work of Hudd et al.[87] for details of the calculations. Their results have been recalculated in the present study with improved solubility product values for the carbide obtained from this investigation (to be discussed later) and the results presented in Table 3.10. Hudd et al.[87] concluded that (i) the general agreement between the experimental data and the predicted values were satisfactory; (ii) for many alloy compositions variation in nonstoichiometry was not particularly important.

The Present Treatment of the Problem

The composition of the carbonitride precipitated in a particular steel is strongly dependent upon the composition of the steel. This is amply illustrated in Table 3.11, wherein all the reported carbonitrides and the respective steel compositions are listed. The degree of nonstoichiometry depends on the amounts of carbon in solution in austenite and most of the steels with highly nonstoichiometric carbonitrides were experimentally found to contain very low amounts of carbon in solution in austenite. By contrast, the steels of Mandry and Dornelas[21] and the one used in the present investigation, which are the only compositions with higher carbon levels, indicate that the degree of nonstoichiometry is less. Referring back to the theoretical tie line relations in the Fe-Nb-C

TABLE 3.10

Recalculated results of Hudd *et al.*[87]

Author	Steel No.	Temp.	Experimental			Calculated			
	(*)	°C	x	y	[%Nb]$^{\gamma}$	x	y	±σ	[%Nb]$^{\gamma}$
Mori *et al.*	CN1 (28)	1000	0.49	0.34	0.015	0.60	0.40	0.05	0.030
		1100	0.42	0.36	0.052	0.50	0.50		0.070
		1200	0.34	0.36	0.096	0.40	0.60		0.125
	CN3 (28)	1000	0.57	0.28	0.005	0.65	0.35	0.05	0.006
		1100	0.51	0.32	0.028	0.65	0.35		0.020
		1200	0.45	0.34	0.078	0.65	0.35		0.052
	CN5 (28)	1000	0.69	0.15	0.020	0.80	0.20	0.01	0.040
		1100	0.65	0.18	0.087	0.80	0.20	0.02	0.091
		1200	0.60	0.23	0.190	0.80	0.20	0.03	0.172
	CN6 (28)	1000	0.73	0.12	0.036	0.86	0.14	0.02	0.060
		1100	0.70	0.14	0.119	0.85	0.15	0.03	0.150
		1200	0.68	0.16	0.210	0.82	0.18	0.03	0.230
	C7 (28)	1000	0.80	0.07	0.019	0.97	0.03	--	0.040
		1100			0.087				0.095
		1200			0.150				0.180
	(27)	1000	0.08	0.88	0.014	0.05	0.95	0.05	0.016
	(27)	1200	0.2-0.3	0.7-0.8	0.109	0.44	0.56	0.08	0.055

Continued......

TABLE 3.10 (Continued)

Author	Steel No. (*)	Temp. °C	Experimental x	Experimental y	Experimental $[\%Nb]^{\gamma}$	Calculated x	Calculated y	Calculated $\pm\sigma$	Calculated $[\%Nb]^{\gamma}$
Mandry and Dornelas	(27)	1050			0.002	0.88	0.12	0.04	0.008
		1100	0.83	0.14	0.020	0.90	0.10	0.04	0.013
		1150			0.034	0.91	0.09	0.04	0.022
Meyer	(27)	900	0.90	0.10	0.005	0.77	0.23	0.06	0.001
		900	0.65	0.35	0.015	0.59	0.41	0.05	0.012

x,y = C/Nb and N/Nb atom ratios, respectively, in the carbonitride NbC_xN_y.

σ = uncertainty in x and y

(*) = refers to the page numbers in this thesis wherein the compositions of the respective steels are given.

TABLE 3.11

Dependence of carbonitride composition on steel chemistry and temperature

Author	Steel No.	Mole Ratio			Temp.	Carbonitride composition	
	(*)	C/Nb	N/Nb	C/N	°C	x	y
Mori et al.	(27)	0.33	1.20	0.27	1000	0.08	0.88
Mori et al.	CN1 (28)	1.14	0.39	2.94	1000 1100 1200	0.49 0.42 0.34	0.34 0.36 0.36
Meyer	(27)	1.84	0.41	4.50	1000	0.54	0.46
Mori et al.	CN3 (28)	3.78	0.51	7.14	1000 1100 1200	0.57 0.51 0.45	0.28 0.32 0.34
	CN5 (28)	0.98	0.18	5.56	1000 1100 1200	0.69 0.65 0.60	0.15 0.18 0.23
	CN6 (28)	0.82	0.13	6.25	1000 1100 1200	0.73 0.70 0.68	0.12 0.14 0.16
	C7 (28)	1.18	0.03	39.0	1000-1300	0.80	0.07
	C8 (28)	0.85	0.02	44.0			

Continued......

TABLE 3.11 (Continued)

Author	Steel No (*)	Mole Ratio C/Nb	Mole Ratio N/Nb	Mole Ratio C/N	Temp. °C	Carbonitride composition x	Carbonitride composition y
Mandry and Dornelas	(27)	21.5	0.36	58.0	950-1150	0.85	0.14
This study	S2 (97)	39.0	0.50	79.0	1000	0.91	0.04

(*) = Refers to the page number in this thesis wherein the compositions of the respective steels are given.

x,y = C/Nb and N/Nb ratios, respectively, in the carbonitride NbC_xN_y

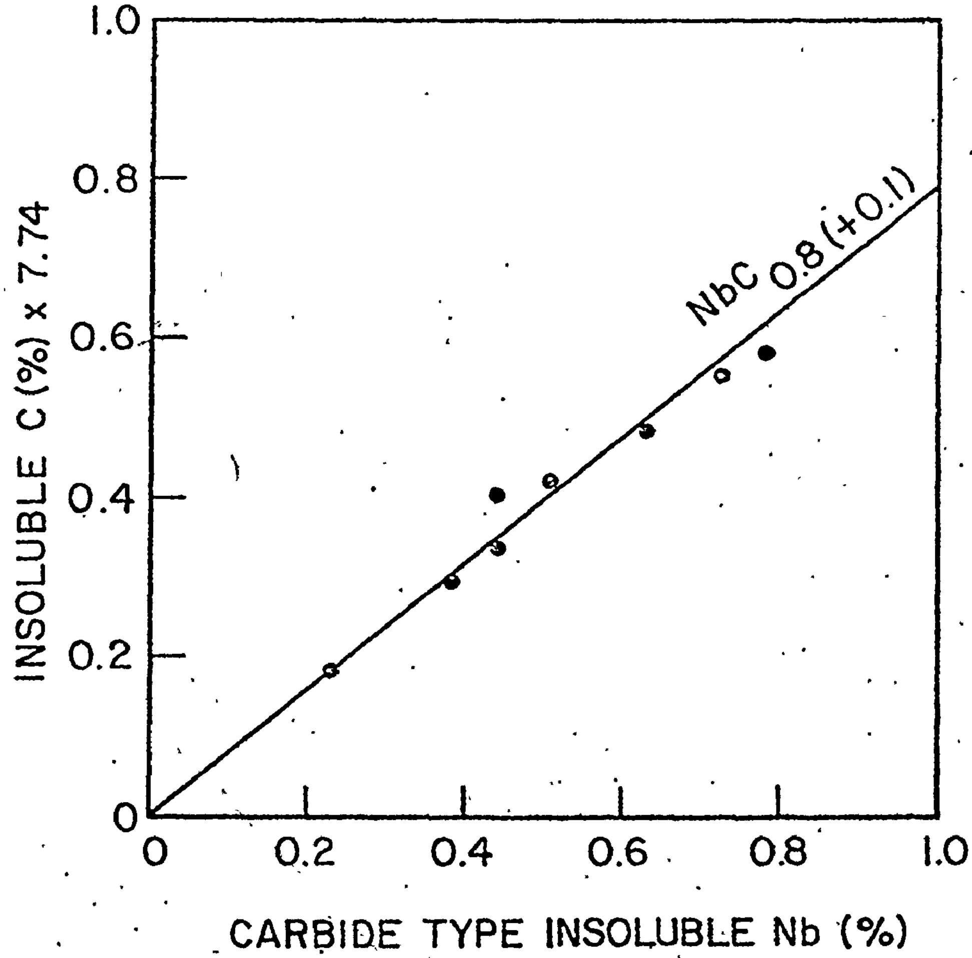

Figure 3.12 Chemical analyses results of Mori *et al.*[7]

system, discussed earlier (Fig. 3.7) an appropriate average carbide composition over the temperature range 1000°-1250°C would appear to be $NbC_{0.93}$ for the composition range of commercial interest and $NbC_{0.9}$ for the complete range of experimental and commercial compositions. On the other hand, the experimental observations (Table 3.11 and Fig. 3.12) suggest that $NbC_{0.87}$ would be a better overall average. Further, referring to the Nb-N phase diagram and the phase relations in the Nb-N system (Fig. 2.4 and Table 2.5) we see that the δ-NbN_x phase in the high temperature stable range has the same crystal structure as the δ-NbC_x phase and a lattice parameter in its stable existence range close to that of $NbC_{0.87}$.

(i) The niobium carbonitride precipitated in steels is a defect compound of approximately fixed nonstoichiometry and the average composition of the carbonitride can therefore be written as $NbC_xN_{0.87-x}$.

(ii) The carbonitride is an ideal mixture of the nonstoichiometric carbide δ-$NbC_{0.87}$ and the nonstoichiometric metastable nitride δ-$NbN_{0.87}$ so that the activities of the carbide and the nitride in the carbonitride can be set equal to their respective concentrations, i.e., $x/0.87$ and $(0.87-x)/0.87$.

In view of the assumption of a fixed nonstoichiometry in tie line relations 3.19, 3.20 become

$$\frac{C_T - [C]}{Nb_T - \frac{x}{0.87}[Nb]} = \frac{\frac{x}{1.87} - C_T}{\frac{x/0.87}{1.87} - Nb_T} \qquad 3.21$$

and

$$\frac{N_T - [N]}{Nb_T - \frac{0.87-x}{0.87}[Nb]} = \frac{\frac{(0.87-x)}{0.87} - N_T}{\frac{(0.87-x)/1.87}{1.87} - Nb_T} \qquad 3.22$$

and thereby one of the variables, i.e., y is eliminated. Note, however, that we have lost the ability to deal with variations in nonstoichiometry.

The ideality assumption allows us to write the solubility products for the reactions representing the formation of $NbC_{0.87}$ and the metastable $NbN_{0.87}$ in the quaternary austenite as

$$K'_C = \frac{[Nb][C]^{0.87}}{x/0.87} \qquad 3.23$$

and

$$K'_N = \frac{[Nb][N]^{0.87}}{(0.87-x)/0.87} \qquad 3.24$$

Correspondingly, the free energy of formation of the carbonitride $NbC_xN_{0.87-x}$ can be written through the ideal solution assumption and Eqs. 3.23 and 3.24 as

$$RT \ln K'_{CN} = RT\{\frac{x}{0.87} \ln K'_C + \frac{0.87-x}{0.87} \ln K'_N - \Delta S^m\} \qquad 3.25$$

where ΔS^m is the entropy of mixing of the carbide and the nitride and is given by

$$\Delta S_m = -\{\frac{x}{0.87} \ln \frac{x}{0.87} + \frac{(0.87-x)}{0.87} \ln \frac{0.87-x}{0.87}\} \qquad 3.26$$

Any two of the Eqs. 3.23-3.25 and the two tie line relations 3.21 and 3.22 can be used to solve for the four unknowns, i.e., [Nb], [C], [N] and x.

Accurate values for the solubility product K'_C are known from the present study. Since there is no information available on the values of K'_N through direct measurements, it is first of all necessary to estimate appropriate values for this quantity over the temperature range of interest. The direct determinations of K'_{CN} discussed in an earlier chapter have been used along with the accurate K'_C values, to estimate the values of K'_N indirectly. These estimated values are tabulated in Table 3.13 along with the K'_C values evaluated in the present study. In turn these values have been substituted into Eqs. 3.23 and 3.24 and together with the tie line relations 3.21 and 3.22 we have recalculated the carbonitride compositions and quaternary austenite compositions corresponding to the direct experiments. The correlations between observations and predictions are shown in Table 3.14 and Fig. 3.15 and will be discussed later.

A diagrammatic representation of the estimated free energies of formation of the carbonitrides are presented in Figs. 3.16 and 3.17. Here log $[\%Nb][\%C]^x[\%N]^y$ values for the experimental results are compared with the proposed free energy curve for the carbonitride $NbC_xN_{0.87-x}$. It is to be noted in all these diagrams that the free energies of formation of the stable ε-NbN are considerably more negative than the estimated free energies of δ-$NbN_{0.87}$ as required by the metastability of the latter compound.

The fixed nonstoichiometric carbonitride is shown in the schematic quaternary phase diagram (Fig. 3.9). Thus, given an alloy composition in the two phase region, any two of Eqs. 3.23-3.25 and the two tie line relations 3.21 and 3.22 can therefore be used to solve for the four unknowns x, [Nb], [C] and [N] and thus determine the complete carbonitride-

TABLE 3.13

T°_C	This study (Experimental) $\log[\%Nb][\%C]^{0.87}$	Estimated $\log[\%Nb][\%N]^{0.87}$
1000	-2.88 ± 0.05	-3.75 ± 0.15
1100	-2.35 ± 0.05	-3.1 ± 0.20
1200	-2.00 ± 0.06	-2.6 ± 0.20
1300	-1.64 ± 0.06	-2.2 ± 0.20

TABLE 3.14

Experimental and predicted austenite-carbonitride equilibrium

Author	Steel No. (*)	Temp. °C	Experimental x	Experimental y	Experimental $[\%Nb]^{\gamma}$	Experimental $[\%C]^{\gamma}$	Experimental $[\%N]^{\gamma}$	Predicted x	Predicted y	Predicted $[\%Nb]^{\gamma}$	Predicted $[\%C]^{\gamma}$	Predicted $[\%N]^{\gamma}$
Mori et al.	CN1 (27)	1000	0.49	0.34	0.015	0.018	0.0027	0.49	0.38	0.018	0.018	0.0018
		1100	0.42	0.36	0.052	0.021	0.0041	0.47	0.40	0.062	0.021	0.0039
		1200	0.34	0.36	0.096	0.025	0.0065	0.46	0.31	0.102	0.023	0.0076
	CN3 (27)	1000	0.57	0.28	0.005	0.086	0.0075	0.54	0.33	0.007	0.087	0.0061
		1100	0.51	0.32	0.028	0.089	0.0074	0.54	0.33	0.022	0.088	0.0068
		1200	0.45	0.34	0.078	0.094	0.0094	0.54	0.33	0.050	0.091	0.0086
	CN5 (27)	1000	0.69	0.15	0.020	0.026	0.0030	0.70	0.17	0.025	0.025	0.0012
		1100	0.65	0.18	0.087	0.035	0.0020	0.68	0.18	0.073	0.030	0.0016
		1200	0.60	0.23	0.190	0.046	0.0014	0.67	0.20	0.120	0.036	0.0013
	CN6 (27)	1000	0.73	0.12	0.036	0.015	0.0013	0.74	0.13	0.044	0.015	0.0001
		1100	0.70	0.14	0.119	0.026	0.0003	0.74	0.13	0.110	0.021	0.0014
		1200	0.68	0.16	0.210	0.036	0.0001	0.72	0.15	0.180	0.030	0.0004
	C7 (27)	1000	0.80	0.07	0.019	0.028	0.0007	0.84	0.03	0.028	0.026	0.0001
		1100			0.087	0.039	0.0017			0.067	0.031	0.0003
		1200			0.150	0.045	0.0023			0.135	0.043	0.0007
	C8 (27)	1000	0.80	0.07	0.036	0.020	0.0007	0.81	0.06	0.044	0.014	0.0002
		1100			0.092	0.023	0.0015			0.108	0.016	0.0012
		1200			0.197	0.030	0.0020			0.210	0.027	0.0022
	(27)	1000	0.08	0.88	0.014	0.0032	0.0063	0.06	0.81	0.014	0.0034	0.0072
Mandry and Dornelas	(27)	950	0.83	0.14	0.004	0.174	0.0023	0.73	0.14	0.003	0.174	0.0023
		1050			0.011	0.174	0.0025	0.76	0.11	0.009	0.175	0.0027
		1100			0.020	0.175	0.0027	0.77	0.10	0.015	0.175	0.0028
		1150			0.034	0.177	0.0029	0.78	0.09	0.025	0.176	0.0031

Continued......

TABLE 3.14 (Continued)

Author	Steel No. (*)	°C	Experimental x	y	$[\%Nb]^{\gamma}$	$[\%C]^{\gamma}$	$[\%N]^{\gamma}$	Predicted x	y	$[\%Nb]^{\gamma}$	$[\%C]^{\gamma}$	$[\%N]^{\gamma}$
Meyer	(27)	900	0.77	0.23	0.005	0.217	0.0040	0.67	0.20	0.001	0.217	0.0040
		900	0.65	0.35	0.015	0.018	0.0018	0.48	0.39	0.010	0.019	0.0010

(*) = Refers to the page number in this thesis wherein the compositions of the respective steels are given.

x,y = C/Nb and N/Nb atom ratios, respectively, in the carbonitride NbC_xN_y

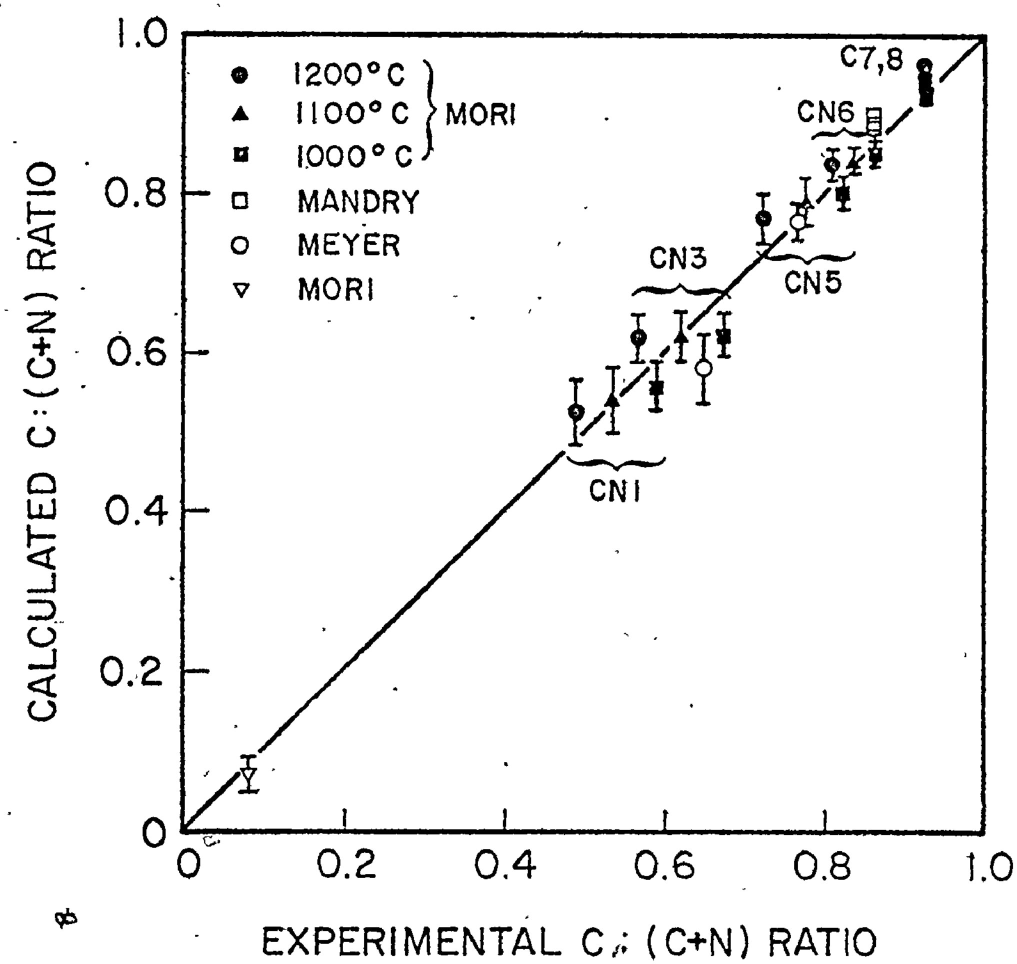

<u>Figure 3.15</u> Correlation of predicted and observed C:(C+N) ratios for the carbonitrides precipitated in steels

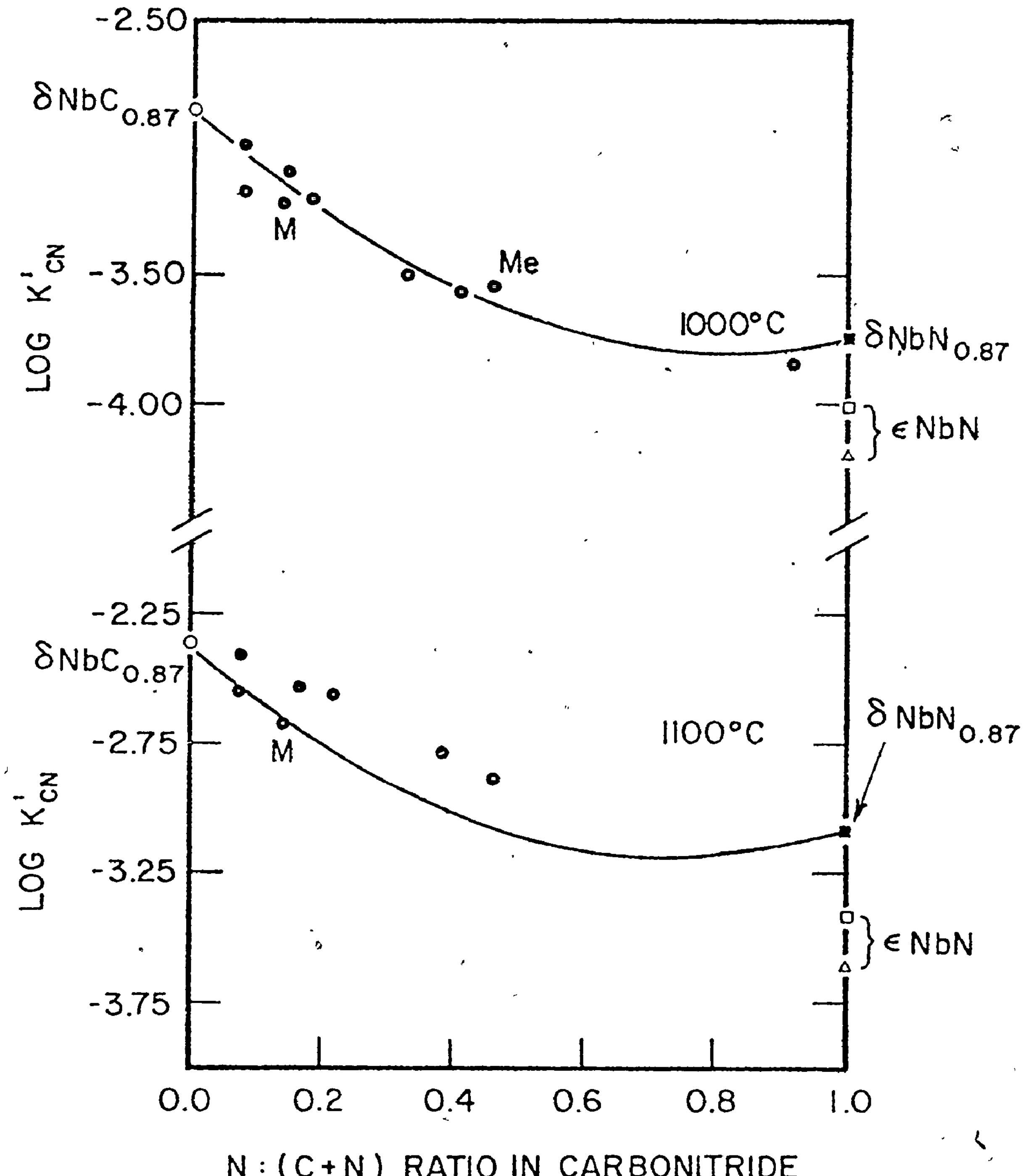

Figure 3.16 Relative free energy-composition diagram

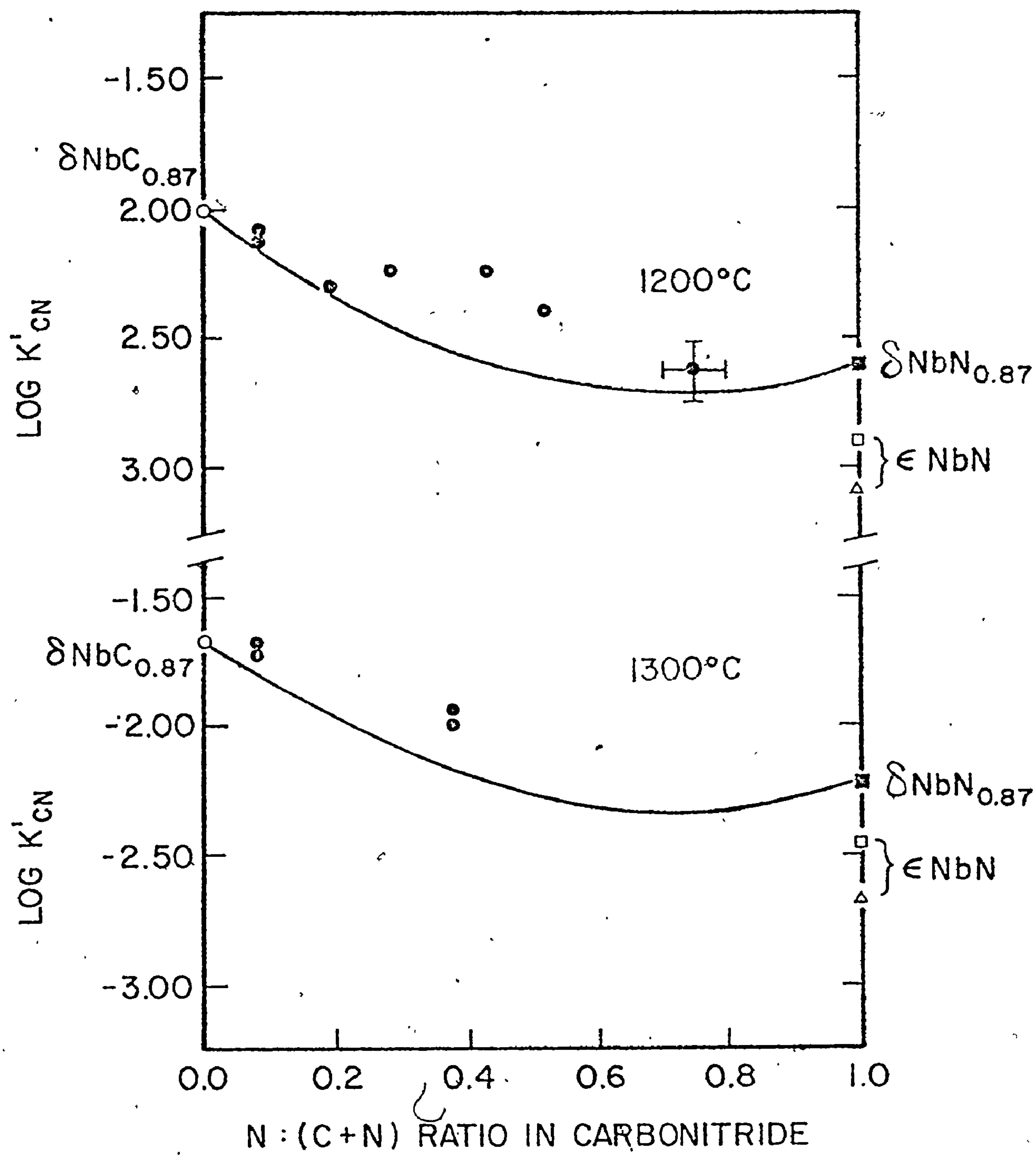

Figure 3.17 Relative free energy-composition diagram

austenite equilibrium including the relative amounts of the two phases.

3.7 THERMODYNAMIC INTERACTIONS OF Mn, Si, Cr, Ni AND Mo WITH NIOBIUM, CARBON AND NITROGEN

To include the effect of alloying elements on the niobium carbide, nitride or carbonitride equilibrium with austenite, a knowledge of the Wagner thermodynamic interaction parameters of the alloying elements with niobium, carbon and nitrogen, i.e., $\varepsilon^{M}_{Nb,C,N}$ is necessary.

If we consider the reactions for the formation of NbC_x or NbN_x in a multi-component austenite, i.e.,

$$[Nb] + x[C] \underset{}{\overset{K_C}{\rightleftarrows}} NbC_x \qquad 3.27$$

$$[Nb] + x[N] \underset{}{\overset{K_N}{\rightleftarrows}} NbN_x \qquad 3.28$$

then the respective equilibrium constants are given by

$$K_C = \frac{a_{NbC_x}}{a_{Nb} \cdot a_C^x} \qquad 3.29$$

$$K_N = \frac{a_{NbN_x}}{a_{Nb} \cdot a_N^x} \qquad 3.30$$

The Henrian (standard state at infinite dilution) activities are given by the Wagner formalism as,

$$\ln a_{Nb} = \ln X^{\gamma}_{Nb} + \sum_{i=1}^{n} \varepsilon^{M}_{Nb} \cdot X^{\gamma}_{M_i} \qquad 3.31$$

$$\ln a_C = \ln X^{\gamma}_C + \sum_{i=1}^{n} \varepsilon^{M}_{C} \cdot X^{\gamma}_{M_i} \qquad 3.32$$

$$\ln a_N = \ln X^{\gamma}_N + \sum_{i=1}^{n} \varepsilon^{M}_{N} \cdot X^{\gamma}_{M_i}, \qquad 3.33$$

all other interaction terms being justifiably neglected.

The solubility products $K'_C = 1/K_C$ and $K'_N = 1/K_N$ for the carbide and nitride reactions are therefore given by

$$\ell n \ K'_C = \ell n \ [Nb][C]^x + \sum_{i=1}^{n} (\varepsilon_{Nb}^{M_i} + \varepsilon_C^{M_i})[M_i] \qquad 3.34$$

$$\ell n \ K'_N = \ell n \ [Nb][N]^x + \sum_{i=1}^{n} (\varepsilon_{Nb}^{M_i} + \varepsilon_N^{M_i})[M_i] \qquad 3.35$$

Recently, Koyama et al.[88,89] have experimentally studied the effects of Mn, Si, Cr and Ni on the solubilities of niobium carbide and nitride in steels. Their experimental equations are listed in Table 3.16. The ε_C^M interaction coefficients are well-known and the ε_N^M interaction coefficients for Mn, Si, Cr, Ni and Mo have been experimentally measured by a number of recent investigators. These are summarized in Table 3.

Using the first four of these and the results of Koyama et al.[88,89] the Wagner interaction coefficients have been independently evaluated through Eq. 3.34 and Eq. 3.35 and compared in Table 3.18. Unfortunately, measurements involving Mo were not carried out. However, in view of the facts that (i) both Mo and Nb have identical interactions with iron (exemplified by the respective Fe-Mo and Fe-Nb phase diagrams[113,114]), (ii) they lie adjacent in the period table (suggesting a possible complete mutual solid solubility in the Mo-Nb binary system[115]) there is a strong likelihood that the interaction between Mo and Nb is negligible. It is therefore justifiable to estimate $\varepsilon_{Nb}^{Mo} \approx 0$. Thus, it is now possible in the inverse calculation to treat the solubility of niobium carbide and nitride satisfactorily in a multi-component austenite containing five additional

TABLE 3.18

Experimental Results of Koyama *et al.*[88,89]

Solubility Product	Experimental Equations	Temp. range
log[%Nb][%N]	$-8500/T + 2.89 + (1085/T - 0.68)[\%Mn] - (48/T + 0.032)[\%Mn]^2$	
log[%Nb][%N]	$-8500/T + 2.89 - (1900/T - 1.103)[\%Si]$	
log[%Nb][%N]	$-8500/T + 2.89 + (1290/T - 0.77)[\%Cr] - (51/T + 0.034)[\%Cr]^2$	1100°C-1250°C
log[%Nb][%N]	$-8500/T + 2.89 + (694/T - 0.44)[\%Ni] - (29/T - 0.0178)[\%Ni]^2$	
log[%Nb][%C]	$-7970/T + 3.31 + (1371/T - 0.900)[\%Mn] - (75/T - 0.0504)[\%Mn]^2$	
log[%Nb][%C]	$-7970/T + 3.31 - (735/T - 0.348)[\%Si]$	
log[%Nb][%C]	$-7970/T + 3.31 + (1113/T - 0.691)[\%Cr] - (38/T - 0.0228)[\%Cr]^2$	1050°C-1150°C
log[%Nb][%C]	$-7970/T + 3.31 + (148/T - 0.0904)[\%Ni] + (8.5/T - 0.0068)[\%Ni]^2$	

	Mn	Si	Cr	Ni
Maximum alloy contents studied (wt-%)	∿ 10.0	∿ 2.0	∿ 10.0	∿ 15.0

TABLE 3.19

Carbon-alloy (ε_C^M) and nitrogen-alloy (ε_N^M) interaction coefficients

Alloying Element	ε_C^M	Ref.
Mn	-5070/T	90
Si	4.84 + 7370/T	91
Cr	7.02 - 21880/T	92
Ni	0.69 + 4600/T	93
Mo	3.86 - 17870/T	105
Alloying Element	ε_N^M	**Ref.**
Mn	17.2 - 31950/T	95
	3.0 - 16140/T	94
	(8.2 - 21000/T) ± 0.5	93
Si	- 35 + 57700/T	96
Cr	9.6 - 26400/T	97
	31.1 - 80000/T	94
	(43 - 92000/T) ± 1	93
Ni	4.5 (1050°C)	98
	4.1 (1250°C)	98
	3000/T	97
Mo	-9552/T	5

TABLE 3.20

Niobium-alloy interaction coefficients evaluated from Koyama's results (Table 3.18) using the interaction coefficients chosen in Table 3.19

Alloying Element	ε_{Nb}^{M}
Mn	175 - 26260/T
Si	-100 + 160640/T
Cr	37 - 72625/T
Ni	∿ 7000/T
Mo(*)	0

* ε_{Nb}^{Mo}, assumed.

alloying elements, i.e., Mn, Si, Cr, Ni and Mo. That is, the carbonitride equilibrium in a multi-component austenite can be predicted by substituting the activities defined by Eqs. 3.31 - 3.33 for the concentrations [Nb], [C] and [N] in Eqs. 3.23 and 3.24 and proceeding as for the quaternary. The last entry in each of the sub-sections of tables 3.19 and 3.20 represents our recommended relation for the interaction parameter to be used in such a phase diagram calculation.

CHAPTER IV

EXPERIMENTAL METHODS

4.1 DETERMINATION OF $\gamma/\gamma+NbC_x$ PHASE BOUNDARY IN THE Fe-Nb-C SYSTEM BY EQUILIBRATION

The binary Fe-C system has been thoroughly studied by gas equilibration techniques by many workers. Chipman[106] has reviewed all the experimental results on the thermodynamic properties of binary Fe-C austenite and found a substantial degree of agreement among them. He has concluded that the data are among the most accurate in the field of metallurgy. More recently, Ban-ya et al.[82,83] have published results of their own experiments, critically compared their results with the existing data and have given accurate relations between carbon activity and carbon composition for binary Fe-C austenite. Their results have proved very useful in the study of the effects of alloying elements.

While determining the influence of an alloying element on the thermodynamics of the binary Fe-C austenite, it is common to equilibrate a series of Fe-M alloys with CO-CO_2 or H_2-CH_4 gas mixtures of carefully measured composition. The initial Fe-M compositions are chosen to be outside or inside the composition range for stability of single-phase austenite depending on whether the objective is to determine phase boundaries in the Fe-M-C system or to study the effect of the alloying element on the activity of carbon in austenite. This procedure is difficult experimentally especially while studying the effects of strong carbide formers which drastically reduce the activity of carbon. At these low carbon activities, the appropriate gas mixtures are almost pure CO or H_2 and the control of the carbon activity is susceptible to very large errors. A simpler technique is to simultaneously equilibrate Fe-M-C alloys and Fe-C alloys with the gas mixtures, and then use the accurately known activity composition relations for the binary Fe-C austenite to determine the carbon activity in the ternary Fe-M-C samples. Most of the reported studies of the effects of alloying elements have used this technique.

The results of such an equilibration method are supposed to have the highest accuracy as compared to other methods. This has been shown to be true with most alloying elements. In the case of niobium, however, the few reported equilibration measurements of the carbide solubility[12,13,16] show considerable disagreement. The uncertainty in the measured solubility limits has often not been reported. Thus there is a strong need for a comprehensive study of the solubility of niobium carbide in austenite over a wide temperature range. Extensive and reliable determinations of the carbide solubility through chemical methods are already available and the results of a properly done equilibration measurement as described above would yield more accurate solubility information and help to check on the consistency of the other data.

The Present Experimental Technique

The sealed capsule technique, employed by Källstrom and Omsen,[107] Heckler and Winchell,[108] Zupp and Stevenson,[109] Nishizawa[110] and Uhrénius and Harvig[111] held definite advantages for the present study. This technique consisted of enclosing a series of high purity Fe-Nb alloys and Fe-C alloys in a thick-walled quartz tube, evacuating the tube to a high vacuum and back-filling it with high purity H_2 gas, sealing the tube to form a capsule and then annealing it at the desired temperature. Carbon gets selectively transferred between the Fe-C and the Fe-Nb alloys which are not in physical contact. The carbon activity obtained within the capsule was determined from the final carbon content of the binary Fe-C alloy samples and the results of Ban-ya, Elliott and Chipman.[83]

The main experimental considerations in this method were:

1) preparation and evaluation of high purity Fe-Nb and Fe-C alloys;
2) accurate temperature control and establishment of a uniform temperature zone;
3) prevention of leakage of H_2 from the quartz tube;
4) establishment of equilibrium with respect to carbon content;
5) investigation of the possibility of transfer of niobium between the samples or of silicon contamination from the quartz capsule; and,
6) carbon analysis. These points are discussed in turn below.

<u>1. Preparation and Evaluation of Materials</u>: High purity Ferro-Niobium alloys supplied by the Shieldalloy Corporation and of the compositions shown in Table 4.1 were diluted to different extents with Ferrovac-E of the composition shown in Table 4.2 by argon-arc-melting. Ten Fe-Nb alloys were prepared. Reproducible Nb analysis on all the samples was carried out by spectrophotometric means. The alloy compositions are given in Table 4.3. The purpose of the present investigation being primarily the determination of the austenite/austenite+NbC_x phase boundary, most of the alloys made had Nb contents which were well outside the composition range for stability of single-phase austenite. The Fe-C samples

TABLE 4.1

Composition of the Ferro-Niobium alloys used in this study

Niobium	62-68%
Tantalum	0.25% Max
Carbon	0.10% Max
Manganese	0.05% Max
Silicon	0.20% Max
Aluminium	1.00% Max
Phosphorous	0.02% Max
Lead	0.01% Max
Tin	0.01% Max
Sulphur	0.01% Max
Nitrogen	0.02% Max
Oxygen	0.10% Max

TABLE 4.2

Composition of the Ferrvac-E iron used in this study

Iron	99.92%
Carbon	0.006
Manganese	0.001
Phosphorous	0.002
Sulphur	0.005
Silicon	0.005
Nickel	0.025
Chromium	0.001
Vanadium	0.005
Tungsten	0.001
Molybdenum	0.001
Cobalt	0.004
Copper	0.001
Tin	0.002
Aluminium	< 0.01
Nitrogen	0.00015
Oxygen	0.0012
Hydrogen	0.00006

TABLE 4.3

Niobium contents of the Fe-Nb alloys made for equilibration studies

	Wt.-% Nb
1)	0.012 ± 0.0010
2)	0.032 ± 0.0010
3)	0.056 ± 0.0010
4)	0.073 ± 0.0024
5)	0.091 ± 0.0030
6)	0.108 ± 0.0040
7)	0.315 ± 0.0050
8)	0.402 ± 0.0060
9)	0.510 ± 0.0070
10)	0.605 ± 0.0080

required for the equilibration were 0.1 to 0.4 wt %C alloys prepared by argon-arc melting of Ferrovac-F and a master high carbon (1.5 wt. %C) alloy. All the alloys were remelted several times to promote homogeneity and then were swaged into rods. The samples for the equilibration runs were obtained by rolling the rod stock to 0.5 mm thick sheets, then cutting the sheet stock into strips.

The quartz tube used for enclosing the specimens was thick-walled. The specimen arrangement is shown in Fig. 4.4. In a typical experiment up to eight alloy samples weighing ∿ 2.0 gms each were equilibrated with Fe-C samples of chosen carbon contents. The quartz tube was evacuated to 10^{-4} mm Hg, back-filled with hydrogen gas to the desired partial pressure and then sealed.

2. Temperature Control: Of obvious importance is control to maintain constant temperature. Control of the temperature profile along the carbon equilibration cell is even more critical, because the equilibrium between the H_2-CH_4 atmosphere and carbon dissolved in the sample shifts with temperature. A Lindberg Heavy Duty furnace was used in the present study. The hot zone was over 10 cms long and the quartz capsules were 7 to 8 cms long. Two Pt-Pt 10%Rh thermocouples calibrated with an external Pt-Pt 13%Rh calibration thermocouple were used to control the temperature across the 8 cm length. The total uncertainty in the temperature measurement including long-time variations was less than ± 4°C below 1100°C and ± 6°C between 1100°C and 1250°C. This is on the basis of (1) the certified accuracy of calibration of the reference thermocouple and its aging characteristics and (2) the accuracy of the measuring potentiometer.

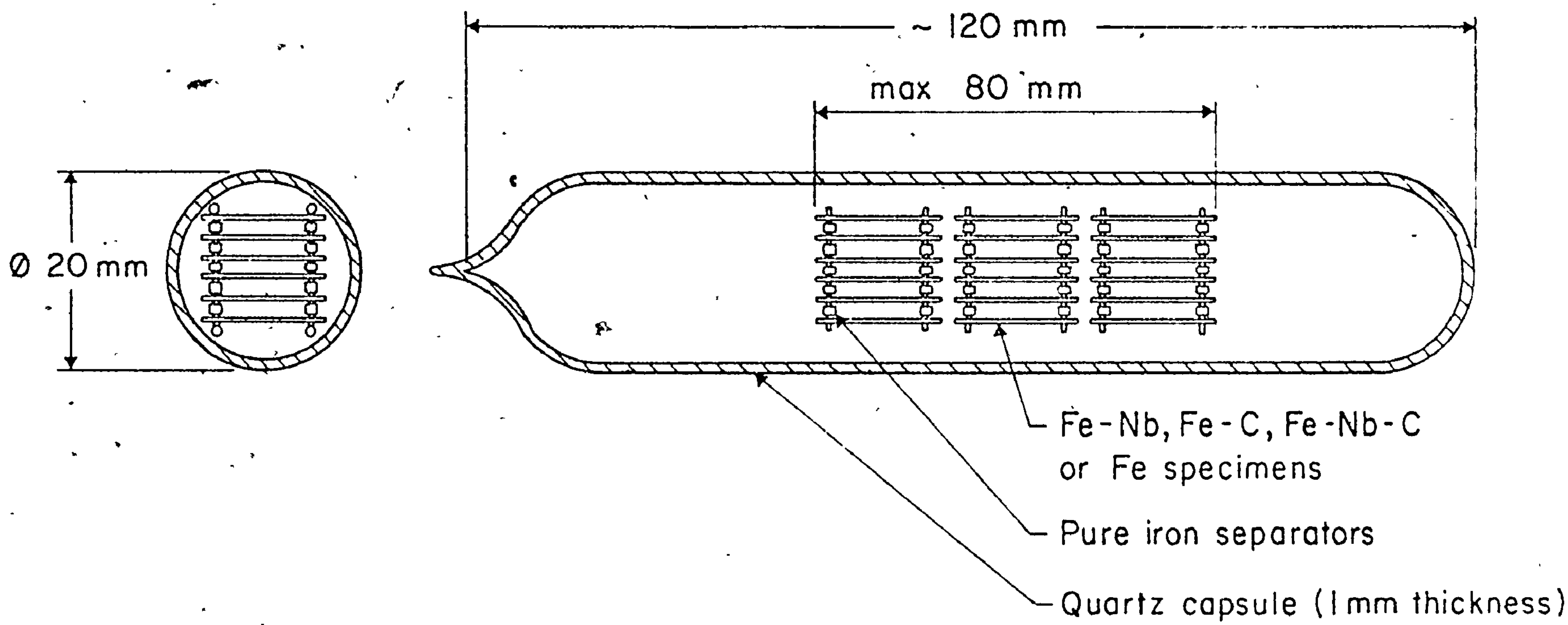

Figure 4.4 Specimen arrangement in the quartz capsule

3. Hydrogen Leakage from the Quartz Tube: It was shown by Nishizawa[110] that hydrogen, which is used as a carrier gas inside the capsules will diffuse out of the quartz tubes to a great extent within a couple of days at 1000°C. To prevent this serious loss of carbon transport capacity, which indeed is low already at the initial hydrogen pressure, a hydrogen pressure at atmospheric level was maintained outside the quartz capsule via a continuous supply of hydrogen through the furnace tube.

4. Establishment of Carbon Equilibrium: For samples of double the size used in this study, it is seen from the literature that equilibrium in a flowing H_2-CH_4 mixture, is attained within a day[12,13] at 1000°C. For the present specimen sizes and the closed capsule technique, preliminary experiments were carried out to check for equilibration times at different temperatures above 1000°C. This was first verified by equilibrating Fe-C, Fe-Nb and a pure Fe sample until the carbon content in the pure Fe sample was the same as in the Fe-C sample. Also, Fe-C, Fe-Nb, Fe-Nb-C alloy samples with the same Nb content were equilibrated until the two alloy samples with the same Nb, reached the same carbon levels. The results are shown in Table 4.5 where the approach to equilibrium from both directions (i.e., carburizing and decarburizing Fe-Nb and Fe-Nb-C alloys) are compared. Up to 1100°C, the niobium carbides dissolve rather slowly and the approach to equilibrium by decarburizing takes longer. The equilibration time in all the runs in this investigation corresponded at least to the times representative of column no. 2 in Table 4.5. All heat treatments were interrupted by quenching the capsules in brine and by breaking them at once. The surfaces were clean in general and there were no traces of oxidation. The Fe-C and the Fe-Nb-C

TABLE 4.5

Approach to Equilibrium

Temperature	Time for Equilibration (hrs) 1	2
1000°C	∿ 78	∿ 96
1050°C	∿ 48	∿ 60
1100°C	∿ 28	∿ 36
1150°C	∿ 16	∿ 20
1200°C	∿ 10	∿ 12
1250°C	∿ 7	∿ 10

1 For carburizing Fe-Nb alloys

2 For decarburizing Fe-Nb-C alloys

samples were analysed for carbon. The presence or absence of the carbides could easily be detected by an optical microscope. A few scanning electron micrographs were taken to get a clear idea of the maximum sizes and size distributions of the carbides.

5. Evaluation of the Selectivity of the Carrier Gas for Carbon: The carrier gas should selectively transfer carbon so that no correction for transfer of Nb is necessary. This behaviour was verified by annealing an Fe-C and a Ferro-niobium master alloy sample for long periods of time at 1000°C and 1250°C and analyzing the Fe-C sample for niobium. In no case was detectable transfer observed. Because silicon can increase the carbon activity, the possibility of transfer of silicon has been thoroughly examined by previous workers who had used the quartz tube technique. Up to 1200°C, no detectable silicon pick up was found in the earlier studies. In the present investigation, a pure Fe-C sample with known Si was enclosed in a H_2 atmosphere and annealed at 1250°C for two days. No detectable increase in the silicon content of the Fe-C sample occurred.

6. Carbon Analysis: Accurate analysis for low carbon, less than 0.12 wt. %C, was necessary and this could easily be achieved by the Leco conductormetric apparatus designed to analyse low carbon. The standard deviation was ± 5 ppm for the reproducibility of carbon determination in the low range (up to about 200 ppm), and a slightly higher value at higher concentrations.

4.2 STUDIES ON PRECIPITATES EXTRACTED FROM NIOBIUM-BEARING STEELS

The literature abounds with information on the methods of extracting inclusions and second-phase particles precipitated in steel. Simple and very efficient electrochemical means for isolating precipitates have been discussed by Blickwede and Cohen,[35] Andrews and Hughes,[36] Walz and Bloom[37] and Gurry et al.[38] These procedures are particularly useful in the context of the present investigation wherein the objective is to identify interstitial phases of niobium precipitated in steels. The principle in all these techniques is the same, i.e., anodic dissolution of the heat treated steel specimen under suitable conditions. Mandry and Dornelas[21] have successfully used a citrate cell for extracting carbonitrides of niobium. The advantage of an electrochemical technique is that it is conducive to extracting relatively large amounts of precipitates in a short time.

The very small amounts of niobium normally found in steels and the need for knowing the fixed and free niobium in order to determine solubility limits of the interstitial phases of niobium has resulted in the evolution of chemical dissolution techniques for isolating these phases and accurate procedures for analysing the extracted residues.[40-43]

Mori et al.,[7,18,14] who have by far done the most extensive studies on niobium compounds precipitated in steel, have used a simple chemical dissolution method to extract the precipitates quantitatively. The chemical analysis of the extracts have been done using the well-established Kawamura technique[40] in which the niobium analysis is done through an accurate spectrophotometric technique. Numerous other chemical analysis procedures are available and have been reviewed by Bhargava and Donoven.[39]

These authors have also given new and accurate procedures for analysing for niobium.

In the present investigation, solubility product determinations and precipitate identifications have been made using chemical and electrochemical methods to isolate the precipitated phases.

Preparation of Materials

Two high purity vacuum melted steels, S1 and S2, whose compositions are given in Table 4.6, were used for the present study. They were analysed particularly for nitrogen, oxygen and sulphur. About 200 gms of specimen were used for each electrolysis to yield adequate quantities of the precipitated carbides after isolation. The samples in the form of thin sheets of 4 cms x 2.5 cms x 0.3 cms were first solution treated at 1200°C and 1300°C, respectively, and quenched into brine. Isothermal heat treatments were then carried out at 1000°C for more than two weeks. The specimens were all sealed in highly evacuated and argon-back-filled quartz capsules and the argon gas at an atmospheric pressure was passed continuously through the furnace tube, around the sealed quartz tubes. The heat treatments were then interrupted by quenching in brine. The specimens always had a clean surface at the end of the heat treatments. They were then cleaned in 6 N HCl for a few minutes and then were ready for electrolysis or chemical dissolution.

Electrochemical Isolation of Precipitates

The cell assembly is shown in Fig. 4.7. An Eberbach low voltage electropolishing unit was used. Up to 50 gms of the specimens could be

TABLE 4.6

Composition of steels used for precipitate isolation studies

Steel No.	Composition, Wt-% Nb	C	N	S	O
S1	0.180	0.030	---	0.004	0.0010
S2	0.026	0.175	0.0026	∿ 0.01	∿ 0.0018

Other impurities (wt.-%) Si ∿ 0.01; P = 0.004

Ni ∿ 0.01; Mn = 0.02

Cr < 0.004, Mo < 0.004; V ∿ 0.002

Cu ∿ 0.01; Sn ∿ 0.002

Al ∿ 0.001; Total Ti ∿ 0.005

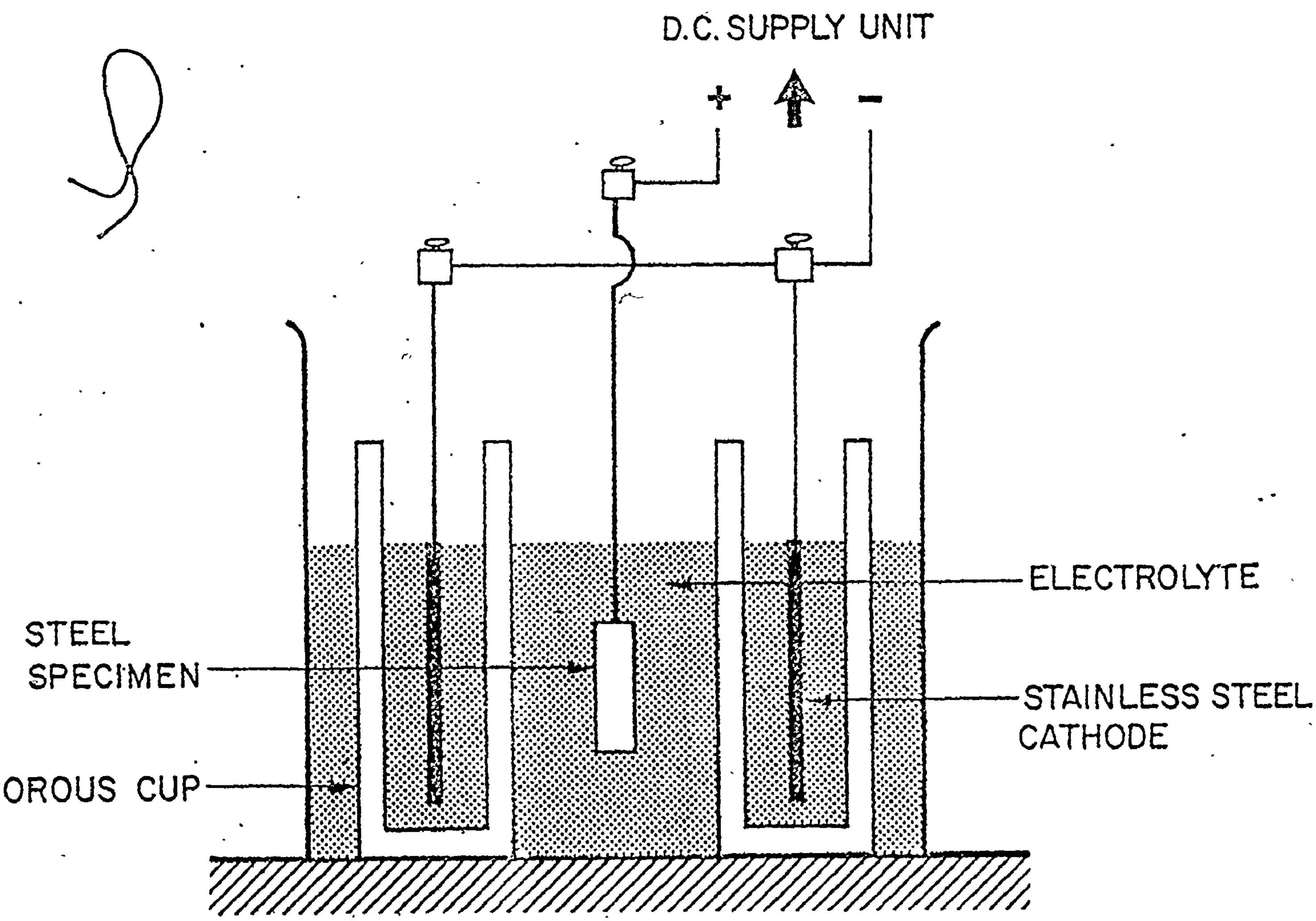

Figure 4.7 The cell assembly

held in the anode holders and the cathodes made of stainless steel plates were surrounded by porous clay cups to prevent the deposited iron from contaminating the electrolyte in which the isolated agglomerated carbides were present around the dissolving anode steel specimens.

The electrolyte consisted of 5% sodium citrate and 2% potassium bromide. The electrolying conditions were 12V and a current density of 5 ma/cm^2. It took less than 4 hrs to dissolve all the anode specimens. A 0.35 μ millipore filter was used to filter the electrolyte and retain the desired coarse residue portions. The residues were then given a series of hot cleaning treatments to dissolve away any unwanted iron and other impurities. 10% HF was used for all the cleaning purposes. The residues were oven-dried and were ready for subsequent identification.

Chemical Dissolution and Isolation of Niobium Carbides for Solubility Determinations

The steel S1, whose composition is given in the earlier section, was used. Specimens in the form of 1 cm x 1 cm x 0.1 cm were solution treated and then heat treated at various temperatures in sealed quartz tubes, in a manner described earlier. A summary of the heat treatment schedules is given in Table 5.15. 8 to 10 gms of the specimen were heat treated at each temperature. A few accurately weighed grams out of this was dissolved each time in cold 6 N HCl. Since the objective was to quantitatively determine the Nb present as precipitate, it was necessary to retain all of the residue. A 0.05 μ special membrane filter was used. The retained residues were washed and analysed for niobium using the Kawamura technique. Soluble niobium was found by subtracting from total niobium in the steel and the soluble carbon was determined from a knowledge of the precipitate compositions obtained through X-ray analysis of carbides extracted from steel S1, discussed in the next section.

Precipitate Identification

X-ray diffraction studies of the residues from steels S1 and S2 were carried out in a Debye-Scherrer cylindrical camera using a Cu-target for the X-ray source and a Ni filter so that only CuK_{α_1} and CuK_{α_2} radiations were involved in the diffraction. To obtain the resolution of the high angle reflections, a larger camera diameter of 114 mm was chosen. To minimize the background radiation, Helium was flushed through the camera throughout the exposure period. Because of the long coarsening treatments given to them, the precipitates were adequately sized to yield the desired high angle resolution. The line positions on the films were measured to deduce the 2θ values for each reflection. Standard extrapolation procedures were used to measure lattice parameters to better than 0.001 A° accuracy, this being adequate enough to identify the non-stoichiometric compounds.

CHAPTER V

EXPERIMENTAL RESULTS

5.1 EQUILIBRATION EXPERIMENTS

The carbon contents (in wt. %) as a function of niobium in the Fe-Nb alloys equilibrated at the various temperatures are shown in Figs. 5.1-5.4. The points on the vertical axis correspond to the carbon gained by the pure iron samples used in each run to check for equilibration (and are also the final carbon contents of the Fe-C samples). Points on each isoactivity line correspond to the alloy compositions within the same capsule, having been equilibrated to the same carbon potential. The carbon contents shown are an average of at least eight carbon analyses of alloy samples from two identical equilibration runs. In view of the large difference in the atomic weights of carbon and niobium, the wt. %Nb of each Fe-Nb-C alloy did not change during equilibration.

The carbon activities indicated on the graphs were calculated from the carbon contents of the binary Fe-C samples using the data of Ban-ya et al.[83]

Each alloy sample was metallographically checked for the presence of precipitated carbides and the samples in the single phase and two phase regions could clearly be delineated.

The point at which each isoactivity line changes slope, corresponds to the $\gamma/\gamma+NbC_x$ equilibrium and also represents the maximum amounts of niobium and carbon that can remain in solution in austenite at that carbon activity before precipitation of NbC_x begins. The uncertainties

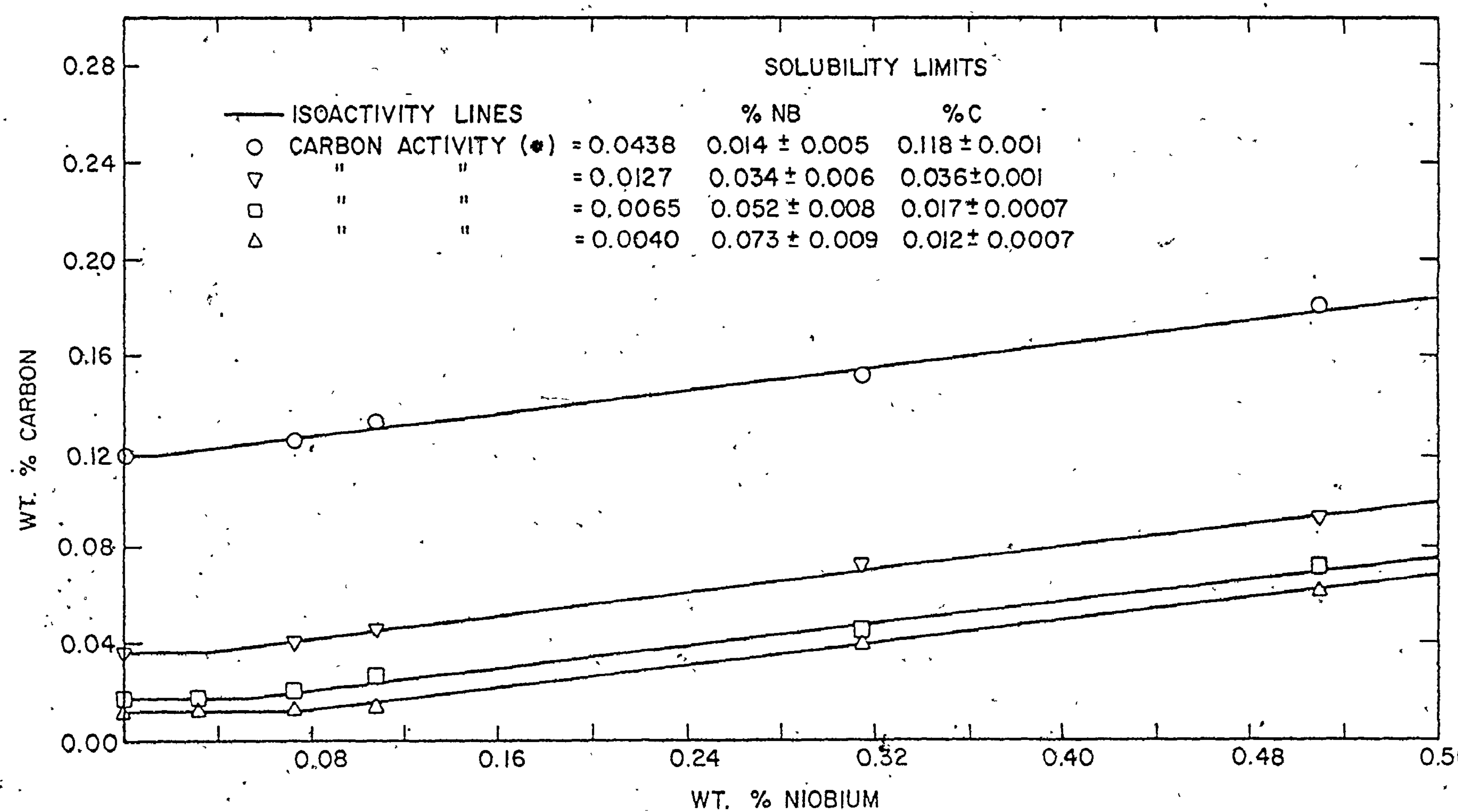

Figure 5.1 CARBON CONTENT OF FE-NB ALLOYS, EQUILIBRATED AT 1000° C

* STANDARD STATE REFERRED TO GRAPHITE

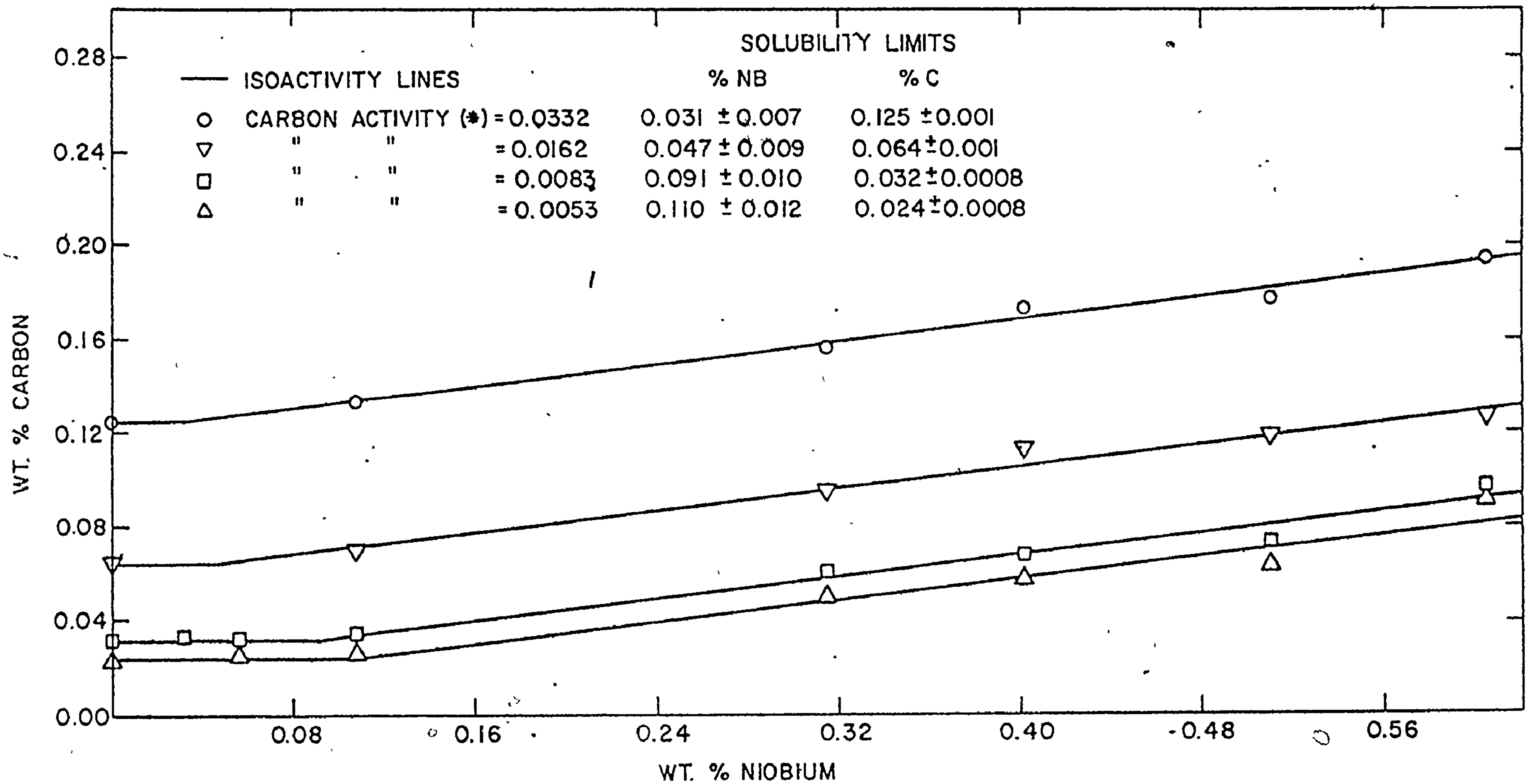

Figure 5.2 CARBON CONTENT OF FE-NB ALLOYS, EQUILIBRATED AT 1100°C

* STANDARD STATE REFERRED TO GRAPHITE

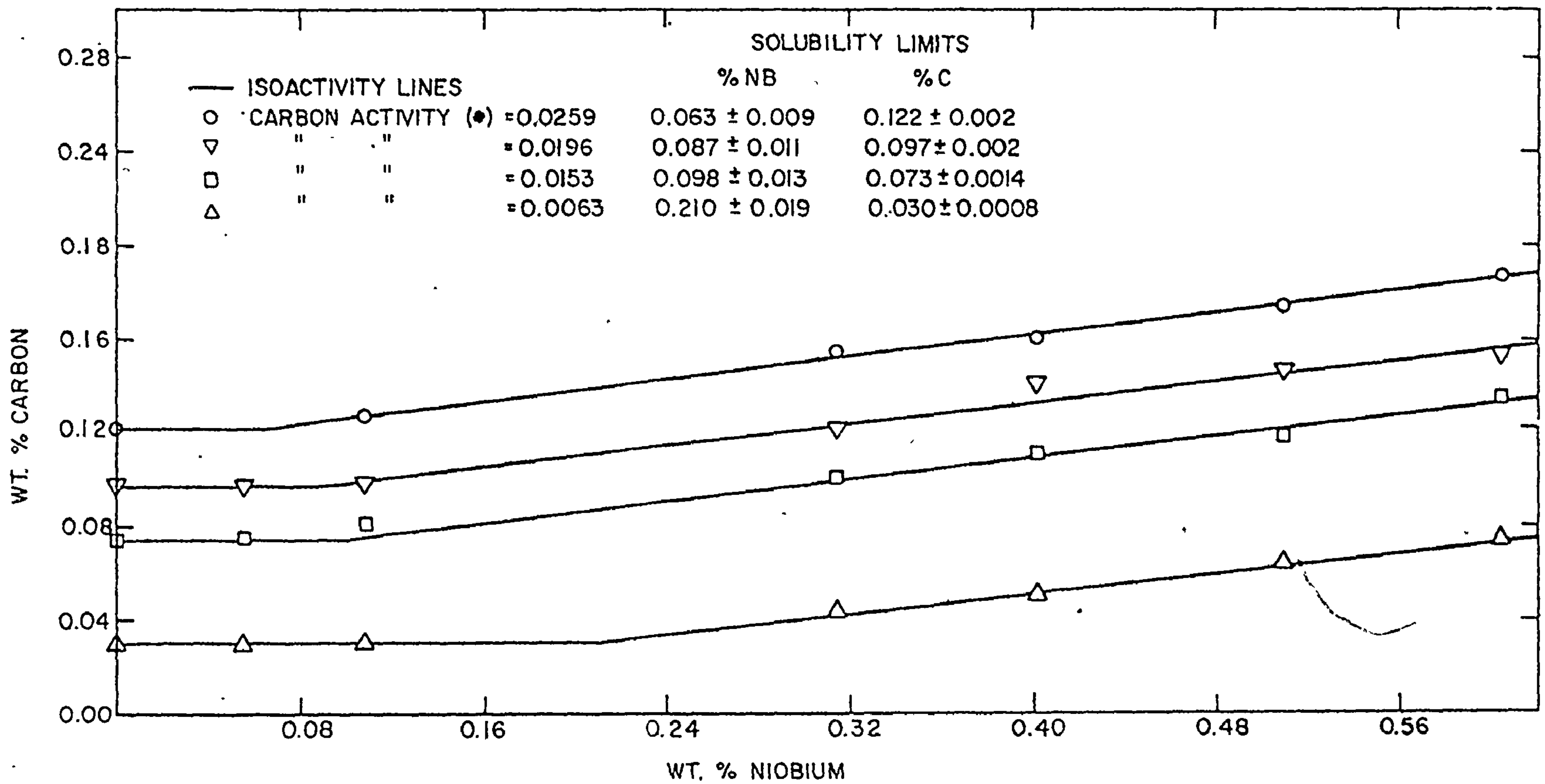

Figure 5.3 CARBON CONTENT OF FE-NB ALLOYS, EQUILIBRATED AT 1200°C

*STANDARD STATE REFERRED TO GRAPHITE

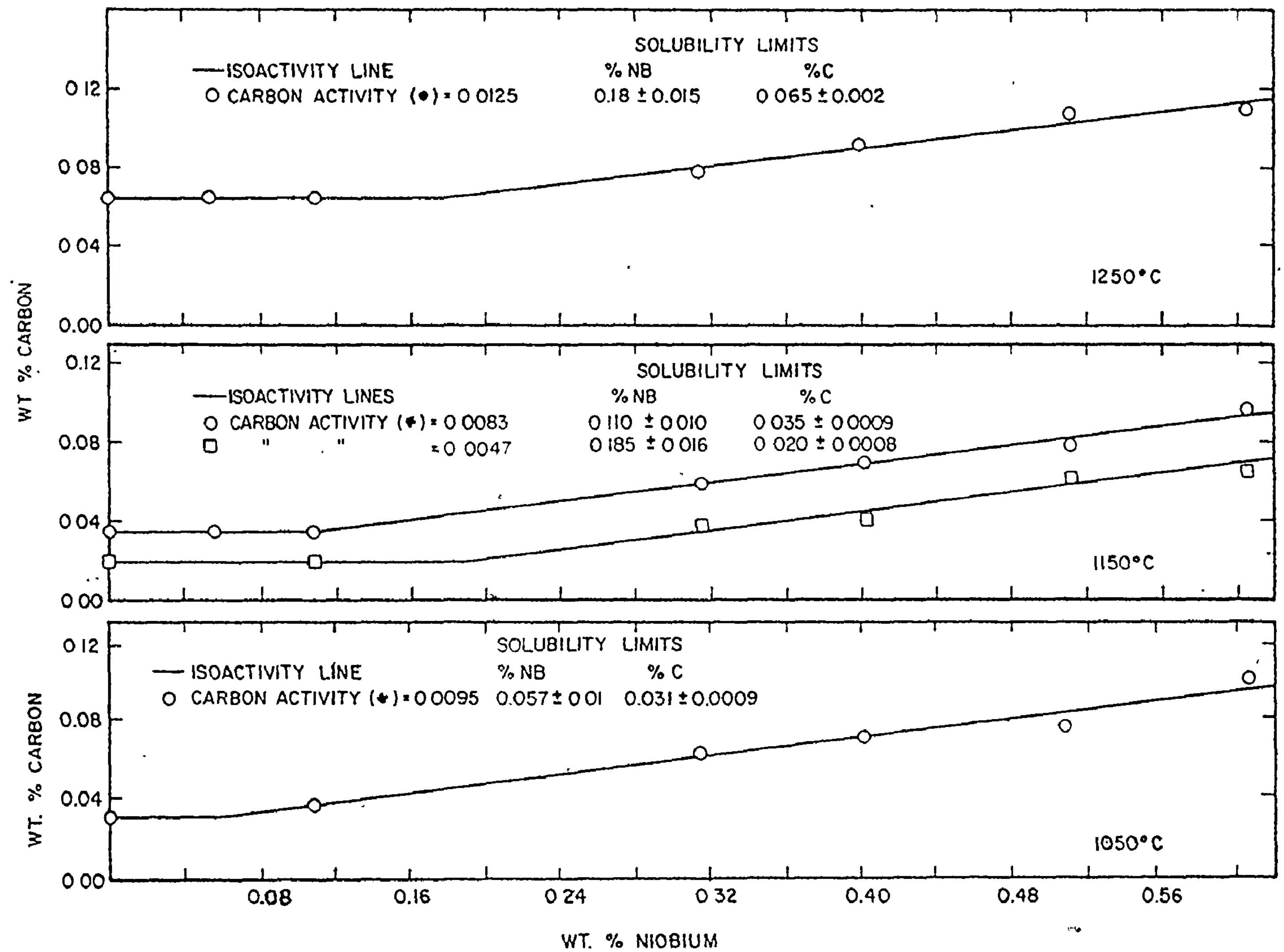

Figure 5.4 CARBON CONTENT OF FE-NB ALLOYS, EQUILIBRATED AT 1050°C, 1150°C AND 1250°C

• STANDARD STATE REFERRED TO GRAPHITE

in both the niobium and carbon contents have been used to estimate the errors in the tie lines. At each carbon activity, the possible changes in slopes of the straight lines that represent the best linear least squares fit of the points in the two phase and the single phase region have been taken into account in arriving at the solubility limits indicated on the graphs. In many cases, however, horizontal lines have necessarily been drawn in the single phase region corresponding to the binary carbon level. The uncertainty recorded for each of the solubility limits represents the maximum deviation and thus corresponds approximately to a 95% confidence limit.

5.2 CHEMICAL ANALYSIS OF EXTRACTED PRECIPITATES

The results of the chemical analysis of carbides extracted from steel S1, are shown in Table 5.5. The carbide present in this steel at 1000°C was identified below as $NbC_{0.9}$. The soluble niobium and carbon were calculated from the total amounts of niobium and carbon in the steel S1 and the mean value of niobium present as carbide.

5.3 IDENTIFICATION OF PRECIPITATES

The results of X-ray analysis of the precipitates extracted from steels S1 and S2, held at 1000°C, are given in Tables 5.6 and 5.7. The lattice parameters of the precipitates are given in the same table along with the respective uncertainties.

The lattice parameter of the precipitate in steel S1 was compared with the results of Kempter et al.[29] and identified as $NbC_{0.9}$. The data of Brauer and Lesser[26] has been utilized to identify the carbonitride

TABLE 5.5

The details of residuum analysis (steel S1)

Temp. of Austenitization T C	950	1000	1050	1100	1150	1200
Holding time (hrs)	120	100	94	48	48	12
Nb 10^3 (gms) present as ppt. per 100 gms. of steel dissolved.						
Residue 1	136	98	84	32	--	--
Residue 2	127	113	104	47	20	--
Residue 3	144	128	102	70	24	--
Residue 4	134	120	90	60	--	--
Mean Value	135	115	95	52	22	0
wt. %Nb in solution in austenite (Total Nb-fixed Nb)	.045	.065	.085	.128	.158	.180
wt. %C in solution (Total %C-fixed Nb x 0.87 x $\frac{12.01}{92.91}$)	.015	.017	.019	.024	.028	--
$\log[\%Nb][\%C]^{0.87}$	-2.93	-2.73	-2.57	-2,30	-2.15	--

$$\log K_C' = 2.7 - \frac{6900}{T} \pm 0.12$$

TABLE 5.6

X-ray Analysis of Precipitate from Steel S1

Diffraction conditions

Type of Camera: Debye-Scherrer cylindrical
Camera diameter: 114 mm
Radiation: CuK_α
Filter: Ni
Exposure time: 6½ hrs.
Atmosphere: Helium

Line	hkℓ	Radiation	R.I.	2θ	$\cancel{\sin^2\theta}$	a(A°)
1	111	$K\alpha_1$	100	35.71	0.0940	4.355
2	200	$K\alpha_1$	75	41.52	0.1256	4.346
3	220	$K\alpha_1$	50	59.83	0.2487	4.369
4	311	$K\alpha_1$	40	71.50	0.3405	4.378
5	222	$K\alpha_1$	20	74.92	0.3699	4.387
6	331	$K\alpha_1$	20	98.90	0.5774	4.419
7	420	$K\alpha_1$	25	102.54	0.6086	4.416
8	420	$K\alpha_2$	15	102.94	0.6120	4.414
9	422	$K\alpha_1$	25	116.84	0.7258	4.429
10	422	$K\alpha_2$	15	117.32	0.7295	4.429
11	333,511	$K\alpha_1$	25	128.70	0.8126	4.440
12	333,511	$K\alpha_2$	15	129.27	0.8165	4.440
13	440	$K\alpha_1$	25	155.38	0.9546	4.460
14	440	$K\alpha_2$	15	156.73	0.9593	4.460

R.I. = Relative Intensity; $K\alpha_1$ = 1.54051 A°; $K\alpha_2$ = 1.54433 A°

Extrapolated lattice parameter = 4.465 ± 0.001 A°

compound = $NbC_{0.9}$

TABLE 5.7

X-ray Analysis of Precipitate from Steel S2

Diffraction conditions

Type of Camera: Debye-Scherrer cylindrical
Camera diameter: 114 mm
Radiation: CuK_α
Filter: Ni
Exposure time: 6½ hrs.
Atmosphere: Helium

Line	hkℓ	Radiation	R.I.	2θ	$\sin^2\theta$	a(A°)
1	111	$K\alpha_1$	100	35.71	0.0940	4.355
2	200	$K\alpha_1$	75	41.51	0.1256	4.351
3	220	$K\alpha_1$	50	59.82	0.2486	4.373
4	311	$K\alpha_1$	40	71.38	0.3404	4.353
5	222	$K\alpha_1$	20	74.88	0.3696	4.393
6	331	$K\alpha_1$	20	98.80	0.5765	4.433
7	420	$K\alpha_1$	25	102.42	0.6075	4.419
8	420	$K\alpha_2$	15	102.82	0.6109	4.418
9	422	$K\alpha_1$	25	116.69	0.7246	4.433
10	422	$K\alpha_2$	15	117.16	0.7282	4.433
11	333,511	$K\alpha_1$	25	128.50	0.8113	4.444
12	333,511	$K\alpha_2$	15	129.09	0.8153	4.444
13	440	$K\alpha_1$	25	154.95	0.9530	4.463
14	440	$K\alpha_2$	15	156.27	0.9577	4.463

R.I. = Relative Intensity; $K\alpha_1$ = 1.54051 A°; $K\alpha_2$ = 1.54433 A°

Extrapolated lattice parameter = 4.469 ± 0.001 A°

compound = $NbC_{0.91}N_{0.04}$

in steel S2 as $NbC_{0.91}N_{0.04}$.

5.4 $\gamma/\gamma+NbC_x$ PHASE BOUNDARIES IN THE TEMPERATURE RANGE 1000°-1250°C

The calculated $\gamma/\gamma+NbC_x$ phase boundaries along with the present experimental information and all the reported solubility data (discussed in Chapter II) are present in Figs. 5.8-5.13.

The following average solubility product is yielded by the results of the present equilibration experiments:

$$\log[\%Nb][\%C]^{0.87} = 3.4 - \frac{7920}{T}$$

~~and th~~is has been calculated as indicated in Table 5.14.

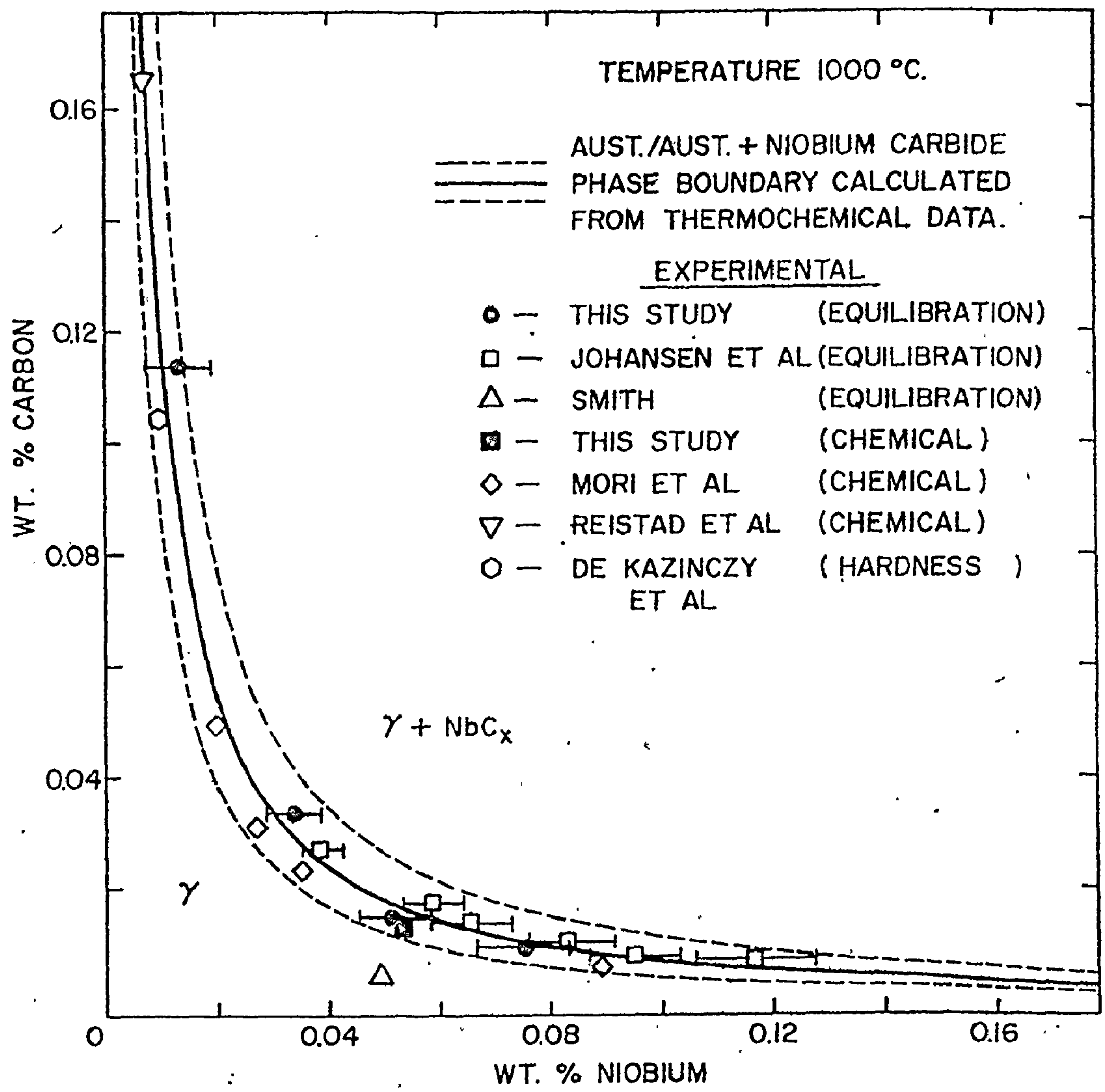

Figure 5.8 $\gamma/\gamma+NbC_x$ phase boundary at 1000°C

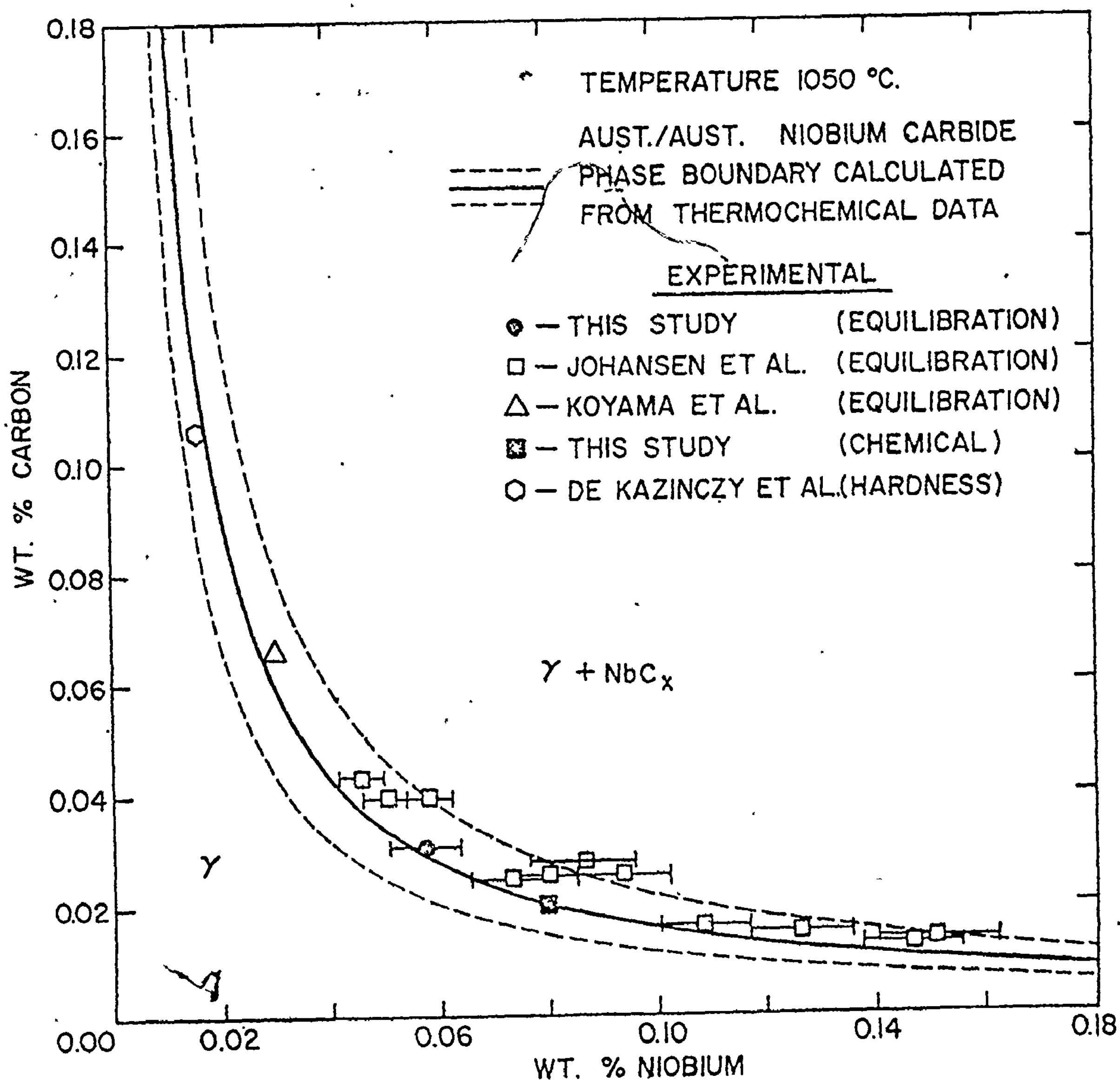

Figure 5.9 $\gamma/\gamma+NbC_x$ phase boundary at 1050°C

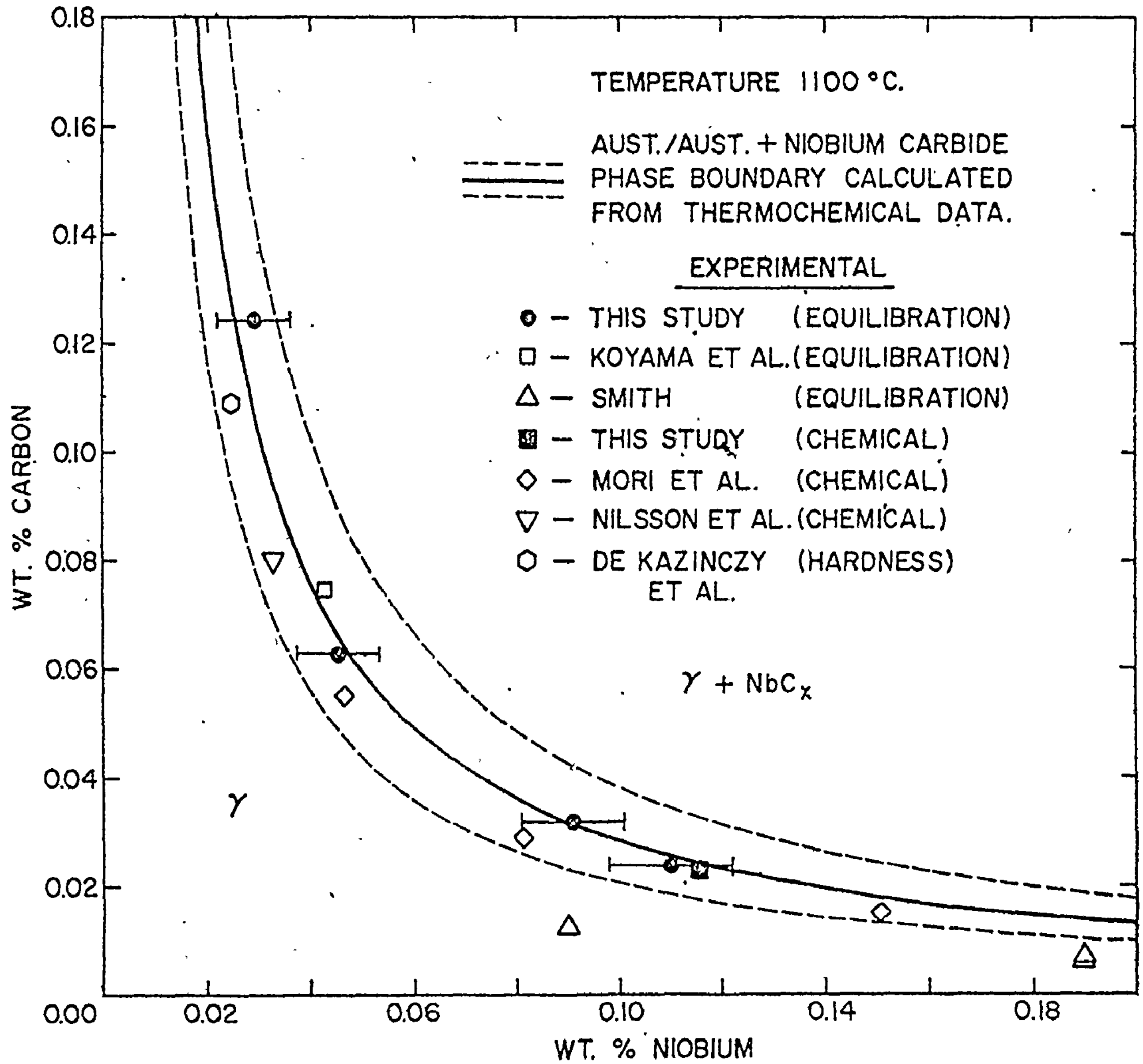

Figure 5.10 $\gamma/\gamma+NbC_x$ phase boundary at 1100°C

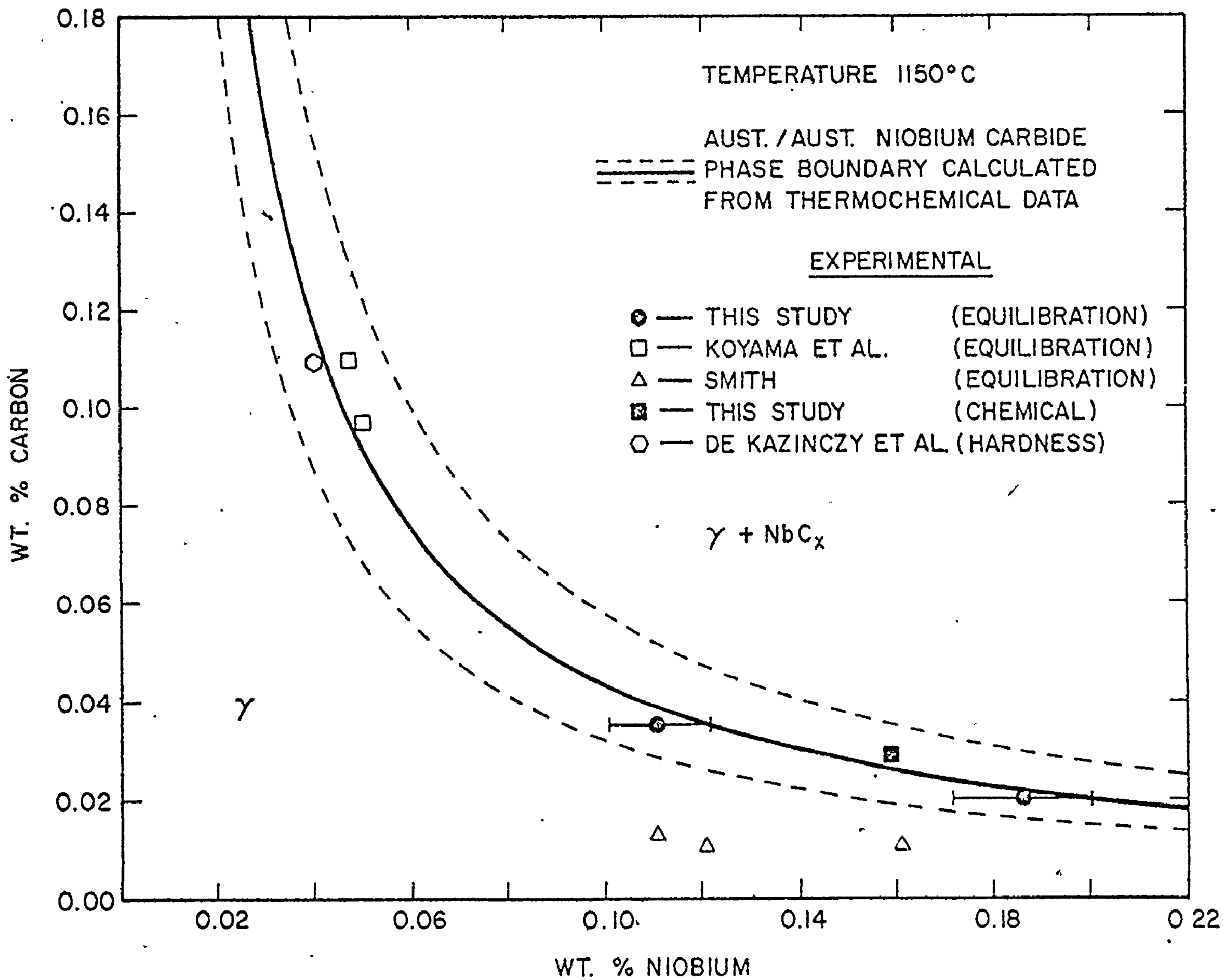

Figure 5.11 $\gamma/\gamma+NbC_x$ phase boundary at 1200°C

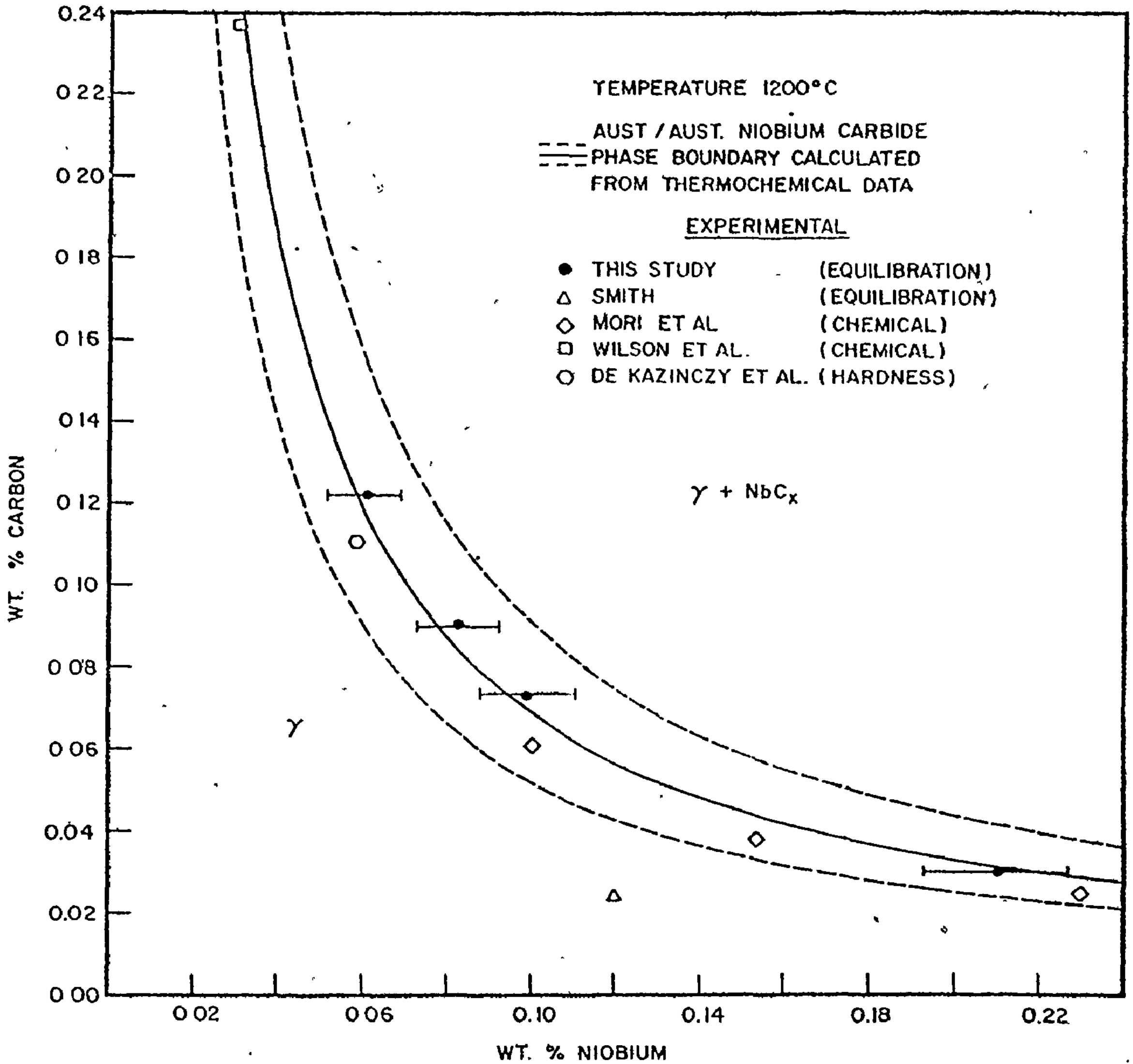

Figure 5.12 γ/γ+NbC_x phase boundary at 1200°C

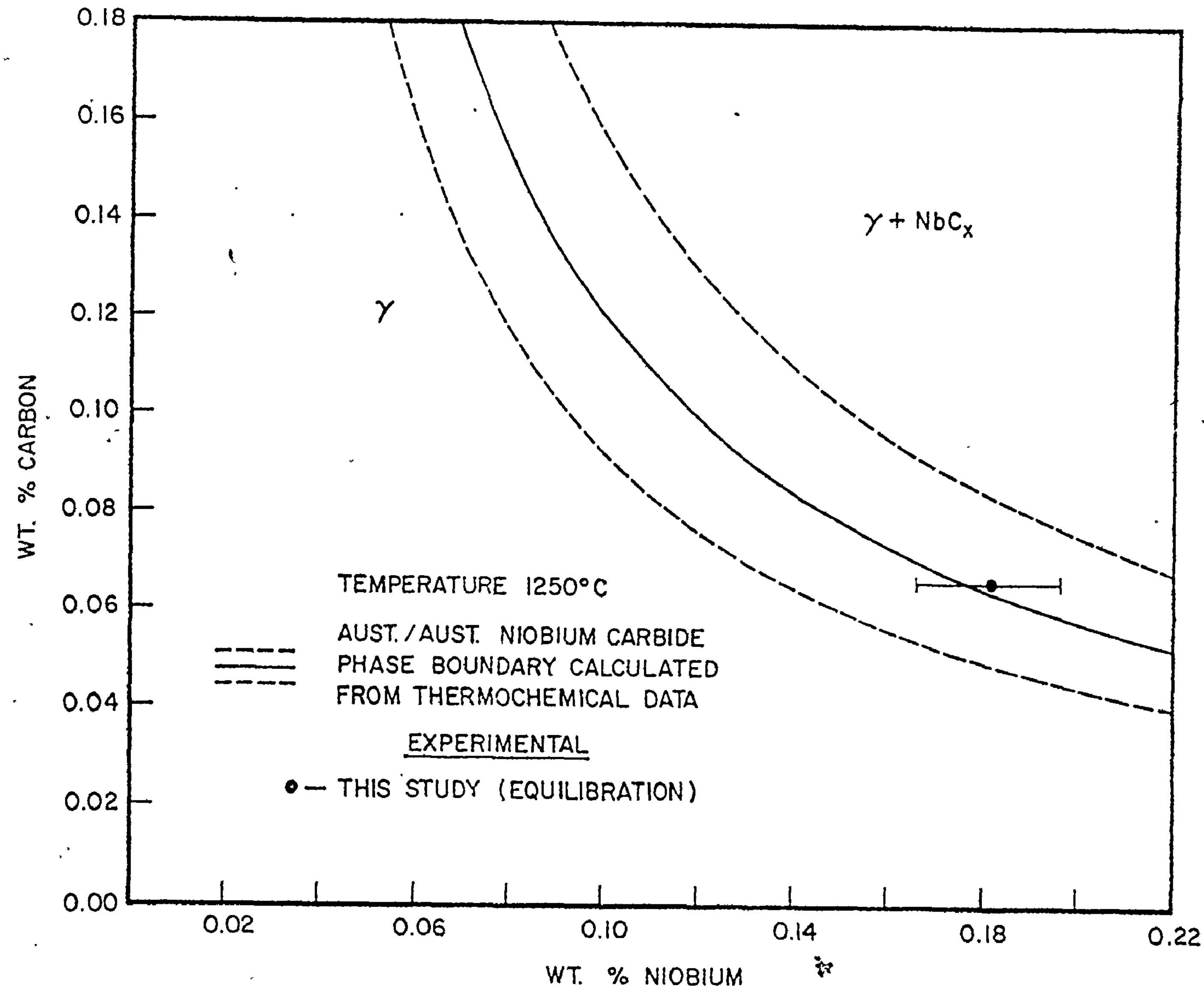

Figure 5.13 $\gamma/\gamma+NbC_x$ phase boundary at 1250°C

TABLE 5.14

Solubility products from equilibration studies

T°C	Solubility Limits %Nb	%C	$\text{Log}[\%Nb][\%C]^{0.87}$
1000	0.014	0.118	-2.66 ± 0.19
	0.034	0.036	-2.72 ± 0.12
	0.052	0.015	-2.85 ± 0.07
	0.073	0.010	-2.88 ± 0.06
1050	0.057	0.031	-2.56 ± 0.06
1100	0.031	0.125	-2.29 ± 0.09
	0.047	0.064	-2.37 ± 0.08
	0.091	0.032	-2.34 ± 0.05
	0.110	0.024	-2.35 ± 0.06
1150	0.110	0.035	-2.23 ± 0.05
	0.185	0.020	-2.21 ± 0.06
1200	0.063	0.122	-2.00 ± 0.07
	0.087	0.097	-1.94 ± 0.06
	0.098	0.073	-2.00 ± 0.06
	0.210	0.030	-2.00 ± 0.05
1250	0.180	0.065	-1.78 ± 0.05

CHAPTER VI

DISCUSSION AND CONCLUSIONS

The first objective of this investigation has been to generate a self-consistent phase diagram for the Fe-Nb-C system over relevant temperature and composition ranges through detailed experiments and theoretical calculations using direct and indirect data available in the literature. The second objective has been to account for the influence of nitrogen and alloying elements and thus extend the earlier results to the quaternary Fe-Nb-C-N and higher order systems.

The empirical equations in Table 3.6, the tie line relations in Fig. 3.7, the solubility products from direct equilibration and residuum analysis experiments, Tables 5.5 and 5.14, and the phase diagrams in Figures 5.8-5.13 describe the complete information obtained through this study, and together these characterize the complete austenite-niobium carbide equilibrium. The estimated solubility products of the metastable cubic nitride (Table 3.13) along with the carbide solubility information has enabled the characterization of the austenite-niobium carbonitride equilibrium via certain justifiable assumptions and the thermodynamic equations generated therefrom (Eqs. 3.21-3.25). The evaluated alloy interactions (Table 3.20) further enable us to include the effect of alloying elements on the solution behaviour of the interstitial phases of niobium in austenite.

In this chapter, the accuracy and completeness of the present experimental and theoretical calculations are first compared with the results of other investigators. The utility of the method devised for predicting carbonitride solubilities are also discussed. Some conclusions regarding the usefulness of the tie line relations (Fig. 3.7) in estimating quaternary solubility information are drawn. The relevance of the present study to practical situations is briefly highlighted and some possibilities for future work suggested.

6.1 ACCURACY OF THE $\gamma/\gamma+NbC_x$ PHASE BOUNDARIES CALCULATED USING THERMOCHEMICAL DATA

The accuracy of the calculated phase diagram depends ultimately on the uncertainties in the recorded free energy of formation (or mixing). These uncertainties arise from (i) the uncertainty in the reference heats of formation ($\Delta H^\circ_f(298)$) values over the composition range of the carbide, (ii) errors in recorded specific heat data over the temperature range, (iii) errors in the activity data for the binary Fe-C system, and (iv) weaknesses in the assumption of ideal solution behaviour for niobium in austenite.

The first error has been shown not to exceed ± 700 cal/mol-niobium at the 2σ level. The uncertainties in the thermal functions of the carbide, carbon and niobium introduce estimated errors of ± 300 cal/mole-niobium, ± 200 cal/mole-carbon and ± 400 cal/mole-niobium, respectively. The carbon activity data of Ban-ya et al.[83] have been shown to be very accurate and the uncertainty is certainly less than ± 150 cal/mole-carbon. The assumption of an ideal behaviour of niobium in austenite should not cause an error greater than ± 400 cal/mole-niobium.

The maximum uncertainty in the integral free energy of mixing of each carbide NbC_x is therefore $\approx \pm (1200/(1+x))$ cal/mole-niobium carbide at the 2σ level. Over the composition range ($x = 0.7$-0.98) of the carbide therefore, the error is not more than 800 cal/mole-carbide Consequently, the uncertainties in the empirical log (%C) values in Table 3.6 that describe the phase boundaries are not greater than the uncertainties indicated. The error bands on Figs. 5.8-5.13 reflect this estimated maximum uncertainty.

Nordberg and Aronsson[6] calculated a solubility product for the carbide $NbC_{0.87}$ using thermochemical data but erroneously estimated the free energy of solution of niobium in austenite as ~ -3500 cal/mole. Largely due to this, their calculated solubility product (Eq. 2.5) was in rather poor agreement with the observations.

In closing this section it is to be remarked that the thermodynamic data base for this system is by far the best among the refractory compounds, resulting in the excellent correlation with experiments to be seen in Figs. 5.8-5.13

6.2 COMPARISON OF THE THERMODYNAMIC CALCULATIONS WITH THE PRESENT AND PUBLISHED CARBIDE SOLUBILITY DATA

Referring to Figs. 5.8-5.13 and the experimental points designated by the term "Equilibration" we see that the predictions, our results and the results of Koyama et al.[88,89] are in excellent agreement. The conspicuous discrepancy in the results of Smith[12] has been attributed to high nitrogen contents in their starting materials.[6] The solubility determinations of Johanssen et al.,[13] though extensive, were subject to systematic errors. They equilibrated a single Fe-Nb-C and Fe samples at different carbon potentials. Subtracting the carbon gained by the pure Fe samples (which is equal to the limiting carbon solubility in the ternary Fe-Nb-C austenite at that carbon activity) from the carbon content of the Fe-Nb-C alloy after equilibration and assuming a stoichiometric carbide NbC, they calculated the soluble niobium by mass balance. This procedure for determining soluble niobium is bound to introduce large systematic errors. This is clearly evidenced in their results at 1050°C and 1000°C. Indeed, whereas their experimental points ought to lie to the left of the phase boundary in view of their incorrect assumption of a stoichiometric carbide, they all lie to the right.

In view of the differing results from the various direct equilibration techniques, we conclude that the closed capsule technique adopted in the present study and proved to be equally efficient at even lower carbon activities,[109-111] is probably the most suitable for studies on strong carbide formers.

The two apparent disadvantages in the present technique are the long equilibration times required and the accompanying problems of temperature control and hydrogen leakage. However, both of these can be overcome by careful experimentation.

Referring next to the experimental points designated by the term "chemical" we note that the results of Mori et al.[7] are the most comprehensive among the carbide solubility data obtained through chemical analysis of isolated precipitates. Their experiments are particularly noteworthy in that the standard deviations in their niobium analyses are only ± 10 ppm. Their solubility determinations agree reasonably well with the presently calculated phase boundaries and all our own results. However, all their values tend to be lower which lends support to their own conclusions that their precipitates may have had small amounts of dissolved nitrogen.

Our own results by the chemical method are less comprehensive and our chemical analyses were less accurate as can be seen in Table 5.5. At the same time, our steel S1 was nitrogen free. Generally, our measurements agree with the predictions and the consensus of experimentation. The measurements of Nilsson et al.,[6] Reistad and Stehlstedt[11] and Wilson[10] are less comprehensive and of limited accuracy as admitted by the respective authors.

Referring finally to the points designed by the term "Hardness" we note that the hardness measurements of de Kazinczy et al.[8] have been recalculated and reinterpreted by Nordberg and Aronsson.[6] The latter's reinterpretation was based on the well-known fact that the hardness of mild steels containing niobium increase linearly with ℓ^{-1}, 'ℓ' being the average distance between particles of niobium carbide precipitated in ferrite (Orowan-type mechanism). This corrected the assumption of de Kazinczy et al.[8] that the mechanism was of the Mott-Nabarro type. The hardness measurements of de Kazinczy et al.[8] shown on the phase diagrams correspond to the recalculated solubility products. While solubility values obtained through hardness measurements involve large uncertainties, they show surprisingly good agreement with theory and the other determinations.

6.3 PRECIPITATE IDENTIFICATION BY X-RAY ANALYSIS

Turning to Fig. 3.7 it is noted that the carbide $NbC_{0.9}$ identified in steel S1 by lattice parameter measurements (Table 5.6) and the corresponding soluble carbon and niobium (Table 5.5) agree very well with the tie line relation at 1000°C. The carbonitride composition $NbC_{0.91}N_{0.04}$ in steel S2 estimated from lattice parameter measurements (Table 5.7) should also be close to the actual value. Indeed, the approximate carbon in solution in austenite at 1000°C for this steel is ≈ 0.16 wt.% so if we add on the nitrogen and treat the total as an equivalent carbon, the nonstoichiometry (x+y) from Fig. 3.7, can be deduced as 0.95. This tends to support the inferences of the X-ray results and to indicate a possible method of estimating the nonstoichiometry of niobium carbonitrides (to be discussed later).

Mori et al.[7] have analysed precipitates chemically and by X-ray means. Their results for the chemical analysis of carbides is given in Fig. 3.12. Besides, they identified carbide compositions between $NbC_{0.85}$ and $NbC_{0.89}$ by X-ray analysis of precipitates extracted from low carbon steels, heat treated at 1000°C. Their carbonitride identifications have been discussed in Chapter II.

6.4 THE ESTIMATED SOLUBILITY PRODUCTS OF METASTABLE NIOBIUM NITRIDE AND THE TREATMENT OF NIOBIUM CARBONITRIDE-AUSTENITE EQUILIBRIUM

The comparisons in Table 3.13 indicate that the inferred solubility products of the metastable nitride represent good estimates. Also, referring to Fig. 3.15 which compares the C:(C+N) values for the predictions and experiments, the agreement is very good. Estimated deviations of the solubility products K'_C and K'_N at the 95% (2σ) level were invoked to estimate the maximum uncertainties in the predicted compositions. The greatest deviations in the predicted ratios are obtained when the deviations in K'_C and K'_N are of opposite sign and these are the deviations (now at possibly greater than the 2σ confidence level) indicated in Fig. 3.15. The uncertainty in the ratio due to the uncertainty of the K' values is greater when equiatomic proportions of carbon and nitrogen are present in the precipitate than when a large excess carbon is present. Since deviations from the theoretical line tend to be random rather than systematic, it appears unlikely that the discrepancies are due only to error in the solubility product values, K'_C and K'_N.

The agreement between prediction and experiment for both the C:(C+N) values and quaternary austenite compositions is considerably better than found by Hudd et al.,[87] suggesting that the revised assumptions concerning a carbonitride of fixed nonstoichiometry are good approximations to the truth. Earlier authors,[6,87] who assumed a stoichiometric carbonitride, had admitted their inability to treat the carbonitride as a nonstoichiometric compound. The present procedure, with the postulation of a metastable nitride, $NbN_{0.87}$, clearly demonstrates that such an improved procedure is possible.

It is noted finally that the predictions of the austenite composition and the C/C+N ratios of the carbonitride are quite insensitive to the assumption of fixed nonstoichiometry (x+y) and to small changes in the particular value of (x+y) chosen. This salutory result, which is a consequence of the extreme diluteness of all the alloys of interest, allows one to make an improved estimate of the nonstoichiometry, without recourse to further iteration of the austenite composition or C/C+N ratios.

If one postulates that for high C/C+N ratios nitrogen substitutes for carbon in a completely neutral manner (recall the ideality assumption for the NbC_x, NbN_x mixture) then the nonstoichiometry can be estimated from Fig. 3.7 by substituting C+N for C in the ordinate. Unfortunately, the data on nonstoichiometry is insufficiently accurate or comprehensive at this time to test this possible refinement.

6.5 RELEVANCE TO COMMERCIAL PRACTICE

It has already been demonstrated that the method devised for predicting the austenite-niobium carbonitride equilibrium can be used to estimate the precipitate fractions. If the method is applied to commercial materials, the calculated amounts of niobium carbide/carbonitride present at equilibrium should be interpreted as maximum possible amounts. Given a steel composition, the temperature for complete solution can be calculated or inversely, the steel chemistry can be adjusted to satisfy desired solution treatments, using the present method.

6.6 SUGGESTIONS FOR FUTURE WORK

In a commercial steel, elements other than carbon and nitrogen (i.e., oxygen and sulphur) will be present which may form compounds with niobium if present in sufficient quantity and the Fe-Nb-C-N equilibrium will be modified. Providing appropriate thermodynamic modelling it should be possible to take into account the influence of oxygen and sulphur in a rigorous way.

The very close similarity in the behaviours of carbon and nitrogen in solution in austenite and the success achieved with the present method indicates that the method should also be applicable to other carbonitrides in steels containing say titanium, tantalum, vanadium or zirconium. The method could also be readily modified to cover carbonitrides containing more than one alloying element, e.g., the mixed carbonitride of niobium and tantalum.[116] Application to steels which form oxy-sulphides is also possible in principle - although in this instance the problem is complex for oxygen and sulphur dissolved in steel behave differently than carbon and nitrogen.

Interaction of carbides and carbonitrides with ferrite is also of great interest since the scavenging effect is to reduce those interstitial solutes which cause strain aging. Extension of Hudd's work[87] using the present methodology would appear to be useful.

REFERENCES

1. C. Wagner: Thermodynamics of alloys, p. 51, Addison-Wesley, Reading, Mass., U.S.A., 1952.
2. S.R. Keown and F.B. Pickering: Proc. Conf. on "Creep Strength in Steel and High Temperature Alloys", p. 134, 1974, London (Metals Society).
3. J. Wadsworth _et al._: Met. Sci., _10_, p. 105, 1976.
4. J. Wadsworth _et al._: Met. Sci., _10_, p. 342, 1976.
5. H. Schenk and E. Steinmetz: Stahleisen-Sonderberichte, _7_, p. 27, p. 32, 1966.
6. H. Nordberg and B. Aronsson: JISI, _206_, p. 1263, 1968.
7. T. Mori _et al._: Tetsu-to-Hagane, _54_, p. 764, 1968.
8. F. de Kazinczy _et al._: Jernkont. Ann., _147_, p. 408, 1963.
9. L. Meyer: Dissertation Claustthal Berg. Hütten, 1966.
10. J.L. Wilson and D. Geiselman: Union Carbide Tech., Rep. R-62-15, 1962.
11. T. Reistad and P. Sehlstedt: Jernkont. Ann., _151_, p. 950, 1967.
12. R.P. Smith: Trans. AIME, _236_, p. 220, 1966.
13. R.H. Johansen _et al._: Trans. AIME, _239_, p. 1651, 1967.
14. J.R. Brown: GKN Group Res. Lab., Rep. no. 796, 1965.
15. K. Narita and S. Koyama: Jap. Inst. of Metals Jl. _52_, p. 292, 1966.
16. S. Koyama _et al._: Jap. Inst. of Metals Jl. _35_, p. 1090, 1971.
17. R.P. Smith: Trans. AIME, _224_, p. 190, 1962.
18. T. Mori _et al._: Tetsu-to-Hagane, _50_, p. 911, 1964.
19. K.J. Irvine _et al._: JISI, _205_, p. 161, 1967.
20. P. Duwez and F. Odell: J. Electrochem. Soc., _97_, p. 279, 1950.

21. P. Mandry and W. Dornelas: Comptes. Rend., 263, p. 1118, 1966.

22. T. Mori et al.: Tetsu-to-Hagane, 51, p. 2031, 1965.

23. E. Storms et al.: J. High-Temp. Sci., 1 , p. 430, 1969.

24. Ya. S. Umanski: Zhur. Fiz. Khim., 14, p. 332, 1940.

25. G. Brauer et al.: Z. anorg. chem., 277, p. 249, 1954.

26. G. Brauer and R. Lesser: Z. Metallkunde., 50, p. 8, 1959.

27. E.K. Storms and N.H. Krikorian: J. Phys. Chem., 63, p. 1747, 1959.

28. C.P. Kempter and M.R. Nadler: J. Chem. Phys., 32, p. 1477, 1960.

29. C.P. Kempter et al.: J. Chem. Phys., 33, p. 1873, 1960.

30. E.K. Storms and N.H. Krikorian: J. Phys. Chem., 64, p. 1471, 1960.

31. R.W. Guard et al.: Trans. TMS-AIME, 239, p. 643, 1967.

32. N. Terao: Jap. J. of App. Phys., 4, p. 353, 1965.

33. N. Terao: J. of the Less Common Met., 23, p. 159, 1971.

34. G. Brauer and R. Lesser: Z. Metallkunde, 50, p. 487, 1959.

35. D.J. Blickwede and M. Cohen: Met. Trans., 185, p. 578, 1949.

36. K.W. Andrews and H. Hughes: Irons and Steel, 31, p. 43, 1958.

37. H. Walz and R.A. Bloom: J. or Metals, 12, p. 928, 1960.

38. R.W. Gurry et al.: Transactions of the ASM, 50, p. 105, 1958.

39. O.P. Bhargava and J.F. Donoven: "Spectrophotometric Determination of Niobium in Steels with PAR Direct and Preconcentration Methods", STELCO Internal Report, 1973.

40. K. Kawamura et al.: Nippon Kinzoku., 32, p. 180, 1968, BISI trans. 6650.

41. P. Schwaab and G. Langenscheid: Metallography, 9 , p. 74, 1971.

42. H.S. Karp et al.: Mat. Res. Bull., 2, p. 311, 1967.

43. G.K. Krapf et al.: JISI, 211, 353, 1973.

44. E.K. Storms: The Refractory Carbides, Academic Press, New York and London, 1967.

45. H.H. Hausner and M.A. Bowman: Fundamentals of Refractory Compounds, p. 67, Plenum Press, New York, 1968.

46. L.E. Toth: Transition Metal Carbides and Nitrides, Academic Press, New York and London, 1971.

47. R.A. Rapp: Physico Chemical Measurements in Metals Research, John Wiley-Interscience Publishers, 1970.

48. E.J. Huber et al.: J. Phys. Chem., 65, 1846, 1961.

49. A.D. Mah and B.J. Boyle: J. Am. Chem. Soc., 77, 6512, 1955.

50. A.N. Kornilov et al.: Moscow Univ., Vestnik Seriia Khim., 17, p. 8, 1962.

51. F.G. Kusenko and P.V. Gel'd: Izv. Sibirsk. Vtd. Akad. Nauk SSSR, 2, p. 46, 1960.

52. A.N. Kornilov et al.: Zh. Fiz. Khim., 40, p. 1070, 1966.

53. W.L. Worrel and J. Chipman: J. Phys. Chem., 68, p. 860, 1964.

54. E. Storms et al.: High. Temp. Sci., 1, p. 430, 1969.

55. R.V. Gel'd and F.G. Kusenko: Izv. Akad. Nauk SSSR, Otd. Tekhn. Nauk, Met. i Toplivo No. 2, p. 79, 1960.

56. D.S. Neel et al.: Air Force Report WADD-TR-60-924, 1960.

57. L.S. Levinson: J. Chem. Phys., 38, p. 2105, 1963.

58. L.B. Pankratz et al.: U.S. Bur. Mines Rept. Invest. 6446, 1964.

59. R.A. McDonald et al.: Proc. Meeting Interagency Chem. Rocket Propulsion Group Thermochem., New York, p. 213, 1963.

60. T.A. Sandenaw and E.K. Storms: Los Alamos Sci. Lab. Report LA-3331, 1965.

61. T.A. Sandenaw and E.K. Storms: J. Phys. Chem. Solids, 27, p. 217, 1966.

62. A.G. Turchanin et al.: Translated from Poroshkovaya Metallurgiya, 11, p. 45, 1971.

63. H.L. Schick: Thermodynamics of Certain Refractory Compounds, Vol. 2, Academic Press, New York-London, 1966.

64. F.M. Jaeger and W.A. Veenatra: Rec. Trav. Chim., 53, p. 677, 1934.

65. G.W. Ziegler: Ph.D. Thesis, Ohio State Univ., Columbus, Ohio.

66. I.B. Fieldhouse et al.: WADC-TR-58-274, 1958, Wright Air Develop. Div., Wright-Patterson, A.F.B., Ohio.

67. G.C. Lowenthal: Australian J. Phys., 16, p. 47, 1963.

68. Ya. A. Kraftmakher: Fiz. Tverd. Tela, 5, p. 950, 1963.

69. D.T. Hawkins and R.L. Orr: J. Chem. Eng. Data, 9, p. 505, 1964.

70. V.A. Kirillin et al.: High Temp. (Engl. Trans.), 3, p. 357, 1965.

71. JANAF Thermochemical Tables, 2nd Edition, D.R. Stull and H. Prophet (Ed.), U.S. Dept. Comm., 1971.

72. "Thermochemical Props. of Inorganic Substances", I. Barin and O. Knacke, Springer-Verlag, New York, 1973.

73. Thermochemistry for Steelmaking, Vol. 1, J.F. Elliott et al., Addison-Wesley Publishing Co., New York, 196

74. K.K. Kelley: U.S. Bur. Mines, Bull. 584, 1960.

75. K.K. Kelley and E.G. King: U.S. Bur. Mines, Bull. 592, 1961.

76. S. Sato and T. Sogabe: Sci. Papers Inst. Phys. Chem. Res. (Tokyo), 38, p. 174, 1941.

77. A.D. Mah and N.L. Gellert: J. Am. Chem. Soc., 78, p. 3261, 1956.

78. L. Kauffman: Trans. TMS-AIME, 224, p. 1006, 1962.

79. R.J. Hawkins: "Thermodynamics of solid Fe-Mn alloys and of Ta and Nb in γ-Fe", Research paper, BSC Corporate Laboratories-University of Sheffield Symposium on Chemical Metallurgy of Iron and Steel, 1973, London (Iron and Steel Inst./Metals Soc.), p. 310.

80. B.B. Argent: "Substitutional Alloys of Iron", Review Paper, ref. 79, p. 301.

81. D. Robinson and B.B. Argent: Met. Sci., 10, p. 219, 1976.

82. S. Ban-ya *et al.*: Met. Trans., 1, p. 1313, 1970.

83. S. Ban-ya *et al.*: Trans. TMS-AIME, 245, p. 1199, 1969.

84. H. Harvig: Jernkont. Ann., 155, p. 157, 1971.

85. M. Hillert and L.I. Staffonson: Acta. Chem. Scand., 24, p. 3618, 1970.

86. M. Hillert and M. Jarl: Met. Trans., 6A, p. 553, 1975.

87. R.C. Hudd *et al.*: JISI, 209, p. 121, 1971.

88. S. Koyama *et al.*: Japan Inst. Met. J., 35, p. 698, 1971.

89. S. Koyama *et al.*: Japan Inst. Met. J., 35, p. 1089, 1971.

90. T. Wada *et al.*: Met. Trans., 2, p. 2199, 1971.

91. T. Wada *et al.*: Met. Trans., 3, p. 1657, 1972.

92. T. Wada *et al.*: Met. Trans., 3, p. 2865, 1972.

93. H.J. Grabke *et al.*: Z. Metallkde., 5, p. 286, 1975.

94. T. Mori *et al.*: Mem. Fac. Eng., Kyoto Univ., 1963, Vol. 25, pp. 164.

95. von Miroslavá Matasová and H. Tůma: Neue Hütte, 7, p. 430, 1973.

96. T. Mori *et al.*: 19th Committee on Reactions in Steel Making, Rep. No. 8022, 1964.

97. I.N. Milinskaya and I.A. Tomlin: Akad. Nauk SSSR Doklady, 174, p. 135, 1973.

98. T. Mori et al.: Mem. Fac. Eng., Kyoto Univ., 1963, Vol. 25, p. 175.

99. G.L. Depoorter: Los Alamos Sci. Lab. Report LA-3744, 1967.

100. W.B. Pearson: Handbook of Lattice Spacings of Metals and Alloys, Pergamon, Vol. 2, 1967.

101. B.B. Argent and B.J. Piearcey, N.P.L. Symposium No. 9 on Intermetallic Compounds, Vol. 1, p. 3, 1958.

102. R.C. Hudd et al.: JISI, 209, p. 121, 1971.

103. W. Roberts and P. Grieveson; Scripta Met., 8, p. 451, 1974.

104. "Aciers de construction métallique à dispersoides", M. Lamberigts and T. Greday, CRM, Brussels, 1975.

105. K.K. Srivastava, Ph.D. Transfer Report, Department of Metallurgy and Materials Science, McMaster University, 1976.

106. J. Chipman: Trans. TMS-AIME, 239, p. 2, 1967.

107. K. Källstrom and A. Omsén: Thesis, Royal Inst. of Techn., Stockholm, 1963.

108. A.J. Hechler and P.G. Winchell: Trans. TMS-AIME, 227, p. 732, 1963.

109. R.R. Zupp and D.A. Stevenson: Trans. TMS-AIME, 236, p. 1316, 1966.

110. T. Nishizawa: Swedish Council Appl. Res. Rep. (4602), 1967.

111. B. Uhrenius and H. Harvig: Met. Sci., 9, p. 67, 1975.

112. Thermodynamics: G.N. Lewis and M. Randall, McGraw-Hill, New York, 1961.

113. Constitution of Binary Alloys, Hansen, McGraw-Hill Book Co., New York, 1958.

114. "Handbook of Binary Phase Diagrams", W.G. Moffat, General Electric Co., New York, 1976.

115. "Compendium of Phase Diagram Data", E. Rudy, AFML-TR-65-2, Part V, 1969.

116. Mori et al.: Trans. ISIJ., 10, p. 350, 1970.